The Dissertation Committee for Haewoon Nam
certifies that this is the approved version of the following dissertation:

Joint Diversity Combining Technique and Adaptive Modulation in Wireless Communications

Committee:

Baxter F. Womack, Supervisor

Earl E. Swartzlander, Jr.

Gustavo de Veciana

Jeffrey G. Andrews

Mohamed-Slim Alouini

Joint Diversity Combining Technique and Adaptive Modulation in Wireless Communications

by

Haewoon Nam, B.S.E., M.S.E.

Dissertation

Presented to the Faculty of the Graduate School of

The University of Texas at Austin

in Partial Fulfillment

of the Requirements

for the Degree of

Doctor of Philosophy

The University of Texas at Austin

December 2006

Dedicated to my wife and my parents
for their endless love and support

Acknowledgments

I would like to thank my advisor, Prof. Baxter F. Womack, for his encouragement, guidance, and support during my years at the University of Texas at Austin. He is a true model as a prefessor with enthusiasm in teaching and a human being with generous friendship.

I am indebted to my committee members for their valuable directions and comments. Prof. Gustavo de Veciana is a truly exceptional instructor and researcher. His lectures are among the best courses that I had taken during my graduate studies. Prof. Jeffrey G. Andrews helped me a lot in various ways. One of his graduate courses was fundamental to much of the work in this dissertation. I would also like to thank Prof. Earl E. Swartzlander, Jr., for taking his valuable time to serve as my committee chair. Special thanks also go to Prof. Mohamed-Slim Alouini for his research direction and advice. His comments and insights were instumental and made my research more fruitful.

I am very grateful to everyone that I worked with at the IBM T.J. Watson research center, Freescale semiconductor, and Samsung Advanced Institute of Technology. Their guidance and insights were influential and helpful throughout the course of my research. I would also like to thank Dr. Youngchai Ko in Korea university for his valuable discussions. Some of the contributions in this dissertation were collaborated with him.

My sincere thanks and gratitude also go to my colleagues who have been in this long academic journey with me at the University of Texas at Austin. My graduate school friends in Austin, graduate school friends in Seoul, undergraduate friends, and high school friends, too numerous to list, are hereby acknowledged. They are great additions to me and my school life have been filled with wonderful memories thanks to them.

I would cordially like to thank the Korean government for the financial support during my doctoral studies at the University of Texas at Austin.

Finally, I would like to dedicate this dissertation to my wife Juyeon Lee, to my boy Brian Janghoon Nam and soon to be born child, to my parents and parents-in-law, and to my brother for their endless love and support. It would have been impossible for me to accomplish this without them.

Haewoon Nam

The University of Texas at Austin
December 2006

Joint Diversity Combining Technique and Adaptive Modulation in Wireless Communications

Publication No. _____

Haewoon Nam, Ph.D.
The University of Texas at Austin, 2006

Supervisor: Baxter F. Womack

Wireless communications has become a major economic sector with an unprecedented growth rate over the past decade. This phenomenal growth rate has increased even faster in the 21st century due to the success of wireless cellular systems and wireless local area networks. Furthermore, a variety of applications for high quality media content running on mobile devices have also fueled this phenomenon. In order to maintain the rapid growth rate and satisfy such a high demand from users, the next generation communication systems must achieve both reliability and high data rate using a limited spectrum, power, and complexity budget. Unfortunately, a harsh and unpredictable wireless radio propagation environment, with issues such as multipath, shadowing effects, and frequency selectivity, makes this goal very challenging.

There are several techniques in wireless communication systems to combat, or even exploit, such a detrimental effect of fading channels. The most popular technique is the diversity combining technique, where multiple replicas of the same signal are used to reduce the amount of fading. By coherently combining these multiple copies of the transmitted signal, this technique provides reliability of the communication link and offers a higher dynamic range. Among other techniques is adaptive modulation, which attempts not to mitigate the fading effect but to take advantage of it by adaptively adjusting the modulation constellation to the instantaneous channel quality. Thus, this technique aims at achieving a high spectral efficiency given a certain level of bit error rate (BER).

This dissertation examines diversity combining techniques and adaptive modulation with an emphasis on how these two different techniques can jointly operate in various wireless systems to achieve both reliability and high spectral efficiency. After a brief introduction to the conventional diversity combining schemes, the adaptive diversity combining schemes are first discussed including a performance analyis. Embedded with a target signal-to-noise ratio (SNR), which may be pre-determined based on the quality of service (QoS) for an application, the adaptive diversity combining schemes achieve a reduced complexity while satisfying the target performance.

Second, a joint diversity combining and adaptive modulation technique in multi-carrier systems is proposed and presented with analytical results. Since the fourth generation (4G) wireless cellular system standards adopt orthogonal frequency division multiplexing (OFDM) as a basic transmission technology, techniques to improve the performance at the cell edge in such multi-carrier systems are becoming very important. Exploiting a diversity

combining technique, the proposed scheme offers an improved spectral efficiency in the low SNR region.

Finally, a simple and practical system based on a switched diversity scheme with adaptive modulation is presented. This system provides a reduced number of channel estimation while satisfying the optimum spectral efficiency compared to a selection diversity system. In addition, the switching threshold is easily manipulated so as to make an efficient use of the trade-off between spectral efficiency and the number of channel estimation. An extension of this scheme into a multiuser scenario is considered. This switch-based multiuser access scheme results in an average feedback load that is lower than using the optimal selection-based multiuser scheme. Numerical results show we can obtain a trade-off between spectral efficiency and the feedback load by choosing the switching threshold appropriately.

Contents

Acknowledgments **v**

Abstract **vii**

List of Tables **xv**

List of Figures **xvi**

Chapter 1 Introduction **1**

1.1 Motivation 1
1.2 Adaptive Modulation 2
1.3 Objective 4
1.4 Organization of Dissertation 5

Chapter 2 Wireless Channel Models **7**

2.1 Introduction 7
2.1.1 Slow and Fast Fading 7
2.1.2 Flat and Frequency Selective Fading 8
2.2 Statistical Fading Channel Models 8
2.2.1 Rayleigh Fading Channel 9
2.2.2 Ricean Fading Channel 10
2.2.3 Nakagami-m Fading Channel 11
2.3 Channel Modeling and Simulation 12

Chapter 3 Conventional Diversity Combining Schemes **15**
3.1 Introduction 15
3.2 Selection Combining (SC) 16
3.3 Switched Combining (SWC) 17
3.4 Maximum Ratio Combining (MRC) 18
3.5 Equal Gain Combining (EGC) 19
3.6 Generalized Selection Combining (GSC) 19

Chapter 4 Low-Complexity Diversity Combining Schemes **21**
4.1 Introduction 21
4.2 Diversity Rich Environment 22
4.3 GSC with Threshold per Branch (T-GSC) 23
4.3.1 Combining Strategy 23
4.3.2 Statistics of the Combined SNR 24
4.3.3 Performance Analysis 25
4.4 Output-Threshold MRC (OT-MRC) 27
4.4.1 Combining Strategy 27
4.4.2 Statistics of the Combined SNR 28
4.4.3 i.i.d. Channel Case 30
4.4.4 Non-i.i.d. Channel Case 33
4.5 Minimum Selection GSC (MS-GSC) 36
4.5.1 Combining Strategy 37
4.5.2 Statistics of the Combined SNR 38
4.5.3 i.i.d. Channel Case 41
4.5.4 Non-i.i.d. Channel Case 48
4.6 Switched Combining with Post-Examining Selection (SECps) . 51
4.6.1 Combining Strategy 52
4.6.2 Statistics of the Combined SNR 52
4.6.3 Performance Analysis 53
4.7 Minimum Estimation and Combining GSC (MEC-GSC) . . . 54
4.7.1 Combining Strategy 55

4.7.2 Statistics of the Combined SNR 55
4.7.3 Performance Analysis 56
4.8 Performance Comparison 57
4.9 Effect of Channel Fading Correlation 63
4.9.1 Statistics of OT-MRC and MEC-GSC 63
4.9.2 Performance Analysis 66
4.9.3 Numerical Results 67
4.10 Practical Aspects 70
4.10.1 Cellular Environment 70
4.10.2 Simulation in an HSDPA Environment 73

Chapter 5 Spectral Efficiency Enhancement in Multicarrier Systems 78

5.1 Introduction 78
5.2 System Model 80
5.3 Proposed Adaptive Scheme 82
5.3.1 Optimal Scheme 82
5.3.2 Hybrid Scheme 83
5.4 Average Spectral Efficiency 85
5.4.1 Conventional Scheme 85
5.4.2 Hybrid Scheme 86
5.5 Outage Probability 90
5.5.1 Conventional Scheme 90
5.5.2 Hybrid Scheme 90
5.6 Average Bit Error Rate 91
5.6.1 Conventional Scheme 91
5.6.2 Hybrid Scheme 91
5.7 Complexity Analysis 93
5.7.1 Optimal Scheme 93
5.7.2 Hybrid Scheme 94
5.8 Numerical Results 94

5.9 Simulation in a Practical Scenario 98
5.9.1 802.16 WiMAX System Environment 98
5.10 Conclusion 102

Chapter 6 Joint Switched Diversity and Adaptive Modulation 103
6.1 Introduction 103
6.2 Switched Diversity Systems with Adaptive Modulation 105
6.2.1 Spectral Efficiency Maximizing Scheme 106
6.2.2 Antenna Switching Minimizing Scheme 109
6.2.3 Adaptive Scheme with Optimum Threshold 111
6.3 Switch-based Multiuser Scheduling 113
6.3.1 System Model 113
6.3.2 Switch-based Scheduling 114
6.3.3 Overall System Spectral Efficiency Maximizing Scheme 115
6.3.4 Feedback Load and Antenna Switching Minimizing Scheme 117
6.3.5 Trade-off Scheme 118
6.4 User Scheduling with Fairness 120
6.4.1 Opportunistic Scheduling Policy 120
6.4.2 Equal Access Scheduling Policy 121
6.5 Feedback Load and Rate 122
6.5.1 Overall System Spectral Efficiency Maximizing Scheme 122
6.5.2 Feedback Load and Antenna Switching Minimizing Scheme 123
6.5.3 Trade-off Scheme 123
6.6 Numerical Results and Simulation 124
6.6.1 Joint Switched Diversity and Adaptive Modulation . . 124
6.6.2 Multiuser Diversity with Switch-based Scheduling . . . 127
6.7 Conclusion and Future Work 129

Chapter 7 Conclusions 132
7.1 Summary and Contributions 132
7.2 Future Work 134
7.2.1 Extensions of Adaptive Diversity Techniques to MIMO 134

7.2.2 Efficient Feedback Schemes in a Multiuser Scenario . . 134

Appendix A Some Derivations **136**

A.1 Derivation of SE_i^+ and SE_i^- 136

A.2 Derivation of $\overline{\mathrm{BER}}_{i,j}^{+}$ and $\overline{\mathrm{BER}}_{i,j}^{-}$ 138

A.3 Derivation of Eq. (6.25) 140

Appendix B Some Integrals involving Average Error Rate Analysis **143**

B.1 Derivation of $\mathcal{I}[\alpha_n, \lambda, \delta]_{y_n}^{y_{n+1}}$ 143

B.2 Derivation of $\mathcal{I}_1[k, a, b]$ 145

B.3 Derivation of $\mathcal{I}_2[k, a, b, c]$ 145

Bibliography **147**

Vita **161**

List of Tables

1.1 Constellation size and switching channel SNR thresholds of ψ-QAM for several target BER values (BER_T) 3

2.1 Statistics of the symbol SNR for various fading channel models 10

3.1 Statistics of the combined SNR for the MRC(L) over various fading channel models 18

4.1 HSDPA simulation parameters 73

5.1 WiMAX simulation parameters 98

5.2 Constellation and switching thresholds for simulation 99

List of Figures

2.1 Wireless channel simulation in Matlab 12
2.2 Wireless channel simulation in LabView 13

3.1 An example for dual-branch selection combining and switched combining 17

4.1 Probability density function of MS-GSC (a) $f(\gamma, L_c)$ for L=10, γ_T=6.8dB, (b) $f(\gamma, L_c)$, for L=10, γ_T=10dB, and (c) $f(\gamma, L_c)$, for L=10, γ_T=11.7dB 43
4.2 Bit error rate performance of the low-complexity diversity combining schemes when L=10 and γ_T=6dB 58
4.3 Average number of combined branches of the low-complexity diversity combining schemes when L=10 and γ_T=6dB 59
4.4 Average number of branch estimations of the low-complexity diversity combining schemes when L=10 and γ_T=6dB 59
4.5 Bit error rate performance of the low-complexity diversity combining schemes when L=10 and γ_T=10dB 60
4.6 Average number of combined branches of the low-complexity diversity combining schemes when L=10 and γ_T=10dB 60
4.7 Average number of branch estimations of the low-complexity diversity combining schemes when L=10 and γ_T=10dB 61

4.8 Bit error rate performance versus normalized SNR threshold ($\frac{\gamma_T}{\overline{\gamma}}$) of the low-complexity diversity combining schemes when L=10 61
4.9 Average number of combined branches versus normalized SNR threshold ($\frac{\gamma_T}{\overline{\gamma}}$) of the low-complexity diversity combining schemes when L=10 62
4.10 Average number of branch estimations versus normalized SNR threshold ($\frac{\gamma_T}{\overline{\gamma}}$) of the low-complexity diversity combining schemes when L=10 62
4.11 Average combined SNR of dual OT-MRC and MEC-GSC over correlated Nakagami-m fading channels for $\gamma_T = 7$ dB 67
4.12 The ratio of average combined SNR of dual OT-MRC to that of MEC-GSC over correlated Nakagami-m fading channels for $\gamma_T = 7$ dB 68
4.13 Average number of combined branches of dual OT-MRC and MEC-GSC over correlated Nakagami-m fading channels for $\gamma_T =$ 7 dB 68
4.14 Bit error rate of dual OT-MRC and MEC-GSC over correlated Nakagami-m fading channels for $\gamma_T = 7$ dB 69
4.15 Average number of combined branches of OT-MRC and MEC-GSC in a cellular environment when $L = 4$ 75
4.16 Average outage probability of OT-MRC and MEC-GSC in a cellular environment when $L = 4$ 75
4.17 Average power consumption of OT-MRC, MS-GSC, and MEC-GSC when $L = 4$ 76

5.1 Conventional adaptive modulation for multi-channel systems. . 81
5.2 Flow chart for the algorithm of the proposed scheme 84
5.3 Average spectral efficiency of the optimal scheme and hybrid scheme ($L = 6$) 95

5.4 Outage probability of the optimal scheme and hybrid scheme ($L = 6$). 95
5.5 Average bit error probability of the optimal scheme and hybrid scheme ($L = 6$). 96
5.6 Comparison of the complexity of the optimal scheme and hybrid scheme. 97
5.7 (a) Average data rate and (b) average data rate gain of the hybrid scheme over the conventional scheme in a WiMAX system environment with 1.25 MHz system bandwidth, and (c) average data rate and (d) average data rate gain in a WiMAX system environment with 5 MHz system bandwidth. 99
5.8 Average data rate gain of the hybrid scheme over the conventional scheme in a multi-cellular WiMAX environment with (a) 1.25 MHz system bandwidth, and (b) 5 MHz system bandwidth. 101
5.9 Average Frame Error Rate of the hybrid scheme and the conventional scheme in a WiMAX system environment with 1.25 MHz system bandwidth. 101

6.1 Optimum switching threshold for SECps with multiple modulation levels 112
6.2 A discrete time division multiplexing system over block fading channels. 113
6.3 Average spectral efficiency of various schemes 125
6.4 Average number of channel estimation (antenna switching) of the various schemes 125
6.5 Average bit error rate of the various schemes 126
6.6 Average overall spectral efficiency for the switch-based multiuser access scheme with various parameters for the number of user $K = 10$ 128

6.7 Average overall spectral efficiency for the switch-based multiuser access scheme with various parameters as a function of the number of users for average channel SNR $\overline{\gamma}$=18dB 129
6.8 Average feedback load for the switch-based multiuser access scheme with various parameters as a function of the number of users for average channel SNR $\overline{\gamma}$=16dB 130
6.9 Average feedback load for the switch-based multiuser access scheme with various parameters for the number of user $K = 10$ 130
6.10 Normalized average feedback load for the switch-based multiuser access scheme with various parameters as a function of the number of users for average channel SNR $\overline{\gamma}$=20dB 131

Chapter 1

Introduction

1.1 Motivation

Over the past decades, wireless communications has had a profound impact on the economy and business. Today, we can not even imagine our daily lives without wireless communications. Since Guglielmo Marconi successfully demonstrated the first application of radio in 1898, the world has seen tremendous advances in wireless transmission, resulting in today's ubiquitous communication systems. Although an article covering tests of a two-way radio conversation in a moving automobile, entitled "Talking by wireless as you travel by train or motor", appeared in the November 7, 1920, issue of the *Boston Sunday Post*, it was not until the 1980s that technologies such as pagers and wireless telephones became widely available. An interested reader in the history of wireless is referred to [1].

As wireless technology has grown, users' insatiable hunger for reliable communications at a higher data rate has increased at an even faster pace. In order to meet such a demand, wireless systems have evolved from the second generation (2G) wireless cellular systems, which are mainly voice communications, into the third generation (3G) and future communications that will support both voice and data traffic over a reliable and high data rate wireless link. Overflowing internet applications and high quality media content, such as

videos, audios, and pictures, have expedited the advancement of technologies for data communications over wireless.

The random and unpredictable nature of wireless channels makes it difficult for wireless systems to accomplish both reliability and high data rate simultaneously. Thus, some form of compensation is required to achieve the reliability of a wireless link. Diversity combining techniques are well known as an effective way of mitigating the adverse effects of wireless fading channels without using expensive resources such as frequency band or/and transmit power [2,3]. Adaptive modulation is another way of accommodating the fading effect of wireless channels, where a different modulation constellation is used for transmission depending on the instantaneous channel quality. Adaptive modulation is known as a near-capacity achieving technique. The joint use of diversity combining techniques and adaptive modulation has a great potential for improving the performance of wireless communication systems by providing both high reliability and high data rate simultaneously [4–6].

Wireless systems always have a certain constraint(s) subject to the given resources. Since processing complexity is an important issue in practical systems, it is desirable for the system designer to identify trade-offs between performance and complexity. Conventional diversity combining schemes, on the other hand, entail an inefficient use of resources because of the fixed mode of operation and fixed number of diversity branches that are combined regardless of channel state. Adaptive selection of diversity branches and a degree of freedom given by discrete-rate adaptive modulation can provide an effective way of using the given resources to trade off performance and complexity.

1.2 Adaptive Modulation

When channel state information is available at both the transmitter and the receiver, the transmission scheme can be adapted according to the channel variation. The non-adaptive system with a fixed modulation needs to set its modulation level or transmission scheme to the worst-case channel conditions

n	ψ	γ_T^n [dB]		
		$\text{BER}_T = 10^{-2}$	$\text{BER}_T = 10^{-3}$	$\text{BER}_T = 10^{-4}$
1	4	7.33	9.64	11.35
2	8	11.84	13.32	16.07
3	16	13.90	16.63	18.23
4	32	17.83	19.79	22.29
5	64	19.73	22.86	24.30
6	128	23.85	25.91	28.24
7	256	25.43	28.94	30.23

Table 1.1: Constellation size and switching channel SNR thresholds of ψ-QAM for several target BER values (BER_T)

to meet the performance requirement, which results in an inefficient utilization of the channel capacity. Thus, it is straightforward that adjusting the power or the modulation level, or both, to the instantaneous channel state will provide much higher spectral efficiency [7–10].

The basic intuition of power adaptation is to adjust the transmit power inverse to the channel quality such that the received signal power stays the same regardless of the channel quality. This zero-forcing type of power adaptation often incurs undesirable events like dramatically increasing transmit power when the channel is very weak. Additionally, regulatory concerns and peak-to-average power ratio problems sometimes inhibit adaptive power allocation from being used in practice. Interestingly, it is known that rate adaptation is the key to achieving high link spectral efficiency, whereas variable-power variable-rate systems provide a small spectral efficiency gain over constant-power variable rate systems in which the latter simplifies the hardware complexity significantly [11]. Throughout this dissertation, we consider adaptive modulation with discrete rate and constant transmission power. Frequently, adaptive coded modulation is used to further achieve a coding gain. Although no coding scheme is considered with adaptive modulation, it can be readily extended to adaptive coded modulation. For example, [9] shows the signal-

to-noise ratio (SNR) thresholds for an adaptive coded modulation are well approximated by an exponential function.

For a rate adaptation, the channel SNR (CNR) range is separated into N + 1 fading regions, each of which is associated with a quadrature amplitude modulation (QAM) signal constellation. The divided CNR regions are defined by the CNR thresholds $0 < \gamma_T^1 < \cdots < \gamma_T^N < \infty$, where γ_T^n is the CNR threshold for 2^{n+1}-QAM. Therefore, the signal whose CNR is higher than γ_T^N is modulated with the highest modulation level, while the signal whose CNR is lower than γ_T^1 has no transmission. Table 1.1 shows the adaptive modulation table for a target bit error rate (BER_T) of 10^{-2}, 10^{-3}, and 10^{-4} when $N = 7$.

1.3 Objective

The primary purpose of this dissertation is to provide a foundational research reference for wireless system designers or researchers who require in-depth knowledge of diversity combining schemes and adaptive modulation with an emphasis on their applications in wireless communication systems.

This dissertation has three objectives. The first objective is to develop novel and practical methods of incorporating diversity techniques and adaptive modulation in various wireless systems and to analyze their theoretical performances. The second is to identify and use the trade-off between complexity and performance in those systems. Since complexity or power consumption is a very critical issue in designing wireless communication systems in practice, this fundamental trade-off needs to be determined and emphasized. In addition, system designers need to consider how to utilize this trade-off. The final goal is to offer manageable analytical expressions that can help researchers or system designers investigate the performance of wireless systems with diversity techniques and adaptive modulation and, further, determine the optimum choice for system design under given resource constraints.

1.4 Organization of Dissertation

This dissertation is organized as follows. Chapter 2 briefly discusses the small scale wireless fading channel models. The statistics of the fading channel models are provided in a table for future reference.

Chapter 3 reviews the various conventional diversity combining schemes that are well-known in the literature. Selection combining (SC), switched combining (SWC), maximum ratio combining (MRC), equal gain combining (EGC), and generalized selection combining (GSC) are briefly explained. Since the low-complexity diversity combining schemes are variants of some of the conventional schemes, the statistics of the output SNR of the conventional schemes are briefly discussed.

Chapter 4 is devoted to an analysis of the theoretical performance of low-complexity diversity combining schemes. These schemes can be divided into two categories: selection based schemes and switching based schemes. GSC with threshold per branch (T-GSC), output thresholds MRC (OT-MRC), minimum selection GSC (MS-GSC), and minimum estimation and combining GSC (MEC-GSC) belong to selection based schemes, whereas switched combining with post-examining selection (SECps) is a switching based scheme. The average number of combined branches, average BER, and outage probability are performance metrics used for evaluating the schemes. Closed-form expressions for such performance metrics of the above schemes are derived. Further, simulation results of the above schemes, based on practical parameters in a cellular environment, are also presented.

Chapter 5 introduces a multi-carrier transmission system used with a diversity combining technique over subcarriers. The proposed system improves the overall spectral efficiency compared to the conventional multi-carrier system when the overall channel quality over multiple subcarriers is extremely bad as is the case at the cell edge. The overall spectral efficiency and bit error rate performance of the proposed system are presented as analytical expressions. Simulation results in a WiMAX system environment demonstrate that

the proposed system obtains a significant spectral efficiency gain in a low SNR region.

Chapter 6 presents a joint switched diversity and adaptive modulation scheme as a transmission technique for low-cost and low-power wireless applications such as wireless personal area networks (WPAN). This joint scheme can achieve full diversity gain as well as high spectral efficiency. More importantly, this scheme can adapt its mode of operation, by a simple change of switching threshold, from the spectral efficiency maximization to the switching overhead minimization, or vice versa, depending on the channel state or the availability of given resources. Later in this chapter, switch-based multiuser scheduling is performed in a multiuser environment using a similar concept in the joint switched diversity and adaptive modulation. Fairness and feedback issues are also discussed.

Finally, Chapter 7 concludes this dissertation with contributions and future work.

Chapter 2

Wireless Channel Models

2.1 Introduction

The performance of wireless communication systems is determined to a large extent by the wireless channel. Since radio wave propagation is a function of uncountable number of factors, i.e., the communication environment, the operating frequency and bandwidth, receiver mobility, and so on, it is impossible to generalize the wireless channel to a single model. However, considerable amount of research have focused on the statistical modeling of the wireless channel in lots of different environment [12–14].

2.1.1 Slow and Fast Fading

The fading channels can be categorized into slow and fast fading depending on the coherence time of the channel, which is defined as the inverse of the maximum Doppler frequency. The fading is said to be slow when the coherence time is strictly larger than the symbol time duration. On the other hand, if the symbol time duration is larger than the coherence time, the channel is fluctuating very frequently over time, which is said to be fast fading.

The mobility of any objects in the environment including the transmitter and receiver induces Doppler frequency. As the mobility increases, Doppler

frequency also increases and, thus, the coherence time shrinks, and vice versa. The slow fading offers some advantages to the complexity of the system. For instance, the frequent channel estimation is not necessary. However, the system can suffer from the reduced overall performance, since the interleaving technique becomes useless due to the long coherence time. In the fast fading, it is difficult to keep track of channel variation by the conventional estimation methods. On the other hand, frequent fluctuation can lead the overall performance improvement especially in multiuser environment. The recent research shows that the intentional channel fluctuation can provide considerable performance enhancement due to multiuser diversity [15].

2.1.2 Flat and Frequency Selective Fading

The flat fading occurs for narrow-band signals when the delay spread is strictly less than the symbol time duration. In frequency-selective fading, on the other hand, the symbol time duration is smaller than the delay spread. Under such conditions, the received signal has multiple echoes of the transmitted waveform that are attenuated and delayed in time, which might induce the inter-symbol interference. For spread-spectrum systems, rake receivers can take advantage of this frequency selectivity by capturing multiple replicas of the transmitted signal to obtain better performance.

Throughout this dissertation, we are considering slow and flat fading channels, since main focus is the performance evaluation of adaptive low-complexity diversity schemes and its application to multi-carrier systems in which each subcarrier is a narrow-band.

2.2 Statistical Fading Channel Models

Fading channel models are characterized by the following statistics:

1. cumulative distribution function (CDF)

The CDF of a random variable γ evaluated at x, where x is an arbitrary value, is defined as

$$F(x) = \Pr[\gamma \leq x] \tag{2.1}$$

2. probability distribution function (PDF)

   The PDF of γ evaluated at x is obtained by differentiating $F(x)$ with respect to x, which is written as

$$f(x) = \frac{d}{dx}F(x) \tag{2.2}$$

3. moment generating function (MGF)

   The MGF is defined as

$$\mathcal{M}_\gamma(s) = \int_0^\infty f(\gamma)e^{s\gamma}d\gamma \tag{2.3}$$

The statistics of various fading channels of interest is summarized in Table 2.1.

2.2.1 Rayleigh Fading Channel

The fading signal amplitude in macro cellular environment in the absence of a line of sight (LOS) component is frequently modelled by the Rayleigh distribution [12]. When the received signal consists of a large number of place waves, the received complex signal $r(t) = r_Q(t) + jr_I(t)$ is viewed as a wide-sense stationary complex Gaussian random process. In the environment with lots of scatterer, $r_Q(t)$ and $r_I(t)$ are identically and independently distributed zero mean Gaussian random variables with variance σ^2. Under these conditions, the magnitude of the received complex envelope is shown as

$$p(x) = \frac{x}{\sigma^2}e^{-\frac{x^2}{2\sigma^2}}, \quad x \geq 0. \tag{2.4}$$

Model	Rayleigh	Ricean	Nakagami-m
Parameter		$K \geq 0$	$m \geq \frac{1}{2}$
PDF ($f(\gamma)$)	$\frac{1}{\overline{\gamma}} e^{-\frac{\gamma}{\overline{\gamma}}}$	$\frac{(1+K)e^{-K}}{\overline{\gamma}} e^{-\frac{1+K}{\overline{\gamma}}\gamma} I_0\left(2\sqrt{\frac{K(1+K)\gamma}{\overline{\gamma}}}\right)$	$\frac{(\frac{m}{\overline{\gamma}})^m \gamma^{m-1}}{\Gamma(m)} e^{-\frac{m\gamma}{\overline{\gamma}}}$
CDF ($F(\gamma)$)	$1 - e^{-\frac{\gamma}{\overline{\gamma}}}$	$1 - Q_1\left(\sqrt{2K}, \sqrt{\frac{2(1+K)\gamma}{\overline{\gamma}}}\right)$	$1 - \frac{\Gamma(m, \frac{m\gamma}{\overline{\gamma}})}{\Gamma(m)}$
MGF ($M(s)$)	$(1 - s\overline{\gamma})^{-1}$	$\frac{1+K}{1+K-s\overline{\gamma}} e^{\frac{s\overline{\gamma}K}{1+K-s\overline{\gamma}}}$	$(1 - \frac{s\overline{\gamma}}{m})^{-m}$

Table 2.1: Statistics of the symbol SNR for various fading channel models

The instantaneous branch SNR therefore follows an exponential distribution given as

$$f(x) = \frac{1}{\overline{\gamma}} e^{-\frac{\gamma}{\overline{\gamma}}}, \quad \gamma \geq 0 \tag{2.5}$$

where $\overline{\gamma} = \mathrm{E}[x^2] = 2\sigma^2$ denotes the average branch SNR.

2.2.2 Ricean Fading Channel

When there is a dominant signal component such as line-of-sight (LOS) path, it is known that the small-scale fading distribution follows Ricean [16]. In this case, $r_Q(t)$ and $r_I(t)$ are Gaussian random variables with non-zero mean $m_I(t)$ and $m_Q(t)$. If $r_Q(t)$ and $r_I(t)$ are uncorrelated and have the same variance σ^2, then the magnitude of the received complex envelope is shown as

$$p(x) = \frac{x}{\sigma^2} e^{-\frac{x^2+s^2}{2\sigma^2}} I_0\left(\frac{xs}{\sigma^2}\right), \quad x \geq 0 \tag{2.6}$$

where $s^2 = m_I^2(t) + m_Q^2(t)$, which denotes the peak power of the dominant signal, and $I_0(\cdot)$ is the modified Bessel function of the first kind and zero order.

The Rice distribution is described in terms of a parameter K that is defined as the ratio of the dominant signal power to the scattered power, that is $K = \frac{s^2}{2\sigma^2}$. Then the magnitude distribution can be rewritten in terms of K

as

$$p(x) = \frac{2x(K+1)}{\Omega} e^{-K} e^{-\frac{(K+1)x^2}{\Omega}} I_0\left(2x\sqrt{\frac{K(K+1)}{\Omega}}\right), \quad x \geq 0, \tag{2.7}$$

where $\Omega = s^2 + 2\sigma^2$. When $K = 0$ the channel exhibits Rayleigh fading, whereas when $K = \infty$ the channel has no fading at all. This type of fading is often observed in microcellular and mobile satellite applications.

2.2.3 Nakagami-m Fading Channel

Nakagami introduced the Nakagami-m channel in the early 1940's to characterize rapid fading in long distance high frequency (HF) channels [17]. The magnitude of the received envelope is given as

$$p(x) = \frac{2m^m x^{2m-1}}{\Gamma(m)\Omega^m} e^{-\frac{mx^2}{\Omega}}, \quad m \geq \frac{1}{2}, \tag{2.8}$$

where $\Omega = \mathrm{E}[x^2]$ and m is the Nakagami fading parameter that ranges from $\frac{1}{2}$ to ∞.

When m approaches infinity, the distribution shows no fading, when $m = 1$ it becomes the Rayleigh distribution, and when $m = \frac{1}{2}$ it becomes a one-sided Gaussian distribution. Since the Ricean distribution contains a Bessel function whereas the Nakagami-m distribution does not, the Nakagami-m distribution is preferred to derive closed-form analytical expressions. Additionally, the Ricean distribution is a special case of the Nakagami-m distribution, it is said that the Nakagami-m is a more general fading channel model. The Nakagami-m distribution is often considered as the best fit to mobile multipath propagation [18, 19].

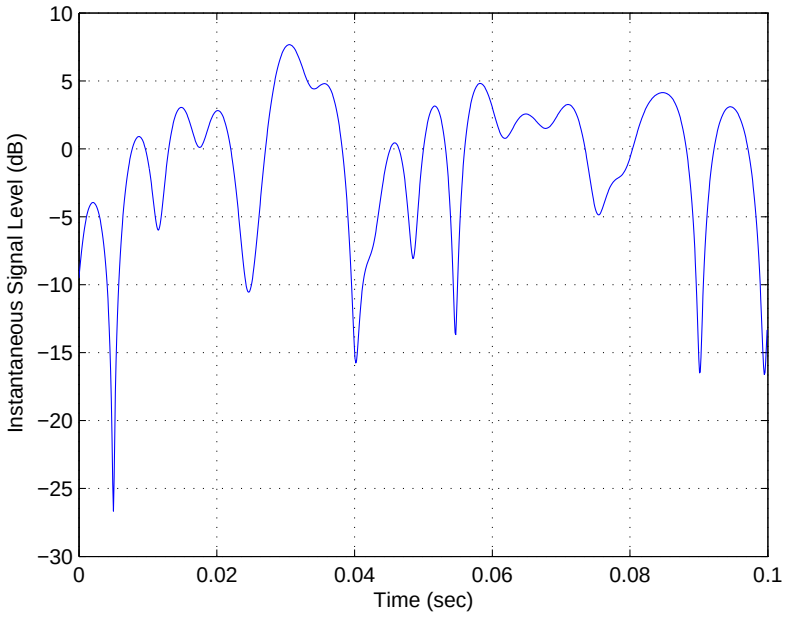

Figure 2.1: Wireless channel simulation in Matlab

2.3 Channel Modeling and Simulation

For the optimum design of wireless systems, an accurate model of the radio propagation channel is very important. The multipath components give rise to temporal dispersion, delay spread, which causes inter-symbol interference. Additionally, the movement of mobile terminals and scattering objects result in fluctuation of the received signal. All these effects impair the detection process of the received signal and increase the bit error rate. To mitigate the interference and improve the signal-to-interference and noise ratio (SINR), an appropriate modulation/coding scheme should be used. Obviously, the optimization of the interference mitigation has to be performed by means of Monte-Carlo-simulations based on accurate stochastic models. Thus, the theoretical and experimental investigation of radio propagation channels as well as the development of stochastic channel models is an important research area for the optimum wireless communication systems design.

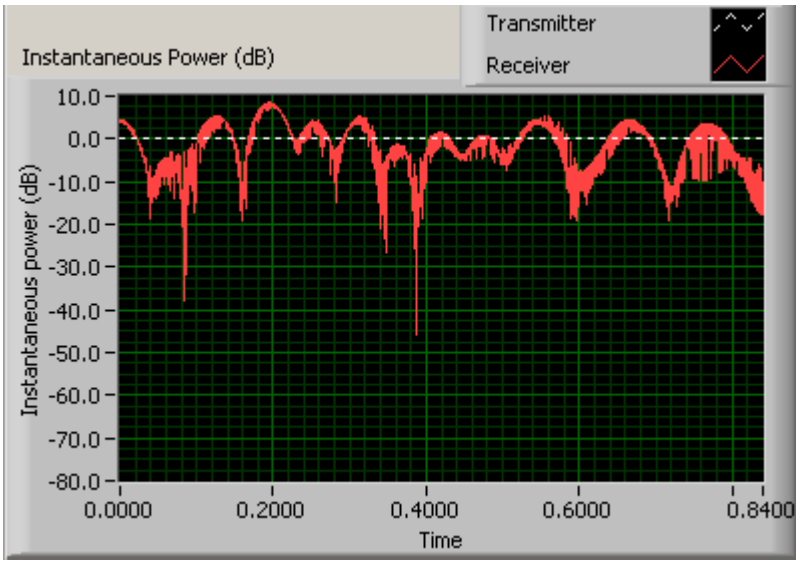

Figure 2.2: Wireless channel simulation in LabView

A tremendous number of channel propagation measurements have been reported for the last several decades. Among lots of different channel measurement environments, an indoor channel is getting more attractive due to the successful deployment of wireless local area network (WLAN). An excellent tutorial of indoor wireless channel modeling is found in [20]. Among the frequency bands for an indoor communications, the 60GHz frequency band has lots of potential for WPAN applications. Reflecting the high interest, the IEEE 802.15.3 task group 3c was formed in march 2005. A physical layer alternative based on millimeter-wave frequency between 57 and 64 GHz for the existing 802.15.3 WPAN standard is being standardized. Along the line, an extensive channel measurement campaign was conducted in the IBM T. J. Watson Research Center [21]. The measurement results in several different indoor places as well as a simple channel model are presented in the paper.

For wide-band indoor channels in general, the Saleh-Valenzuela is frequently used as a channel model [22]. The IEEE 802.15.3a standard group adopted it as the channel model for ultra wideband (UWB) [23]. Thanks to the National Instrument's support, a wireless channel simulator for narrow-band

channel models, such as Rayleigh and Ricean channel, as well as a wide-band channel model, Saleh-Valenzuela, was developed and commercialized as a part of modulation toolkit in LabView. Fig. 2.2 shows the figure captured from the simulator in LabView.

Chapter 3

Conventional Diversity Combining Schemes

3.1 Introduction

Diversity combining techniques have been studied extensively over the past several decades in various areas, such as wireless communications, radar, and navigation systems. There are a number of methods for combining the signals received on multiple diversity branches. Among the conventional diversity combining schemes, MRC is known to be the optimum in the sense that it increases the effect of the branch with high SNR while reducing the effect of branches with small SNR [12,24,25]. EGC is similar to MRC in the sense that all the branches are aligned in phase but the same weight is multiplied in all the branches regardless of their SNR [26,27]. In SC, the branch yielding the highest SNR is always used. By selecting only the strongest branch, the complexity of receivers can be minimized while achieving the diversity gain. The SWC scheme, however, switches to another branch only if the received signal on the current branch falls below the pre-determined SNR threshold [28–30]. The big advantage of switched combining is that only a single radio frequency (RF) chain is needed. To bridge the gap between MRC and SC, GSC selects a certain

fixed number of strong paths and combines them in the way of MRC [31]. A comparison of some of these schemes is available in the literature [32–34] and an excellent tutorial about diversity techniques is found in [35].

3.2 Selection Combining (SC)

Since the strategy is to choose the branch with the highest SNR, it requires each branch to have its own dedicated receiver structure. Thus, the output SNR is written as

$$\gamma_{sc} = \max\{\gamma_1, \gamma_2, \cdots, \gamma_L\}, \tag{3.1}$$

where L is the number of branches. For independent distributed branches, the CDF of the SC, or equivalently the outage probability, is given by

$$F_{sc}(x) = \Pr[\gamma_1 < x, \cdots, \gamma_L < x] = \prod_{i=1}^{L} F(\gamma_i < x). \tag{3.2}$$

If the branches are identically faded, then (3.2) is simply given as

$$F_{sc}(x) = [F_{\gamma}(x)]^L. \tag{3.3}$$

Differentiating (3.3) gives the PDF

$$f_{sc}(x) = L \cdot [F_{\gamma}(x)]^{L-1} f_{\gamma}(x) \tag{3.4}$$

The average SNR of the combiner output is then given by

$$\overline{\gamma}_{sc} = \int_0^{\infty} x f_{sc}(x) dx. \tag{3.5}$$

The average error probability with SC is obtained by averaging the error probability over the PDF of SC and is given by

$$P_b = \int_0^{\infty} P_b(x) f_{sc}(x) dx, \tag{3.6}$$

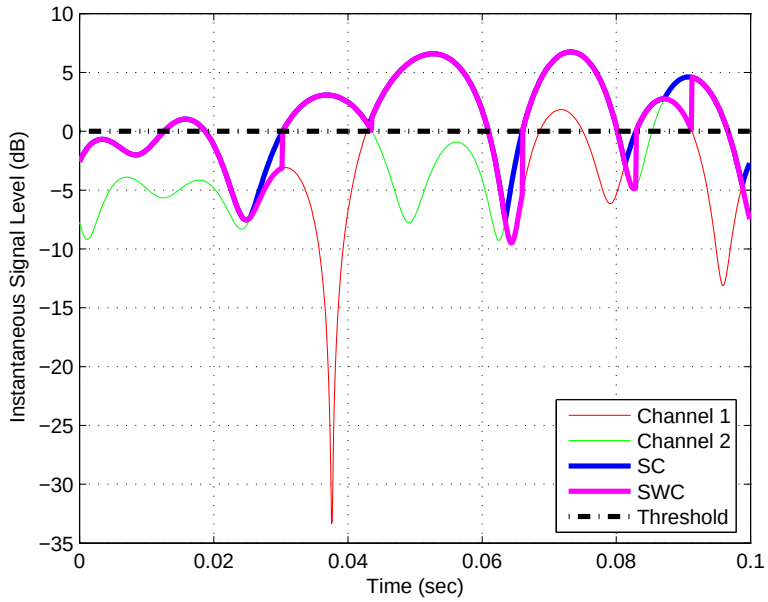

Figure 3.1: An example for dual-branch selection combining and switched combining

where $P_b(x)$ is the BER in additive white Gaussian noise (AWGN).

3.3 Switched Combining (SWC)

While SC requires an estimation of all L branches and a comparison between them simultaneously, a switched combiner scans each of the branches sequentially until in finds a branch whose SNR exceeding a specified threshold. As long as the received signal remains above the threshold, the combiner uses the selected branch until the SNR drops below the threshold. If this happens, the combiner begins to find another branch. If all signals are below the threshold, the combiner can either switch to a random branch or choose the branch with the maximum SNR.

Let γ_1 and γ_2 be the SNRs associated with the two diversity branches. Assume that branch 1 is currently in use. Then, the CDF of the output SNR

Model	PDF ($f_L(\gamma)$)	CDF ($F_L(\gamma)$)
i.i.d. Rayleigh	$\frac{\gamma^{L-1}}{(L-1)!\overline{\gamma}^L}e^{-\frac{\gamma}{\overline{\gamma}}}$	$1-\frac{\Gamma(L,\frac{\gamma_T}{\overline{\gamma}})}{\Gamma(L)}$
non-i.i.d. Rayleigh [36]	$\sum_{j=1}^{L}\prod_{\substack{k=1\\k\neq j}}^{L}\frac{\overline{\gamma}_j{}^{L-2}}{\overline{\gamma}_j-\overline{\gamma}_k}e^{-\frac{\gamma}{\overline{\gamma}_j}}$	$1-\sum_{j=1}^{L}\prod_{\substack{k=1\\k\neq j}}^{L}\frac{\overline{\gamma}_j{}^{L-1}}{\overline{\gamma}_j-\overline{\gamma}_k}e^{-\frac{\gamma}{\overline{\gamma}_j}}$
i.i.d. Nakagami-m	$\frac{\gamma^{Lm-1}}{\Gamma(Lm)}\left(\frac{m}{\overline{\gamma}}\right)^{Lm}e^{-\frac{m\gamma}{\overline{\gamma}}}$	$1-\frac{\Gamma(Lm,\frac{\gamma_T}{\overline{\gamma}})}{\Gamma(Lm)}$

Table 3.1: Statistics of the combined SNR for the MRC(L) over various fading channel models

for SWC is written by

$$\Pr[\gamma_{swc}<x]=\begin{cases}\Pr[(\gamma_1<\gamma_T)\bigcap(\gamma_2<x)], & x<\gamma_T,\\ \Pr[(\gamma_T\leq\gamma_1<x)\bigcup(\gamma_1\leq\gamma_T\bigcap\gamma_2\leq x)], & x\geq\gamma_T,\end{cases}\tag{3.7}$$

The region $x<\gamma_T$ corresponds to the case where a switch from γ_1 to γ_2 occur but the received SNR x is still below γ_T. On the other hand, the region $x\geq\gamma_T$ corresponds to the case when either γ_1 is above γ_T or γ_1 is below γ_T so that a switch to γ_2 happens and the received SNR x becomes above γ_T. Fig. 3.1 illustrates the operation of SC and SWC in a dual-branch system.

3.4 Maximum Ratio Combining (MRC)

In the SC and SWC shown above, the output of the combiner is equal to the one of the branches. In MRC, however, the output is a weighted sum of all branches. The combined SNR of MRC is written as

$$\gamma_{mrc}=\sum_{i=1}^{L}\gamma_i\tag{3.8}$$

where γ_i is the instantaneous SNR of ith branch. The output SNR increases linearly with the number of diversity branches L.

The CDF and the PDF of the combined output SNR for the MRC over various fading channels are tabularized in Table 3.1. Not only independent channel environment [37], but correlated channels is also considered in the literature [38]. We denote the MRC with L diversity branches as MRC(L) which will be used for the performance comparisons later on.

3.5 Equal Gain Combining (EGC)

Although MRC provides the optimal performance, it is often difficult to measure the magnitude of each branch SNR. EGC is similar to MRC because all the branches are co-phased, but is a simpler scheme in the sense that branches are not weighted regardless of their magnitude. This scheme is useful in practice for equal-power modulation techniques such as M-phase shift keying (PSK). The output SNR is then given by

$$\gamma_{egc} = \frac{1}{N_0 L}\left(\sum_{i=1}^{L} r_i\right)^2, \tag{3.9}$$

where r_i is the received signal from ith branch and N_0 is the noise power. Unfortunately, the CDF and PDF for EGC are very difficult to derive. For EGC with $L = 2$ over i.i.d. Rayleigh channels, the CDF is given in a closed-form as

$$F_{egc}(x) = 1 - e^{-\frac{2x}{\overline{\gamma}}} - \sqrt{\frac{\pi x}{\overline{\gamma}}} e^{-\frac{x}{\overline{\gamma}}} \left\{1 - 2Q\left(\sqrt{\frac{2x}{\overline{\gamma}}}\right)\right\}. \tag{3.10}$$

It is known that a closed-form for the CDF does not exist when $L > 2$ [12].

3.6 Generalized Selection Combining (GSC)

The GSC scheme has received considerable attention in the literature for the past several years. This is due to the fact that a good compromise between

performance and complexity is achieved in GSC. It is also known as hybrid selection/maximal-ratio combining scheme (HS/MRC). In the GSC scheme, the L_c strongest branches out of L available branches are coherently combined, which is denoted as GSC(L, L_c). The output SNR of GSC is given by

$$\gamma_{gsc} = \sum_{i=1}^{L_c} \gamma_{(i)} \tag{3.11}$$

where $\gamma_{(i)}$ is the instantaneous SNR of ith strongest branch, that is $\gamma_{(1)} \geq \gamma_{(2)} \cdots \geq \gamma_{(L)}$ [39].

The GSC scheme is analyzed in various different channel environments. [40–42] shows the performance of GSC over i.i.d. Rayleigh channels. Non-i.i.d. Rayleigh channel is considered in [43, 44]. The analysis is extended to i.i.d. Nakagami-m [45–48] and correlated Nakagami-m channels [49]. [50] introduces a different technique, so called the virtual branch, to analyze the performance. The summary of detailed analysis of the GSC scheme over various fading channels will be discussed later.

Chapter 4

Low-Complexity Diversity Combining Schemes

4.1 Introduction

Although MRC provides the best performance, it needs multiple receive chains from RF to baseband and also requires a channel estimation from each diversity branch, which results in high hardware and processing complexity and power consumption. The GSC scheme provides a considerable performance gain over SC, but it still needs to estimate all the branches in order to select a subset of branches according to their signal strength.

Most communication systems require a certain level of quality of service (QoS) depending on the application. In general, QoS is defined by both signal quality and delay requirement, which involve some notion of medium access layer (MAC) functionality. In this dissertation, however, we consider the QoS at every instant time such that a certain level of signal quality guarantees the given QoS.

In a fading channel environment, the received signal SNR fluctuates over a wide range. Even with diversity combining techniques, the combined SNR sometimes far exceeds the SNR required for satisfactory communications,

which results in the overuse of diversity combining branches. Therefore, it can be seen that the complexity of the combining scheme can be reduced if the number of branches is adaptively decided based on the knowledge of the SNR required for the QoS.

In line with this, absolute threshold GSC (AT-GSC) and normalized threshold GSC (NT-GSC) are presented in [51]. In those schemes, a uniform threshold is tested against each of branch SNRs independently on a per branch basis. On the other hand, minimum-selection GSC (MS-GSC), proposed by Kim *et. al.*, uses a threshold to be tested against the combined SNR [52]. Recently, in [53] and [54], a thorough analysis of MS-GSC schemes has been presented over independent and identically distributed (i.i.d.) Rayleigh fading channels. [55] analyzed the error performance of MS-GSC over non-independent and identically distributed (non-i.i.d.) Rayleigh fading channels. Yang and Alouini proposed output-threshold MRC (OT-MRC) and showed its performance over i.i.d. Rayleigh fading channels [56]. In [57] the detailed analysis of OT-MRC over more generalized fading channel models is provided by considering i.i.d. Nakagami-m with integer m and non-i.i.d. Rayleigh fading channels. As a variant of switched combining, switched combining with post-examining selection (SECps) is proposed in [58]. Recently, minimum estimation and combining GSC (MEC-GSC) has been proposed in [59].

4.2 Diversity Rich Environment

The current and imminent wireless communication systems are operating in diversity rich environments. A straightforward example is the WLAN system, such as 802.11a/b/g, which targets mainly an indoor environment and is already being successfully deployed. Since a plethora of multipath exist in such an environment, it is impractical to combine all these paths even though it is optimal from the performance perspective.

The conventional diversity combining schemes are typically effectively operating in worst channel conditions [59]. In an excellent channel condition,

however, combining all the branches in an MRC fashion can lead to an excessive combined signal. Therefore, it is efficient to select a variable number of branches adaptively depending on channel variations under the condition that the combined signal SNR satisfies the performance requirement.

Thus, in diversity-rich environments, such as an indoor communication scenario, the trade-off relationship between performance and complexity becomes a crucial decision factor in designing communication systems.

4.3 GSC with Threshold per Branch (T-GSC)

In [60], a receiver diversity combining scheme is proposed, which allows the number of combined branches to be a variable whose value is determined by the strength of the branch SNRs. Along this line, [51] proposed two conditional combining schemes, AT-GSC and NT-GSC, where each branch is tested against a pre-determined threshold and is selected only if the branch SNR exceeds the threshold. The two schemes differ from each other in the way that the threshold is determined.

4.3.1 Combining Strategy

Consider a diversity combiner with L available branches. Let γ_l, for $l = 1, \cdots, L$, denotes the instantaneous SNR of the lth branch. In AT-GSC, define γ_T as a fixed branch threshold. If γ_l exceeds γ_T, then the branch is selected to be combined. Thus, we can define the combined SNR as

$$\gamma^{AT} = \sum_{i=1}^{L} \gamma_l' \tag{4.1}$$

where

$$\gamma_l' = \begin{cases} \gamma_l, & \gamma_l \geq \gamma_T \\ 0, & \gamma_l < \gamma_T. \end{cases} \tag{4.2}$$

In NT-GSC, on the other hand, γ_T is defined as $\gamma_T = \eta_T \gamma_{\max}$ where $0 \leq \eta_T \leq 1$ and $\gamma_{\max} = \max[\gamma_1, \cdots, \gamma_L]$. All the branches whose SNR is equal to or greater than γ_T are selected to be combined. Thus, the combined SNR is written as

$$\gamma^{NT} = \sum_{i=1}^{L_c} \gamma_{(i)} \tag{4.3}$$

where $\gamma_{(i)}$ represents the instantaneous SNR of ith strongest branch.

4.3.2 Statistics of the Combined SNR

The PDF of γ_l' is expressed as

$$f_{\gamma_l'}(\gamma_l') = \begin{cases} F_{\gamma_l}(\gamma_l)\delta(\gamma_l'), & \gamma_l' = 0 \\ 0, & 0 < \gamma_l' \leq \gamma_T \\ f_{\gamma_l}(\gamma_l'), & \gamma_l' \geq \gamma_T \end{cases} \tag{4.4}$$

where $f_{\gamma_l}(x)$ and $F_{\gamma_l}(x)$ are the PDF and CDF of γ_l evaluated at x. Substituting (4.4) into (2.3), the MGF of AT-GSC is presented as

$$\mathcal{M}_\gamma^{AT}(s) = \prod_{l=1}^{L} \left[F_{\gamma_l}(\gamma_T) + \int_{\gamma_T}^{\infty} f_{\gamma_l}(\gamma_l') e^{s\gamma_l'} d\gamma_l' \right] \tag{4.5}$$

Since NT-GSC can be viewed as a conventional GSC whose number of combined branches is a random variable , the moment generating function (MGF) of NT-GSC is given as

$$\mathcal{M}_\gamma^{NT}(s) = \sum_{l=1}^{L} \Pr[Lc = l] \mathcal{M}_\gamma^{GSC}(s, Lc = l) \tag{4.6}$$

where $\mathcal{M}_{\gamma}^{GSC}(s, Lc = l)$ is the MGF of the conventional GSC when $L_c = l$ branches are selected, which is given by

$$\Pr[Lc = l] = l\binom{L}{l}\sum_{k=0}^{L-l}\binom{L-l}{k}(-1)^k\sum_{m=0}^{l-1}\binom{l-1}{m}\frac{(-1)^m}{m+1+\eta_T(l-m-1+k)}.$$

4.3.3 Performance Analysis

Average Error Probability

AT-GSC

For i.i.d. Rayleigh channels, the average BER of AT-GSC is given [41, eq. (25)] by

$$P_b^{AT} = \frac{\sum_{k=1}^{L}\binom{L}{k}[1-e^{-\frac{\gamma_T}{\overline{\gamma}}}]^{L-k}}{1-[1-e^{-\frac{\gamma_T}{\overline{\gamma}}}]^L}\frac{1}{\pi}\int_0^{\frac{\pi}{2}}\left[\frac{\sin^2\phi}{g\overline{\gamma}+\sin^2\phi}e^{-\frac{\gamma_T}{\overline{\gamma}}(\frac{g\overline{\gamma}+\sin^2\phi}{\sin^2\phi})}\right]^k d\phi, \quad (4.7)$$

which has been known to have no closed-form. However, using the integral equation $\mathcal{I}_2(k, a, b)$ introduced in Chapter B, the closed-form is found and is represented as

$$P_b^{AT} = \frac{\sum_{k=1}^{L}\binom{L}{k}[1-e^{-\frac{\gamma_T}{\overline{\gamma}}}]^{L-k}}{1-[1-e^{-\frac{\gamma_T}{\overline{\gamma}}}]^L}\,\mathcal{I}_1\left[k, g\overline{\gamma}, \frac{k\gamma_T}{\overline{\gamma}}\right] \quad (4.8)$$

where $\mathcal{I}_1[k, a, b]$ is defined in (B.10). To the author's best knowledge, (4.8) is a novel closed-form for the average BER of AT-GSC.

NT-GSC

The average BER of NT-GSC is evaluated as a weighted sum of the average BER of the conventional GSC for every possible number of branches combined

and is simply given by

$$P_b^{NT} = \sum_{i=1}^{L} \Pr[Lc = i] P_b^{GSC}[E, Lc = i] \tag{4.9}$$

where $P_b^{GSC}[E, Lc = i]$ denotes the average BER for GSC with $Lc = i$ branches combined, which is known for i.i.d and non-i.i.d. Rayleigh [41], i.i.d. Nakagami-m [47, 61], and non-i.i.d. Nakagami-m [48].

Outage Probability

Let $\gamma_{\min}$ denote the outage threshold against which the combined SNR is compared.

AT-GSC

Based on the PDF of the combined SNR given in [41, eq. (32)], the outage probability of AT-GSC over i.i.d. Rayleigh channels is expressed as

$$\begin{aligned} P_{out}^{AT}(\gamma_{\min}) = & \sum_{m=0}^{\min(L, \lfloor \gamma_{\min}/\gamma_T \rfloor)} \binom{L}{m} e^{-\frac{\gamma_T m}{\overline{\gamma}}} (1 - e^{-\frac{\gamma_T m}{\overline{\gamma}}})^{L-m} \\ & \times \left\{ 1 - e^{-\frac{\gamma_{\min} - m\gamma_T}{\overline{\gamma}}} \sum_{j=0}^{m-1} \frac{1}{(m-1-j)!} \left(\frac{\gamma_{\min} - m\gamma_T}{\overline{\gamma}} \right)^{m-j-1} \right\} \end{aligned} \tag{4.10}$$

NT-GSC

Similarly, the outage probability of NT-GSC over i.i.d. Rayleigh channels is given as

$$P_{out}^{NT}(\gamma_{\min}) = \sum_{l=1}^{L} \Pr[Lc = l] P_{out}^{GSC}(Lc = l) \tag{4.11}$$

where $P_{out}^{GSC}(Lc = l)$ is the outage probability for GSC and is known for i.i.d. Rayleigh [41, eq. (42)], non-i.i.d. Rayleigh [62], and i.i.d. Nakagami-m

channels [47].

4.4 Output-Threshold MRC (OT-MRC)

The OT-MRC starts with an arbitrary single branch for the signal detection and increase the number of branches for the combining only if the combined signal SNR is below a certain pre-determined threshold. Since the OT-MRC aims at reducing the complexity by combining the minimum number of branches while satisfying the pre-determined threshold over fading channel, the number of combining branches becomes a random variable which depends highly on the average SNR per branch.

The OT-MRC scheme over i.i.d. fading channel is somewhat easily understandable and its performance might be expected since the average SNR at each diversity path is the same over all available branches. However, the results should be different for the case of non-i.i.d. fading channels. Since the average SNR for each branch is not the same, the performance will be more sensitive to the SNR of each branch. We can think of two different extreme examples to see the effect of non-i.i.d. fading channels on the complexity of the OT-MRC. At first, if it starts with the branch of the strongest SNR, the average combined SNR over non-i.i.d fading channel can be larger than the case over i.i.d. fading channel. Thus, a smaller number of branches will be used for combining when a certain output threshold is given. On the other hand, an excessive number of branches could be used for combining when it happens to start with a branch of the lowest SNR. To investigate the sensitivity of the combined SNR, the analysis of OT-MRC over non-i.i.d. fading channel is even more important.

4.4.1 Combining Strategy

As defined previously, let γ_l denotes the instantaneous SNR of the lth branch. We denote the OT-MRC with L available branches as OT-MRC$(L; \gamma_T)$ where

γ_T is the pre-determined output threshold, which may be set for the satisfactory communications.

The OT-MRC($L;\gamma_T$) starts with comparing the instantaneous SNR of the first branch[1], γ_1, against γ_T. If $\gamma_1 \geq \gamma_T$, then it stops, and only the first branch is used for the signal detection. In this case the combined output SNR, Γ, is equal to γ_1. If $\gamma_1 < \gamma_T$, then it compares the combined output SNR of the first and second branches against γ_T. If $\gamma_1 + \gamma_2 \geq \gamma_T$, then the first and second branch are combined, and the combined output SNR is $\Gamma = \gamma_1 + \gamma_2$. Otherwise, it keeps combining other branches until Γ becomes greater than γ_T. Whenever Γ surpasses γ_T, it stops checking the rest of the branches and employs MRC with the selected branches.

4.4.2 Statistics of the Combined SNR

In OT-MRC($L;\gamma_T$), the number of branches to be used for the combining, denoted by L_c, is a random variable (RV) depending on the channel statistics as well as γ_T. Since the probability of the combined SNR being less or greater than a certain value is a function of two random variables, instantaneous SNR of each branch and L_c, the joint CDF, $F(\gamma, L_c)$, and PDF, $f(\gamma, L_c)$, of Γ and L_c are derived, respectively, as follows. Based on the combining strategy of OT-MRC, we can write the joint CDF as [56, eq. (2)]

$$F(\gamma, L_c) = \begin{cases} \Pr[\gamma_T \leq \gamma_1 < \gamma], & \gamma_T \leq \gamma, 1 \leq L_c < 2, \\ \Pr[\sum_{k=1}^{L_c-1} \gamma_k < \gamma_T \ \& \ \gamma_T \leq \sum_{k=1}^{L_c} \gamma_k < \gamma], & \gamma_T \leq \gamma, 2 \leq L_c \leq L, \\ \Pr[\sum_{k=1}^{L} \gamma_k < \gamma], & \gamma_T > \gamma, L_c = L. \end{cases} \tag{4.12}$$

[1]There is no order in numbering the branch. We here mean that the ordering is arbitrary regardless of the signal strength.

It is easy to see from (4.12) that the probability of $\gamma_T \leq \gamma$ and $1 \leq L_c < 2$ is the same as that of the receiver with no diversity, and the probability for $\gamma_T > \gamma$ and $L_c = L$ follows that of the conventional MRC with L branches. The probability of $\gamma_T \leq \gamma$ and $2 \leq L_c \leq L$ can be easily written as the following integration form.

$$F^*(\gamma, L_c) = \int_0^{\gamma_T} \cdots \int_0^{\gamma_T - \sum_{k=1}^{L_c-2} \gamma_k} \int_{\gamma_T - \sum_{k=1}^{L_c-1} \gamma_k}^{\gamma - \sum_{k=1}^{L_c-1} \gamma_k} f_{\gamma_1, \cdots, \gamma_{L_c}}(\gamma_1, \cdots, \gamma_{L_c}) d\gamma_{L_c} \cdots d\gamma_1. \tag{4.13}$$

where $\gamma_T \leq \gamma$. Note that due to the assumption of independent fading channels, the joint PDF of $\{\gamma_l\}_{l=1}^{L_c}$ can be simply written as

$$f_{\gamma_1, \cdots, \gamma_{L_c}}(\gamma_1, \cdots, \gamma_{L_c}) = \prod_{l=1}^{L_c} f_{\gamma_l}(\gamma_l), \tag{4.14}$$

where $f_{\gamma_l}(\gamma_l)$ corresponds to the PDF of the SNR for the lth branch. If the channel statistics is known and the PDF of the combined SNR over the channel can be derived, then we can simplify (4.12) using (4.13) and (4.14) as

$$F(\gamma, L_c) = \begin{cases} \int_{\gamma_T}^{\gamma} f_1(\tau) d\tau, & \gamma_T \leq \gamma, 1 \leq L_c < 2, \\ \int_0^{\gamma_T} f_{L_c-1}(\tau) \int_{\gamma_T - \tau}^{\gamma - \tau} f_1(\eta) d\eta d\tau, & \gamma_T \leq \gamma, 2 \leq L_c \leq L, \\ \int_0^{\gamma} f_L(\tau) d\tau, & \gamma_T > \gamma, L_c = L, \end{cases} \tag{4.15}$$

where $f_{l_c}(\gamma)$ is the PDF of the combined SNR for the MRC receiver with l_c diversity branches. By differentiating (4.15) with respect to γ^2, we have the

[2]In fact, the joint PDF of Γ and L_c can be obtained by differentiating the CDF with respect to both γ and L_c. However, since L_c takes the discrete value, the resulting joint PDF is simply the one differentiated with respect to γ with a delta function, $\delta(L_c)$. Without loss of generality we here remove the delta function.

joint PDF of Γ and L_c as

$$f(\gamma, L_c) = \begin{cases} f_1(\gamma), & \gamma_T \leq \gamma, L_c = 1, \\ \displaystyle\int_0^{\gamma_T} f_{L_c-1}(\tau) f_1(\gamma - \tau) d\tau, & \gamma_T \leq \gamma, L_c = 2, \cdots, L, \\ f_L(\gamma), & \gamma_T > \gamma, L_c = L, \end{cases} \tag{4.16}$$

which agrees with [56, eq. (5)].

The MGF is very useful in that the average error performance can be easily evaluated based on it [2]. We can write the MGF of the combined output SNR using (4.16) as

$$\begin{aligned} \mathcal{M}(s) &= \int_0^{\infty} e^{s\gamma} \sum_{L_c=1}^{L} f(\gamma, L_c)\ d\gamma \\ &= \int_0^{\gamma_T} e^{s\gamma} f_L(\gamma) d\gamma + \sum_{L_c=1}^{L} \int_{\gamma_T}^{\infty} e^{s\gamma} f(\gamma, L_c) d\gamma. \end{aligned} \tag{4.17}$$

4.4.3 i.i.d. Channel Case

Statistics

Substituting the PDF of the instantaneous SNR at each branch as well as the PDF of the combined output SNR of the MRC with $L-1$ diversity branches, all of which are shown in Chapter 2, into (4.16), the joint PDF of Γ and L_c for OT-MRC over various fading channels can be derived. For Nakagami-m channels, the joint PDF is given as [57, eq. (6)]

$$f(\gamma, L_c) = \begin{cases} e^{-\frac{m\gamma}{\overline{\gamma}}} \left(\dfrac{m}{\overline{\gamma}}\right)^{L_c m} \dfrac{\gamma^{L_c m - 1}}{\Gamma(L_c m)} I\left(\dfrac{\gamma_T}{\gamma}, (L_c - 1)m, m\right), & \gamma_T \leq \gamma, L_c = 1, \cdots, L, \\ e^{-\frac{m\gamma}{\overline{\gamma}}} \left(\dfrac{m}{\overline{\gamma}}\right)^{Lm} \dfrac{\gamma^{Lm-1}}{\Gamma(Lm)}, & \gamma_T > \gamma, L_c = L, \end{cases} \tag{4.18}$$

where $I(x, p, q)$ is the regularized beta function [63, eq. (8.392)]. As a special case, the joint PDF for Rayleigh fading channels can be derived with the fading parameter $m = 1$.

Substituting (4.18) into (4.17) and using the series representation of the incomplete beta function, we obtain the closed-form of MGF for Nakagami-m channels with integer m as

$$\begin{aligned}\mathcal{M}(s) = &\sum_{L_c=1}^{L} \left(\frac{\gamma_T m}{\overline{\gamma}}\right)^{L_c m} \sum_{i=0}^{m-1} \frac{e^{-\gamma_T(\frac{m}{\overline{\gamma}}-s)}}{(L_c m - m + i)!} \left[\gamma_T\left(\frac{m}{\overline{\gamma}} - s\right)\right]^{i-m} \\ &+ \left(\frac{m}{m - s\overline{\gamma}}\right)^{Lm} \left\{1 - e^{-\gamma_T(\frac{m}{\overline{\gamma}}-s)} \sum_{k=0}^{Lm-1} \frac{1}{k!}\left[\gamma_T\left(\frac{m}{\overline{\gamma}} - s\right)\right]^{k}\right\}.\end{aligned} \tag{4.19}$$

Performance Analysis

Average Number of Combined Branches

While the conventional MRC has the fixed complexity due to the fixed number of combined branches, the number of combining branches for OT-MRC is a RV. Thus, its statistical average is meaningful to look into the complexity of the OT-MRC. The average number of branches can be obtained by calculating

$$\overline{L_c} = \sum_{L_c=1}^{L} L_c \int_0^{\infty} f(\gamma, L_c) d\gamma \tag{4.20}$$

Given the joint PDF in (4.16), we have the following relationship

$$\int_0^{\infty} f(\gamma, L_c) d\gamma = \int_0^{\gamma_T} f_{L_c-1}(\gamma) d\gamma - \int_0^{\gamma_T} f_{L_c}(\gamma) d\gamma, \quad L_c = 2, \cdots, L-1. \tag{4.21}$$

Using (4.52), we can rewrite (4.51) as

$$\overline{L_c} = L - \sum_{L_c=1}^{L-1} F_{L_c}^{(c)}(\gamma_T) \tag{4.22}$$

where $F_n^{(c)}(x)$ is the complementary CDF of n-branch MRC evaluated at x. Substituting the complementary CDF of combined SNR into (4.53) gives the average number of branches of OT-MRC for Nakagami-m channels as

$$\overline{L_c} = L - \sum_{L_c=1}^{L-1} \frac{\Gamma(L_c m, \frac{\gamma_T m}{\overline{\gamma}})}{\Gamma(L_c m)}, \tag{4.23}$$

where $\Gamma(\alpha, x)$ is the incomplete gamma function [63, eq. (8.350)]. As special cases, we can show that $\overline{L_c} = 1$ when $\gamma_T \to 0$ and $\overline{L_c} = L$ when $\gamma_T \to \infty$, which are also understood by the mode of operation.

Outage Probability

The outage probability, P_{out}, is defined as the probability that the combined SNR is below an outage threshold, $\gamma_{\min}$.

$$P_{out} = \int_0^{\gamma_{\min}} \sum_{L_c=1}^{L} f(\gamma, L_c) d\gamma. \tag{4.24}$$

Switching the order of integration and summation, we obtain the outage probability as

$$P_{out} = \begin{cases} \dfrac{\Gamma(Lm) - \Gamma(Lm, \frac{\gamma_{\min} m}{\overline{\gamma}})}{\Gamma(Lm)}, & \gamma_{\min} < \gamma_T \\ 1 - \dfrac{\Gamma(m, \frac{\gamma_{\min} m}{\overline{\gamma}})}{\Gamma(m)} - \displaystyle\sum_{L_c=1}^{L-1} \sum_{i=0}^{m-1} \frac{(-1)^i}{i!(L_c m + i)} \left(\frac{\gamma_T m}{\overline{\gamma}}\right)^{L_c m + i} \frac{\Gamma(m-i, \frac{\gamma_{\min} m}{\overline{\gamma}})}{\Gamma(L_c m)\Gamma(m-i)}, & \gamma_{\min} \geq \gamma_T. \end{cases} \tag{4.25}$$

As shown in (4.25), the outage probability follows that of the conventional MRC when the normalized outage threshold $\gamma_{\min}/\overline{\gamma}$ is less than γ_T. On the other hand, the outage performance degrades dramatically when $\gamma_{\min}/\overline{\gamma}$ becomes bigger than γ_T, which can be understood by the mode of operation.

Average Error Rate

Using the MGF-based approach [64, eq. (20)] with the alternative Q function in [65], we can easily calculate the average symbol/bit error rate (SER/BER) over fading channels for various modulations. For example the average BER for BPSK modulation can be calculated as

$$P_b = \frac{1}{\pi}\int_0^{\frac{\pi}{2}} \mathcal{M}\left(-\frac{1}{\sin^2\theta}\right) d\theta \tag{4.26}$$

Substituting (4.19) into (4.98) and after some manipulation, we can derive the closed-form expression for the average BER of OT-MRC over i.i.d. Nakagami-m channels as

$$\begin{aligned} P_b = &\sum_{L_c=1}^{L}\sum_{i=0}^{m-1} \frac{1}{(L_c m - m + i)!}\left(\frac{\gamma_T m}{\overline{\gamma}}\right)^{L_c m - m + i} \mathcal{I}_1\left[m-i, \frac{\overline{\gamma}}{m}, \frac{\gamma_T m}{\overline{\gamma}}\right] \\ &+ \mathcal{J}\left[\frac{\overline{\gamma}}{m}, Lm\right] - \sum_{k=0}^{Lm-1}\frac{1}{k!}\left(\frac{\gamma_T m}{\overline{\gamma}}\right)^k \mathcal{I}_1\left[Lm-k, \frac{\overline{\gamma}}{m}, \frac{\gamma_T m}{\overline{\gamma}}\right] \end{aligned} \tag{4.27}$$

where $\mathcal{I}_1[k, a, b]$ is defined in (B.10),

$$\mathcal{J}[c, m] = \left(\frac{1-\mu}{2}\right)^m \sum_{k=0}^{m-1}\binom{m+k-1}{k}\left(\frac{1+\mu}{2}\right)^k, \tag{4.28}$$

and $\mu = \sqrt{\frac{c}{1+c}}$ [66, eq. (14.4-15)].

4.4.4 Non-i.i.d. Channel Case

Statistics

Using the PDF of the MRC combined output SNR shown in Chapter 3 and substituting them with the PDF of a single channel into (4.16), we obtain the

joint PDF for non-i.i.d. Rayleigh channels as

$$f(\gamma, L_c) = \begin{cases} \sum_{j=1}^{L_c} \prod_{\substack{k=1 \\ k\neq j}}^{L_c} \frac{\overline{\gamma}_j{}^{L_c-2}}{\overline{\gamma}_j - \overline{\gamma}_k} e^{-\frac{\gamma}{\overline{\gamma}_{L_c}} + \gamma_T\left(\frac{1}{\overline{\gamma}_{L_c}} - \frac{1}{\overline{\gamma}_j}\right)}, & \gamma_T \leq \gamma, L_c = 1, \cdots, L, \\ \sum_{j=1}^{L} \prod_{\substack{k=1 \\ k\neq j}}^{L} \frac{\overline{\gamma}_j{}^{L-2}}{\overline{\gamma}_j - \overline{\gamma}_k} e^{-\frac{\gamma}{\overline{\gamma}_j}}, & \gamma_T > \gamma, L_c = L, . \end{cases} \tag{4.29}$$

For i.i.d. Rayleigh fading case, that is, $\overline{\gamma}_1 = \overline{\gamma}_2 = \cdots = \overline{\gamma}_L = \overline{\gamma}$, (4.29) has a 0/0 form, which is indeterminate. Taking the limit and applying L'Hospital's rule, we can have

$$\lim_{\overline{\gamma}_1, \cdots, \overline{\gamma}_L \to \overline{\gamma}} f(\gamma, L_c) = \begin{cases} \frac{\gamma_T^{L_c-1}}{\Gamma(L_c)\overline{\gamma}^{L_c}} e^{-\frac{\gamma}{\overline{\gamma}}}, & \gamma_T \leq \gamma, L_c = 1, \cdots, L, \\ \frac{\gamma^{L-1}}{\Gamma(L)\overline{\gamma}^{L}} e^{-\frac{\gamma}{\overline{\gamma}}}, & \gamma_T > \gamma, L_c = L, \end{cases} \tag{4.30}$$

which reduces to (4.18) evaluated at $m = 1$.

Substituting (4.29) into (4.17) gives the MGF of output SNR over non-i.i.d. Rayleigh channel as

$$\begin{aligned} \mathcal{M}(s) = & \sum_{L_c=1}^{L} \sum_{j=1}^{L_c} \frac{\overline{\gamma}_{L_c}}{1 - s\overline{\gamma}_{L_c}} \prod_{\substack{k=1 \\ k\neq j}}^{L_c} \frac{\overline{\gamma}_j{}^{L_c-2}}{\overline{\gamma}_j - \overline{\gamma}_k} e^{-\gamma_T\left(\frac{1}{\overline{\gamma}_j} - s\right)} \\ & + \sum_{j=1}^{L} \frac{\overline{\gamma}_j}{1 - s\overline{\gamma}_j} \prod_{\substack{k=1 \\ k\neq j}}^{L} \frac{\overline{\gamma}_j{}^{L-2}}{\overline{\gamma}_j - \overline{\gamma}_k} \left(1 - e^{-\gamma_T\left(\frac{1}{\overline{\gamma}_j} - s\right)}\right). \end{aligned} \tag{4.31}$$

Performance analysis

Suppose the average SNR of lth branch follows an exponential multipath power delay profile (PDP) characterized by $\overline{\gamma}_l = \overline{\gamma}_1 \exp(-\beta(l-1))$, where β is a decay factor, $0 \leq \beta \leq 1$, and $l = 1, \cdots, L$. Since OT-MRC does not order diversity branches, the average performance depends on the average SNR of each

selected branch. Thus, average performance given a set of selected branches needs to be again averaged over all the possible selections to calculate overall average performance. Let S_i denote the ith selection, where $1 \leq i \leq L!$. For instance, $S_1 = \{\overline{\gamma}_1, \overline{\gamma}_2, \cdots, \overline{\gamma}_L\}$ and $S_{L!} = \{\overline{\gamma}_L, \overline{\gamma}_{L-1}, \cdots, \overline{\gamma}_1\}$. The average performance can be calculated by $\sum_{i=1}^{L!} \frac{A(S_i)}{L!}$ where $A(S_i)$ is a performance metric for S_i.

Average Number of Combined Branches

Substituting the complementary CDF of combined SNR for MRC over non-i.i.d. Rayleigh channels tabularized in Chapter 3 into (4.53), we can obtain the number of combined branches given S_1 as

$$\overline{L_c}(S_1) = L - \sum_{L_c=1}^{L-1} \sum_{j=1}^{L_c} \prod_{\substack{k=1 \\ k \neq j}}^{L_c} \frac{\overline{\gamma}_j{}^{L_c-1}}{\overline{\gamma}_j - \overline{\gamma}_k} e^{-\frac{\gamma_T}{\overline{\gamma}_j}} \tag{4.32}$$

With the use of L'Hospital's rule, we can easily see that, for i.i.d. case, (4.32) is equal to (4.23) evaluated $m = 1$, which is also given in [56, eq. (13)].

By averaging over all the possible branch selections, the average number of combined branches is given by

$$\overline{L_c} = L - \sum_{L_c=1}^{L-1} \sum_{j_1=1}^{L} \cdots \sum_{\substack{j_{L_c}=1 \\ j_{L_c} \neq j_1, \\ \cdots, \\ j_{L_c} \neq j_{L_c-1}}}^{L} \prod_{k=1}^{L_c-1} \frac{L_c \overline{\gamma}_{j_1}{}^{L_c-1} e^{-\frac{\gamma_T}{\overline{\gamma}_{j_1}}}}{(L - L_c + 1)_{L_c} (\overline{\gamma}_{j_1} - \overline{\gamma}_{j_{k+1}})} \tag{4.33}$$

Outage probability

The outage probability over non-i.i.d. Rayleigh channels can be obtained by substituting (4.29) into (4.24) and taking average over all the branch selections

is given as

$$P_{\text{out}} = \begin{cases} \displaystyle\sum_{j=1}^{L} \prod_{\substack{k=1 \\ k\neq j}}^{L} \frac{\overline{\gamma}_j{}^{L-1}}{\overline{\gamma}_j - \overline{\gamma}_k} \left(1 - e^{-\frac{\gamma_{\min}}{\overline{\gamma}_j}}\right), & \gamma_{\min} < \gamma_T \\ \displaystyle 1 - \sum_{L_c=1}^{L-1} \sum_{j_1=1}^{L} \cdots \sum_{\substack{j_{L_c}=1 \\ j_{L_c}\neq j_1, \\ \cdots, \\ j_{L_c}\neq j_{L_c-1}}}^{L} \prod_{k=1}^{L_c-1} \frac{L_c \overline{\gamma}_{L_c} \overline{\gamma}_{j_1}{}^{L_c-1} e^{-(\frac{\gamma_T}{\overline{\gamma}_{j_1}} + \frac{\gamma_{\min}-\gamma_T}{\overline{\gamma}_{L_c}})}}{(L-L_c+1)_{L_c}(\overline{\gamma}_{j_1} - \overline{\gamma}_{j_{k+1}})}, & \gamma_{\min} \geq \gamma_T \end{cases} \tag{4.34}$$

Average Error Rate

With substitution (4.31) into (4.98) and averaging over all possible selections, the average BER for BPSK modulation can be written as

$$\begin{aligned} P_b = & \sum_{j=1}^{L} \prod_{\substack{k=1 \\ k\neq j}}^{L} \frac{\overline{\gamma}_j{}^{L-1}}{\overline{\gamma}_j - \overline{\gamma}_k} \left\{ \frac{1}{2}\left(1 - \sqrt{\frac{\overline{\gamma}_j}{1+\overline{\gamma}_j}}\right) - \mathcal{I}_1\left[1, \overline{\gamma}_j, \frac{\gamma_T}{\overline{\gamma}_j}\right] \right\} \\ & + \sum_{L_c=1}^{L-1} \sum_{j_1=1}^{L} \cdots \sum_{\substack{j_{L_c}=1 \\ j_{L_c}\neq j_1, \\ \cdots, \\ j_{L_c}\neq j_{L_c-1}}}^{L} \prod_{k=1}^{L_c-1} \frac{L_c \overline{\gamma}_{L_c} \overline{\gamma}_{j_1}{}^{L_c-2} \, \mathcal{I}_2[1, \overline{\gamma}_j, \frac{\gamma_T}{\overline{\gamma}_j}, \overline{\gamma}_{L_c}]}{(L-L_c+1)_{L_c}(\overline{\gamma}_{j_1} - \overline{\gamma}_{j_{k+1}})}, \end{aligned} \tag{4.35}$$

where $\mathcal{I}_1[k, a, b]$ and $\mathcal{I}_2[k, a, b, c]$ are defined in (B.10) and (B.14), respectively.

4.5 Minimum Selection GSC (MS-GSC)

The two conditional GSC with individual threshold schemes, AT-GSC and NT-GSC, outperforms the GSC systems in the sense that branches with low SNR are circumvented and branches with high SNR are selected to be combined. However, they are not optimized in terms of power consumption since there are cases that the number of selected branches is overused. To cope with this drawback the minimum selection GSC (MS-GSC) scheme was pro-

posed in [52], where the target SNR to meet a certain QoS expressed in BER is predetermined, and the number of selected branches changes adaptively to meet this target SNR so that the number of selection for the combining is minimized. With the knowledge of the target SNR for the desired QoS, the MS-GSC scheme minimizes the complexity while satisfying the desired performance by switching the combined SNR surplus into the reduction of the number of branches for the combining. By minimizing the number of selected branches under the constraint on the target SNR the power consumption can be minimized accordingly. Numerical results show that the MS-GSC scheme can take advantage of selecting the minimum number of diversity branches over a wide range of the average SNR per branch.

In [54] and [53], the analysis of MS-GSC scheme was presented over i.i.d. Rayleigh fading channels by providing the MGF of the combined SNR and the distribution function of the number of selected branches in closed-forms. [55] extended the analysis by considering non-i.i.d. Rayleigh fading channels. In this Chapter we introduce a different approach to pursue the detailed analysis of MS-GSC over i.i.d. and non-i.i.d. Rayleigh fading channels. The approach herein is more general compared to [53] and [55], since the analytical expressions can also be applied to the analysis for correlated channel models.

4.5.1 Combining Strategy

As defined previously, let γ_l denotes the instantaneous SNR of the lth branch. We denote the MS-GSC with L available branches as MS-GSC$(L;\gamma_T)$ where γ_T is the pre-determined output threshold, which may be set for the satisfactory communications. Let $\gamma_{(1)} \geq \gamma_{(2)} \geq \cdots \geq \gamma_{(L)} \geq 0$ be the ordered statistics obtained by sorting out $\{\gamma_k\}_{k=1}^{L}$ in descending order of magnitude.

Let Γ denote the coherently combined SNR of L_c strongest branches, i.e., $\gamma = \sum_{i=1}^{L_c} \gamma_{(i)}$, when L_c branches are selected by the combiner. The operation of MS-GSC combiner is as follows. First, $\{\gamma_{(k)}\}_{k=1}^{L}$ are sorted out in descending order of magnitude. At the second stage, the largest SNR $\gamma_{(1)}$

is first compared with γ_T. If $\gamma_{(1)} \geq \gamma_T$, then $L_c = 1$ and only the branch with the largest SNR is used for the combining ($\Gamma = \gamma_{(1)}$), which is exactly the same as SC with L branches. However, if $\gamma_{(1)} < \gamma_T$, then the combiner increase L_c by 1 ($L_c = 2$) and check if $\gamma_{(1)} + \gamma_{(2)} \geq \gamma_T$. If so, it stops with $\Gamma = \gamma_{(1)} + \gamma_{(2)}$, otherwise increase L_c by 1 again ($L_c = 3$). This procedure goes on until either L_c on the condition $\sum_{i=1}^{L_c} \gamma_{(i)} \geq \gamma_T > \sum_{i=1}^{L_c-1} \gamma_{(i)}$ is found or $\sum_{i=1}^{L} \gamma_{(i)} < \gamma_T$ is met. If $\sum_{i=1}^{L} \gamma_{(i)} < \gamma_T$, signals from all available branches should be combined in a fashion of MRC to get the performance as close to γ_T as possible, which is exactly the same as the case of conventional MRC with L branches. When $\sum_{i=1}^{k} \gamma_{(i)} \geq \gamma_T > \sum_{i=1}^{k-1} \gamma_{(i)}$, the minimum number of branches for the combining on the condition that the combined SNR is larger than γ_T is L_c.

4.5.2 Statistics of the Combined SNR

In MS-GSC($L; \gamma_T$), the number of branches to be used for the combining, denoted by L_c, is a random variable (RV) depending on the channel statistics as well as γ_T. We now want to find the statistics for MS-GSC($L; \gamma_T$). Since the probability of the combined SNR being less or greater than a certain value is a function of two random variables, instantaneous SNR of each branch and the number of selected branches, the joint CDF of Γ and L_c, denoted by $F(\gamma, L_c)$, is derived as follows.

$$F(\gamma, L_c) = \begin{cases} \Pr[\gamma_T \leq \gamma_{(1)} < \gamma], & \gamma_T \leq \gamma, 1 \leq L_c < 2 \\ \Pr[\sum_{k=1}^{L_c-1} \gamma_{(k)} < \gamma_T \ \& \ \gamma_T \leq \sum_{k=1}^{L_c} \gamma_{(k)} < \gamma], & \gamma_T \leq \gamma, 2 \leq L_c \leq L, \\ \Pr[\sum_{k=1}^{L} \gamma_{(k)} < \gamma], & \gamma_T > \gamma, L_c = L. \end{cases} \tag{4.36}$$

As described in the mode of operation, the probability for $\gamma_T \leq \gamma$ and $1 \leq L_c < 2$ is the same as that of SC, and the probability for $\gamma_T > \gamma$ and $L_c = L$ follows that of MRC with L branches. On the other hand, $\Pr[\sum_{k=1}^{L_c-1} \gamma_{(k)} <$

γ_T & $\gamma_T \leq \sum_{k=1}^{L_c} \gamma_{(k)} < \gamma]$, denoted by $F^*(\gamma, L_c)$, can be rewritten as the following expression.

$$
\begin{aligned}
F^*(\gamma, L_c) = & P[\sum_{k=1}^{L_c} \gamma_{(k)} \leq \gamma] - P[\sum_{k=1}^{L_c} \gamma_{(k)} \leq \gamma_T] \\
& - \Bigg\{ P[\gamma_T \leq \sum_{k=1}^{L_c} \gamma_{(k)} \leq \gamma, \sum_{k=1}^{L_c-1} \gamma_{(k)} > \gamma_T, \gamma_{(1)} < \gamma_T, \frac{\gamma_T}{L_c - 1} \leq \gamma_{(L_c-1)} \leq \frac{\gamma}{L_c - 1}] \\
& + P[\gamma_T \leq \sum_{k=1}^{L_c} \gamma_{(k)} \leq \gamma, \sum_{k=1}^{L_c-1} \gamma_{(k)} > \gamma_T, \gamma_{(1)} < \gamma_T, 0 \leq \gamma_{(L_c-1)} \leq \frac{\gamma_T}{L_c - 1}] \\
& - P[\gamma_T \leq \sum_{k=1}^{L_c} \gamma_{(k)} \leq \gamma, \sum_{k=1}^{L_c-1} \gamma_{(k)} > \gamma_T, 0 \leq \gamma_{(L_c-1)} \leq \gamma_{(L_c)}] \Bigg\},
\end{aligned}
\tag{4.37}
$$

which can be represented with an integration form using $f_{\gamma_{(1)},\cdots,\gamma_{(L_c)}}(\gamma_{(1)}, \cdots, \gamma_{(L_c)})$, the joint PDF of the $\{\gamma_{(k)}\}_{k=1}^{L_c}$. By differentiating the joint CDF with respect to γ[3], we obtain the joint PDF of Γ and L_c, $f(\gamma, L_c)$, as

$$
f(\gamma, L_c) = \begin{cases} f_{SC}(\gamma), & \gamma_T \leq \gamma < \infty, \ L_c = 1, \\ f^*(\gamma, L_c), & \gamma_T \leq \gamma < \frac{L_c}{L_c - 1}\gamma_T, \ L_c = 2, \cdots, L, \\ f_{MRC}(\gamma), & 0 \leq \gamma < \gamma_T, \ L_c = L, \end{cases} \tag{4.38}
$$

where $f_{SC}(\gamma)$ and $f_{MRC}(\gamma)$ are the PDF of SC and MRC with L branches, respectively. $f^*(\gamma, L_c)$ is derived, by differentiating the joint CDF with respect

[3]In fact, the joint PDF of Γ and L_c can be obtained by differentiating the joint CDF with respect to both γ and L_c. However, since L_c takes the discrete value, the resulting joint PDF is simply the one differentiated with respect to γ with a delta function, $\delta(L_c)$. Without loss of generality we herein remove the delta function.

to γ and applying the Leibnitz rule [67, p. 121], as

$$f^*(\gamma, L_c) = \int_0^{\frac{\gamma}{L_c}} \int_{\gamma_{(L_c)}}^{\frac{\gamma-\gamma_{(L_c)}}{L_c-1}} \cdots \int_{\gamma_{(3)}}^{\frac{\gamma-\sum_{i=3}^{L_c}\gamma_{(i)}}{2}} f_{\gamma_{(1)},\cdots,\gamma_{(L_c)}}(\gamma_{\Sigma_2^{L_c}}, \gamma_{(2)}, \cdots, \gamma_{(L_c)}) d\gamma_{(2)} \cdots d\gamma_{(L_c)}$$
$$- \Bigg(\int_{\frac{\gamma_T}{L_c-1}}^{\frac{\gamma}{L_c-1}} \int_{\gamma_{(L_c-1)}}^{\frac{\gamma-\gamma_{(L_c-1)}}{L_c-2}} \cdots \int_{\gamma_{(2)}}^{\gamma-\sum_{i=2}^{L_c-1}\gamma_{(i)}} f_{\gamma_{(1)},\cdots,\gamma_{(L_c)}}(\gamma_{(1)}, \cdots, \gamma_{(L_c-1)}, \gamma_{\Sigma_1^{L_c-1}}) d\gamma_{(1)} \cdots d\gamma_{(L_c-1)}$$
$$+ \sum_{i=2}^{L_c-1} \left\{ f_i^+(\gamma, L_c) - f_i^-(\gamma, L_c) \right\} \Bigg), \tag{4.39}$$

where

$$f_i^+(\gamma, L_c) = \int_0^{\frac{\gamma_T}{L_c-1}} \int_{\gamma_{(L_c-1)}}^{\frac{\gamma_T-\gamma_{(L_c-1)}}{L_c-2}} \cdots \int_{\gamma_{(L_c-i+2)}}^{\frac{\gamma_T-\sum_{k=L_c-i+2}^{L_c-1}\gamma_{(k)}}{L_c-i+1}} \underbrace{\int_{\frac{\gamma_T-\sum_{k=L_c-i+1}^{L_c-1}\gamma_{(k)}}{L_c-i}}^{\frac{\gamma-\sum_{k=L_c-i+1}^{L_c-1}\gamma_{(k)}}{L_c-i}}}_{i\text{th integral}} \int_{\gamma_{(L_c-i)}}^{\frac{\gamma-\sum_{k=L_c-i+1}^{L_c-1}\gamma_{(k)}}{L_c-i-1}}$$
$$\cdots \int_{\gamma_{(2)}}^{\gamma-\sum_{k=2}^{L_c-1}\gamma_{(k)}} f_{\gamma_{(1)},\cdots,\gamma_{(L_c)}}(\gamma_{(1)}, \cdots, \gamma_{(L_c-1)}, \gamma_{\Sigma_1^{L_c-1}}) d\gamma_{(1)} \cdots d\gamma_{(L_c-1)}, \tag{4.40}$$

$$f_i^-(\gamma, L_c) =$$
$$\int_0^{\gamma-\gamma_T} \int_{\gamma_{(L_c-1)}}^{\frac{\gamma_T-\gamma_{(L_c-1)}}{L_c-2}} \cdots \int_{\gamma_{(L_c-i+2)}}^{\frac{\gamma_T-\sum_{k=L_c-i+2}^{L_c-1}\gamma_{(k)}}{L_c-i+1}} \underbrace{\int_{\frac{\gamma_T-\sum_{k=L_c-i+1}^{L_c-1}\gamma_{(k)}}{L_c-i}}^{\frac{\gamma-\gamma_{(L_c-1)}-\sum_{k=L_c-i+1}^{L_c-1}\gamma_{(k)}}{L_c-i}}}_{i\text{th integral}} \int_{\gamma_{(L_c-i)}}^{\frac{\gamma-\gamma_{(L_c-1)}-\sum_{k=L_c-i+1}^{L_c-1}\gamma_{(k)}}{L_c-i-1}}$$
$$\cdots \int_{\gamma_{(2)}}^{\gamma-\gamma_{(L_c-1)}-\sum_{k=2}^{L_c-1}\gamma_{(k)}} f_{\gamma_{(1)},\cdots,\gamma_{(L_c)}}(\gamma_{(1)}, \cdots, \gamma_{(L_c-1)}, \gamma_{\Sigma_1^{L_c-1}}) d\gamma_{(1)} \cdots d\gamma_{(L_c-1)}, \tag{4.41}$$

$$\gamma_{\Sigma_2^{L_c}} = \gamma - \sum_{i=2}^{L_c} \gamma_{(i)}, \quad \text{and} \quad \gamma_{\Sigma_1^{L_c-1}} = \gamma - \sum_{i=1}^{L_c-1} \gamma_{(i)}.$$

(4.38) is a general expression that can be used with any joint PDF of ordered branch SNRs $f_{\gamma_{(1)},\cdots,\gamma_{(L)}}(\gamma_{(1)},\cdots,\gamma_{(L)})$. Notice that $f^*(\gamma, L_c)$ is only defined in the region of $\gamma_T \leq \gamma < \frac{L_c}{L_c-1}\gamma_T$ for $L_c = 2,\cdots,L$ and is zero otherwise.

4.5.3 i.i.d. Channel Case

Joint PDF

When $\{\gamma_k\}_{k=1}^{L}$ are i.i.d., the joint PDF of the $\{\gamma_{(k)}\}_{k=1}^{L_c}$ is expressed as [67, p. 246]

$$f_{\gamma_{(1)},\cdots,\gamma_{(L_c)}}(\gamma_{(1)},\cdots,\gamma_{(L_c)}) = L_c!\binom{L}{L_c}[F_\gamma(\gamma_{(L_c)})]^{L-L_c}\prod_{k=1}^{L_c} f_\gamma(\gamma_{(k)}), \qquad (4.42)$$

where $f_\gamma(\gamma)$ and $F_\gamma(\gamma)$ correspond to the PDF and the CDF of the instantaneous SNR at each branch, respectively. For i.i.d. Rayleigh fading channel, the joint PDF of the $\{\gamma_{(k)}\}_{k=1}^{L_c}$ is given as

$$f_{\gamma_{(1)},\cdots,\gamma_{(L_c)}}(\gamma_{(1)},\cdots,\gamma_{(L_c)}) = L_c!\binom{L}{L_c}\left[1-\exp\left(-\frac{\gamma}{\overline{\gamma}_{L_c}}\right)\right]^{L-L_c}\prod_{k=1}^{L_c}\frac{1}{\overline{\gamma}_k}\exp\left(-\frac{\gamma}{\overline{\gamma}_k}\right). \qquad (4.43)$$

where $\bar{\gamma}_k$ is the average SNR at the kth branch, i.e., $\bar{\gamma}_k = E[\gamma_k]$. Substituting (4.43) into (4.39) and after some mathematical manipulations, the joint PDF of MS-GSC over i.i.d. Rayleigh fading channel for $\gamma_T \leq \gamma < \frac{L_c\gamma_T}{L_c-1}$ and $L_c = 2,\cdots,L$, is given as

$$f^*(\gamma, L_c) = \binom{L}{L_c}e^{-\frac{\gamma}{\overline{\gamma}}}\left[\frac{(L_c\gamma_T-(L_c-1)\gamma)^{L_c-1}}{(L_c-1)!\overline{\gamma}^{L_c}} + \sum_{n=1}^{L-L_c}\binom{L-L_c}{n}(-1)^{n+L_c-1}\frac{1}{\overline{\gamma}}\left(\frac{L_c}{n}\right)^{L_c-1}\right.$$
$$\left.\times\left\{e^{-\frac{\gamma}{L_c\overline{\gamma}}n} - e^{-\frac{\gamma-\gamma_T}{\overline{\gamma}}n}\sum_{k=0}^{L_c-2}\frac{1}{k!}\left(\frac{-(L_c\gamma_T-(L_c-1)\gamma)n}{L_c\overline{\gamma}}\right)^k\right\}\right] \qquad (4.44)$$

It is not surprising that (4.44) has a similar form with the PDF for the conventional GSC given in [41, eq. (16)], since MS-GSC is a variant of GSC. Notice that (4.44) reduces to the PDF of the combined SNR at the SC output given in [41, eq. (17)] when γ_T goes down to zero, since the combiner will only take the branch with highest SNR regardless of its value.

$$\lim_{\gamma_T \to 0} f(\gamma, L_c) = \frac{L}{\overline{\gamma}} \sum_{n=0}^{L-1} \binom{L-1}{n} (-1)^n e^{-\frac{\gamma}{\overline{\gamma}}(1+n)}, 0 \leq \gamma \leq \infty. \tag{4.45}$$

On the other hand, (4.44) becomes the PDF of the combined SNR at the MRC output given in [41, eq. (18)] when γ_T approaches infinity, because the combined SNR will never reach γ_T.

$$\lim_{\gamma_T \to \infty} f(\gamma, L_c) = \frac{\gamma^{L-1} e^{-\frac{\gamma}{\overline{\gamma}}}}{(L-1)! \overline{\gamma}^L}, 0 \leq \gamma \leq \infty. \tag{4.46}$$

Substituting (4.44) into (4.38) and using the well-known PDF of SC and MRC, the joint PDF of the combined SNR and the number of selected branches for MS-GSC over i.i.d. Rayleigh fading channel is derived as

$$f(\gamma, L_c) = \begin{cases} \dfrac{L}{\overline{\gamma}} \displaystyle\sum_{n=0}^{L-1} \binom{L-1}{n} (-1)^n e^{-\frac{\gamma}{\overline{\gamma}}(1+n)}, & \gamma_T \leq \gamma < \infty, L_c = 1, \\ f^*(\gamma, L_c), & \gamma_T \leq \gamma < \frac{L_c \gamma_T}{L_c - 1}, L_c = 2, \cdots, L, \\ e^{-\frac{\gamma}{\overline{\gamma}}} \dfrac{\gamma^{L-1}}{(L-1)! \overline{\gamma}^L}, & 0 \leq \gamma < \gamma_T, L_c = L. \end{cases} \tag{4.47}$$

where $f^*(\gamma, L_c)$ is defined in (4.44). For a better understanding, the joint PDFs for $L = 10$ and $\gamma_T = 6.8, 10$, and 11.7 dB are illustrated in Fig. 4.1(a), 4.1(b), and 4.1(c), respectively.

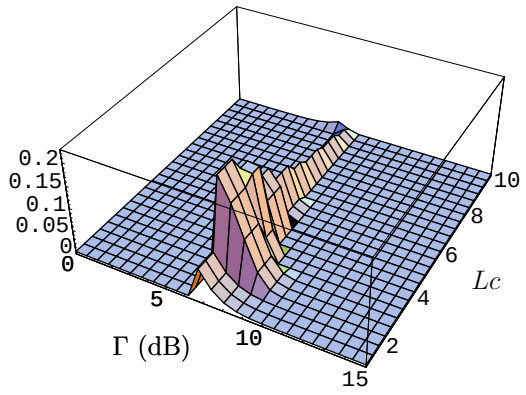

(a)

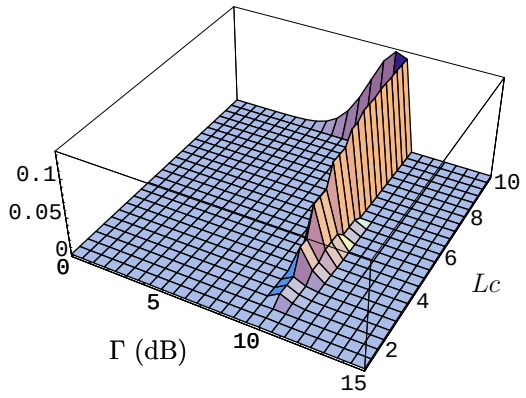

(b)

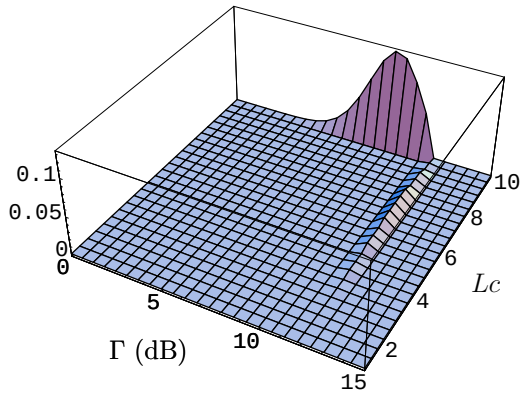

(c)

Figure 4.1: Probability density function of MS-GSC (a) $f(\gamma, L_c)$ for L=10, γ_T=6.8dB, (b) $f(\gamma, L_c)$, for L=10, γ_T=10dB, and (c) $f(\gamma, L_c)$, for L=10, γ_T=11.7dB

$$\mathcal{M}(s) = \sum_{k=0}^{L-1} \binom{L-1}{k} \frac{L(-1)^k}{1+k-\overline{\gamma}s} e^{-(\frac{k+1}{\overline{\gamma}}-s)\gamma_T} + \frac{(1-s\overline{\gamma})^{-L}}{(L-1)!}\gamma[L, \frac{\gamma_T}{\overline{\gamma}}(1-s\overline{\gamma})]$$
$$+ \sum_{l=2}^{L} \binom{L}{l} \Bigg\{ e^{-\frac{\gamma_T l(1-\overline{\gamma}s)}{\overline{\gamma}(l-1)}} \frac{(l-1)^{l-1}}{(l-1)!(\overline{\gamma}s-1)^l}\gamma[l, \frac{\gamma_T(1-\overline{\gamma}s)}{\overline{\gamma}(1-l)}]$$
$$+ \sum_{n=1}^{L-l} \binom{L-l}{n} (-1)^{n+l-1} \frac{l}{(l+n-l\overline{\gamma}s)(l-2)!} \Bigg\{ \left(\frac{l}{n}\right)^{l-1} e^{-\gamma_T\left(\frac{l+n}{l\overline{\gamma}}-s\right)}\gamma[l-1, -\frac{n\gamma_T}{l\overline{\gamma}}]$$
$$- \left(\frac{l-1}{n+1-\overline{\gamma}s}\right)^{l-1} e^{-\frac{l\gamma_T}{l-1}\left(\frac{l+n}{l\overline{\gamma}}-s\right)}\gamma[l-1, \frac{(n+1-\overline{\gamma}s)\gamma_T}{(1-l)\overline{\gamma}}] \Bigg\} \Bigg\} \tag{4.49}$$

MGF

The MGF of MS-GSC can be derived as

$$\mathcal{M}(s) = \int_{\gamma_T}^{\infty} e^{s\gamma} f_{SC}(\gamma)d\gamma + \sum_{L_c=2}^{L} \int_{\gamma_T}^{\frac{L_c\gamma_T}{L_c-1}} e^{s\gamma} f^*(\gamma, L_c)d\gamma + \int_0^{\gamma_T} e^{s\gamma} f_{MRC}(\gamma)d\gamma. \tag{4.48}$$

Substituting (4.47) into (4.48), the MGF is derived as (4.49) on top of the page, where $\gamma[m, x]$ is the incomplete gamma function [63, eq. (8.350.2)] defined as

$$\gamma[m, x] = \int_0^x y^{m-1}e^{-y}dy = (m-1)!\left(1 - e^{-x}\sum_{n=0}^{m-1}\frac{x^n}{n!}\right). \tag{4.50}$$

Performance Analysis

Average Number of Combined Branches

As mentioned previously, the minimum number of the strongest branches is taken while satisfying the target SNR, γ_T, the number of selected branches becomes a random variable that varies from 1 to L depending on channel statistics. Thus, it is important to find the average number of combined branches

to look into the complexity of MS-GSC. The average number of branches can be obtained by calculating

$$\overline{L_c} = \sum_{L_c=1}^{L} L_c \int_0^{\infty} f(\gamma, L_c) d\gamma \tag{4.51}$$

where $f(\gamma, L_c)$ is in (4.47). Using the following relationship

$$\int_0^{\infty} f(\gamma, L_c) d\gamma = \int_0^{\gamma_T} f_{(L_c-1)}(\gamma) d\gamma - \int_0^{\gamma_T} f_{(L_c)}(\gamma) d\gamma, \quad L_c = 2, \cdots, L-1, \tag{4.52}$$

we can rewrite (4.51) as

$$\overline{L_c} = 1 + \sum_{L_c=1}^{L-1} F_{(L_c)}(\gamma_T) \tag{4.53}$$

where $F_{(n)}(x)$ and $f_{(n)}(x)$ are the CDF and PDF of GSC, which are available in closed-form in [41]. Alternatively, the average number of branches can be calculated as

$$\overline{L_c} = \int_{\gamma_T}^{\infty} f_{SC}(\gamma) d\gamma + \sum_{L_c=2}^{L} L_c \int_{\gamma_T}^{\frac{L_c \gamma_T}{L_c-1}} f^*(\gamma, L_c) d\gamma + L \int_0^{\gamma_T} f_{MRC}(\gamma) d\gamma. \tag{4.54}$$

Substituting (4.47) into (4.54), the average number of selected branches is shown in (4.55) on top of next page.

Average error rate

Using the MGF approach, the average BER of MS-GSC for BPSK is given by

$$P_b = \sum_{n=0}^{L-1} \binom{L-1}{n} \frac{L(-1)^n}{n+1} \mathcal{I}_1\left(\frac{\overline{\gamma} g}{n+1}, \gamma_T \frac{n+1}{\overline{\gamma}}\right) + \mathcal{J}\left[\overline{\gamma} g, L\right] - \mathcal{J}_1\left[L, \overline{\gamma} g, \frac{\gamma_T}{\overline{\gamma}}\right] + P_b^* \tag{4.56}$$

$$\overline{L_c} = \sum_{n=0}^{L-1} \binom{L-1}{n} \frac{L(-1)^n}{1+n} e^{-\frac{\gamma_T}{\overline{\gamma}}(1+n)} + \frac{L}{(L-1)!}\gamma[L, \frac{\gamma_T}{\overline{\gamma}}]$$
$$+ \sum_{L_c=2}^{L} L_c \binom{L}{L_c} \Bigg\{ \frac{(L_c-1)^{L_c-1}}{(L_c-1)!} e^{-\frac{L_c\gamma_T}{\overline{\gamma}(L_c-1)}} (-1)^{L_c} \gamma[L_c, \frac{\gamma_T}{\overline{\gamma}(1-L_c)}]$$
$$+ \sum_{n=1}^{L-L_c} \binom{L-L_c}{n} (-1)^{n+L_c-1} \frac{L_c}{(n+L_c)(L_c-2)!} \Bigg\{ \left(\frac{L_c}{n}\right)^{L_c-1} e^{-(\frac{n+L_c}{L_c\overline{\gamma}})\gamma_T} \gamma[L_c-1, -\frac{\gamma_T n}{\overline{\gamma} L_c}]$$
$$- \left(\frac{L_c-1}{n+1}\right)^{L_c-1} e^{-(\frac{n+L_c}{(L_c-1)\overline{\gamma}})\gamma_T} \gamma[L_c-1, \frac{\gamma_T(n+1)}{\overline{\gamma}(1-L_c)}] \Bigg\} \Bigg\}. \tag{4.55}$$

---

where

$$P_b^* = \sum_{L_c=2}^{L} \frac{1}{\pi} \int_0^{\frac{\pi}{2}} \int_{\gamma_T}^{\frac{L_c\gamma_T}{L_c-1}} \exp\Big[-\frac{g\gamma}{\sin^2\theta} \Big] f^*(\gamma, L_c) d\gamma d\theta \tag{4.57}$$

which is derived as (4.58) on top of next page using (4.44), where $\mathcal{J}_1[k, a, b]$ is in (B.7) and $\mathcal{I}_2[k, a, b, c]$ is defined in (B.14).

Outage probability

Let γ_{min} denote the outage threshold against which the combined SNR is compared. The outage probability P_{out} is defined as the probability that the combined SNR falls below a given outage threshold γ_{min}, which is given as

$$P_{out} = \Pr[\Gamma < \gamma_{min}] = \sum_{L_c=1}^{L} \int_0^{\gamma_{min}} f(\gamma, L_c)\ d\gamma. \tag{4.59}$$

$$P_b^* = \sum_{L_c=2}^{L} \binom{L}{L_c} \Bigg\{ (1-L_c)^{L_c-1} \Bigg(\sum_{i=0}^{L_c-1} \frac{1}{i!} \Bigg(\frac{\gamma_T}{\overline{\gamma}(1-L_c)} \Bigg)^i \mathcal{I}_1 \Bigg[L_c - i, \overline{\gamma} g, \frac{\gamma_T}{\overline{\gamma}} \Bigg] - \mathcal{I}_1 \Bigg[L_c, \overline{\gamma} g, \frac{\gamma_T L_c}{\overline{\gamma}(L_c-1)} \Bigg] \Bigg) + \sum_{n=1}^{L-L_c} \binom{L-L_c}{n} (-1)^n \left(-\frac{L_c}{n} \right)^{L_c-1} \Bigg\{ \frac{L_c}{L_c+n} \Bigg(\mathcal{I}_1 \Bigg[1, \frac{L_c \overline{\gamma} g}{L_c+n}, \frac{(L_c+n)\gamma_T}{L_c \overline{\gamma}} \Bigg] - \mathcal{I}_1 \Bigg[1, \frac{L_c \overline{\gamma} g}{L_c+n}, \frac{(L_c+n)\gamma_T}{(L_c-1)\overline{\gamma}} \Bigg] \Bigg) + \sum_{k=0}^{L_c-2} \frac{1}{n+1} \Bigg(\frac{n(L_c-1)}{L_c(n+1)} \Bigg)^k \Bigg(\mathcal{I}_2 \Bigg[k+1, \frac{g L_c \overline{\gamma}}{L_c+n}, \frac{\gamma_T(L_c+n)}{\overline{\gamma}(L_c-1)}, \frac{\overline{\gamma} g}{n+1} \Bigg] - \sum_{j=1}^{k} \frac{1}{j!} \Bigg(\frac{\gamma_T(n+1)}{\overline{\gamma}(1-L_c)} \Bigg)^j \mathcal{I}_2 \Bigg[k+1-j, \overline{\gamma} g, \frac{\gamma_T}{\overline{\gamma}}, \frac{\overline{\gamma} g}{n+1} \Bigg] \Bigg) \Bigg\} \Bigg\} \tag{4.58}$$

Substituting (4.47) into (4.59), we can write the outage probability as

$$P_{out} = \begin{cases} \dfrac{1}{(L-1)!} \gamma(L, \dfrac{\gamma_T}{\overline{\gamma}}) + \displaystyle\sum_{L_c=1}^{L-n} \int_{\gamma_T}^{\gamma_{min}} f^*(\gamma, L_c) d\gamma \\ \quad + \displaystyle\sum_{L_c=L-n+1}^{L} \int_{\gamma_T}^{\frac{L_c}{L_c-1}\gamma_T} f^*(\gamma, L_c) d\gamma, \quad \gamma_{min} \geq \gamma_T, \\ \dfrac{1}{(L-1)!} \gamma(L, \dfrac{\gamma_{min}}{\overline{\gamma}}), \qquad \gamma_{min} < \gamma_T, \end{cases} \tag{4.60}$$

where $f^*(\gamma, L_c)$ is defined in (4.44) and n is chosen to satisfy $A_n \gamma_T \leq \gamma_{min} < A_{n+1}\gamma_T$ for the given γ_{min}, where

$$A_n = \begin{cases} 1, & n = 0 \\ 1 + \frac{1}{L-n}, & n = 1, \cdots, L-1 \\ \infty, & n = L \end{cases}.$$

4.5.4 Non-i.i.d. Channel Case

Joint PDF

When the $\{\gamma_k\}_{k=1}^{L}$ are independent and non-identically distributed (non-i.i.d), the joint PDF of the $\{\gamma_{(k)}\}_{k=1}^{Lc}$ is expressed as

$$f_{\gamma_{(1)},\cdots,\gamma_{(Lc)}}(\gamma_{(1)},\cdots,\gamma_{(Lc)}) = \sum_{i_1=1}^{L}\sum_{\substack{i_2=1\\ i_2\neq i_1}}^{L}\cdots\sum_{\substack{i_{Lc}=1\\ i_{Lc}\neq i_1,i_2,\cdots,i_{Lc-1}}}^{L}\prod_{k=1}^{Lc} f_{\gamma_k}(\gamma_k)\prod_{\substack{j=1\\ j\neq i_1,i_2,\cdots,i_{Lc}}}^{L} F_{\gamma_j}(\gamma_{Lc}) \tag{4.61}$$

where $f_{\gamma_k}(\gamma)$ and $F_{\gamma_k}(\gamma)$ correspond to the PDF and the CDF of the instantaneous SNR for the kth branch, respectively. For non-i.i.d. Rayleigh fading channel, (4.61) is given by [41, eq. (45)]

$$f_{\gamma_{(1)},\cdots,\gamma_{(Lc)}}(\gamma_{(1)},\cdots,\gamma_{(Lc)}) = \sum_{i_1=1}^{L}\sum_{\substack{i_2=1\\ i_2\neq i_1}}^{L}\cdots\sum_{\substack{i_{Lc}=1\\ i_{Lc}\neq i_1,i_2,\cdots,i_{Lc-1}}}^{L}\prod_{k=1}^{Lc}\frac{1}{\overline{\gamma}_{i_k}}e^{-\frac{\gamma_k}{\overline{\gamma}_{i_k}}}\prod_{\substack{j=1\\ j\neq i_1,i_2,\cdots,i_{Lc}}}^{L}\left(1-e^{-\frac{\gamma_{Lc}}{\overline{\gamma}_j}}\right) \tag{4.62}$$

Using the PDF of SC and MRC over non-i.i.d. Rayleigh fading channel shown in [43, eq. (4)] and [57, eq. (25)], respectively, and substituting (4.62) into (4.39), the joint PDF for MS-GSC over non-i.i.d. Rayleigh fading channel can be represented as

$$f(\gamma,L_c) = \begin{cases} \displaystyle\sum_{i=1}^{L}\frac{1}{\overline{\gamma}_i}e^{-\frac{\gamma}{\overline{\gamma}_i}}\prod_{\substack{j=1\\ j\neq i}}^{L}(1-e^{-\frac{\gamma}{\overline{\gamma}_j}}), & \gamma_T\le\gamma<\infty, L_c=1,\\ f^*(\gamma,L_c), & \gamma_T\le\gamma<\frac{L_c\gamma_T}{L_c-1}, L_c=2,\cdots,L,\\ \displaystyle\sum_{i=1}^{L}\frac{\overline{\gamma}_i{}^{L-2}}{\prod_{\substack{j=1\\ j\neq i}}^{L}(\overline{\gamma}_i-\overline{\gamma}_j)}e^{-\frac{\gamma}{\overline{\gamma}_i}}, & 0\le\gamma<\gamma_T, L_c=L, \end{cases} \tag{4.63}$$

where $f^*(\gamma, L_c)$ is given as

$$f^*(\gamma, L_c) = C(L, L_c)\left\{ e^{(A(l_{L_c-2}, L_c)-\tau)(\gamma-\gamma_T)-B(l_{L_c-2})\gamma} - e^{-\gamma(B(L_c)+\frac{\tau}{L_c})} \right\} \quad (4.64)$$

with

$$\begin{aligned} C(L, L_c) = &\sum_{i_1=1}^{L} \sum_{\substack{i_2=1 \\ i_2 \neq i_1}}^{L} \cdots \sum_{\substack{i_{L_c}=1 \\ i_{L_c} \neq i_1, \cdots, i_{L_c-1}}}^{L} \sum_{\tau \in T^L_{i_1, \cdots, i_{L_c}}} \text{sign}(\tau) \prod_{m=1}^{L_c} \frac{1}{\overline{\gamma}_{i_m}} \\ &\times \sum_{l_0 \in \{1\}} \sum_{l_1 \in \{l_0, 2\}} \cdots \sum_{l_{L_c-2} \in \{l_{L_c-3}, L_c-1\}} \prod_{m=0}^{L_c-3} \frac{\text{sign}(l_m)}{A(l_m, m+2)} \frac{\text{sign}(l_{L_c-2})}{A(l_{L_c-2}, L_c) - \tau}, \\ A(k, L_c) = &\frac{1}{k}\left(\sum_{m=1}^{k} \frac{L_c - k}{\overline{\gamma}_{i_m}} - \sum_{m=k+1}^{L_c} \frac{k}{\overline{\gamma}_{i_m}}\right), \quad B(k) = \frac{1}{k} \sum_{m=1}^{k} \frac{1}{\overline{\gamma}_{i_m}}, \text{ and} \\ \text{sign}(l_m) = &\begin{cases} 1, & l_m = m+1 \\ -1, & l_m = l_{m-1} \end{cases}. \end{aligned} \quad (4.65)$$

$T^L_{i_1, \cdots, i_{L_c}}$ are a set obtained by expanding the logarithm of the absolute value of each term in the product $\prod^{L}_{\substack{j=1 \\ j \neq i_1, \cdots, i_{L_c}}} (1 - e^{-\frac{\gamma_{L_c}}{\overline{\gamma}_j}})$, and $\text{sign}(\tau)$ is the corresponding sign of each term in the expansion [41].

MGF

Substituting (4.63) into (4.48), the MGF is given in (4.66) on top of next page, where

$$D(L_c) = A(l_{L_c-2}, L_c) - B(l_{L_c-2}) - \tau \text{ and } E(L_c) = B(l_{L_c-2}) + \frac{\tau}{L_c}. \quad (4.67)$$

$$\mathcal{M}(s) = \sum_{i=1}^{L} \sum_{\tau \in T_i^L} \frac{\text{sign}(\tau)}{\overline{\gamma}_i(\frac{1}{\overline{\gamma}_i} - s + \tau)} e^{-(\frac{1}{\overline{\gamma}_i} - s + \tau)\gamma_T} + \frac{1}{E(L_c) - s} \left(e^{-\frac{L_c \gamma_T}{L_c - 1}(E(L_c) - s)} - e^{-\gamma_T (E(L_c) - s)} \right) \Bigg\}$$
$$+ C(L, L_c) \Bigg\{ \frac{1}{D(L_c) + s} \left(e^{-\frac{L_c \gamma_T}{L_c - 1}(E(L_c) - \frac{A(l_{L_c - 2}, L_c)}{L_c} - s)} - e^{-\gamma_T (B(l_{L_c - 2}) - s)} \right)$$
$$+ \sum_{j=1}^{L} \frac{{\overline{\gamma}_j}^{L-1}}{\prod_{\substack{k=1 \\ k \neq j}}^{L} (\overline{\gamma}_j - \overline{\gamma}_k)} \frac{1}{1 - s\overline{\gamma}_j} \left(1 - e^{-\gamma_T (\frac{1}{\overline{\gamma}_j} - s)} \right) \tag{4.66}$$

Performance Analysis

Average number of branches

Substituting (4.63) into (4.54), we can show that the average number of branches for the combining can be calculated as

$$\overline{L}_c = L + \sum_{i=1}^{L} \sum_{\tau \in T_i^L} \frac{\text{sign}(\tau)}{\overline{\gamma}_i(\frac{1}{\overline{\gamma}_i} + \tau)} e^{-(\frac{1}{\overline{\gamma}_i} + \tau)\gamma_T} - L \sum_{j=1}^{L} \frac{{\overline{\gamma}_j}^{L-1}}{\prod_{\substack{k=1 \\ k \neq j}}^{L_c} (\overline{\gamma}_j - \overline{\gamma}_k)} e^{-\frac{\gamma_T}{\overline{\gamma}_j}}$$
$$+ \sum_{L_c=2}^{L} L_c \cdot C(L, L_c) \Bigg\{ \frac{1}{D(L_c)} \left(e^{-\frac{L_c \gamma_T}{L_c - 1}(E(L_c) - \frac{A(l_{L_c - 2}, L_c)}{L_c})} - e^{-\gamma_T B(l_{L_c - 2})} \right) \tag{4.68}$$
$$+ \frac{1}{E(L_c)} \left(e^{-\frac{L_c \gamma_T}{L_c - 1} E(L_c)} - e^{-\gamma_T E(L_c)} \right) \Bigg\}$$

Average error rate

Using the MGF in (4.66), the BER for BPSK is derived in (4.69) on top of next page.

$$
\begin{aligned}
P_b(E) = & \sum_{i=1}^{L} \sum_{\tau \in T_i^L} \frac{1}{\pi} \int_0^{\frac{\pi}{2}} \frac{\mathrm{sign}(\tau)}{\overline{\gamma}_i (\frac{1}{\overline{\gamma}_i} + \frac{1}{\sin^2\theta} + \tau)} e^{-(\frac{1}{\overline{\gamma}_i} + \frac{1}{\sin^2\theta} + \tau)\gamma_T} d\theta \\
& + C(L, L_c) \Bigg\{ \frac{1}{\pi} \int_0^{\frac{\pi}{2}} \frac{1}{D(L_c) - \frac{1}{\sin^2\theta}} \left(e^{-\frac{L_c \gamma_T}{L_c - 1}(E(L_c) - \frac{A(l_{L_c-2}, L_c)}{L_c} + \frac{1}{\sin^2\theta})} - e^{-\gamma_T (B(l_{L_c-2}) + \frac{1}{\sin^2\theta})} \right) d\theta \\
& + \frac{1}{\pi} \int_0^{\frac{\pi}{2}} \frac{1}{E(L_c) + \frac{1}{\sin^2\theta}} \left(e^{-\frac{L_c \gamma_T}{L_c - 1}(E(L_c) + \frac{1}{\sin^2\theta})} - e^{-\gamma_T (E(L_c) + \frac{1}{\sin^2\theta})} \right) \Bigg\} d\theta \\
& + \sum_{j=1}^{L} \frac{\overline{\gamma}_j{}^{L-1}}{\prod_{\substack{k=1 \\ k \neq j}}^{L} (\overline{\gamma}_j - \overline{\gamma}_k)} \frac{1}{\pi} \int_0^{\frac{\pi}{2}} \frac{1}{1 + \frac{1}{\sin^2\theta} \overline{\gamma}_j} \left(1 - e^{-\gamma_T (\frac{1}{\overline{\gamma}_j} + \frac{1}{\sin^2\theta})} \right) d\theta
\end{aligned}
\tag{4.69}
$$

Outage probability

Substituting (4.63) into (4.59), the outage probability is obtained as

$$
P_{out} = \begin{cases}
1 - \sum_{j=1}^{L} \frac{\overline{\gamma}_j{}^{L-1}}{\prod_{\substack{k=1 \\ k \neq j}}^{L_c} (\overline{\gamma}_j - \overline{\gamma}_k)} e^{-\frac{\gamma_T}{\overline{\gamma}_j}} + \sum_{L_c=1}^{L-n} \int_{\gamma_T}^{\gamma_{min}} f^*(\gamma, L_c) d\gamma \\
\quad + \sum_{L_c=L-n+1}^{L} \int_{\gamma_T}^{\frac{L_c}{L_c-1}\gamma_T} f^*(\gamma, L_c) d\gamma, \quad \gamma_{min} \geq \gamma_T, \\
1 - \sum_{j=1}^{L} \frac{\overline{\gamma}_j{}^{L-1}}{\prod_{\substack{k=1 \\ k \neq j}}^{L_c} (\overline{\gamma}_j - \overline{\gamma}_k)} e^{-\frac{\gamma_{min}}{\overline{\gamma}_j}}, \qquad \gamma_{min} < \gamma_T,
\end{cases}
\tag{4.70}
$$

where $f^*(\gamma, L_c)$ is defined in (4.64) and n is chosen to satisfy $A_n \gamma_T \leq \gamma_{min} < A_{n+1}\gamma_T$ for the given γ_{min}.

4.6 Switched Combining with Post-Examining Selection (SECps)

In [68], switch and examine combining (SEC) is proposed, in which switched diversity schemes are generalized into multibranch scenarios. Recently, SECps

is proposed in [58]. Performance improvement is achieved with SECps in that the branch with the best SNR is selected when all available branches are unacceptable, whereas SEC chooses a random branch.

4.6.1 Combining Strategy

The SEC first compares SNR of the current branch, denote by γ_1, against the threshold. If $\gamma_1 \geq \gamma_T$, then the receiver continues to use the current branch. However, if $\gamma_1 < \gamma_T$, γ_2 needs to be estimated and compared against γ_T. If $\gamma_2 \geq \gamma_T$, the receiver switches to the second branch for reception. Otherwise, the third branch is examined. This process is continued until either an acceptable branch is found or all available branches are examined but no acceptable branch is found. Unlike SEC, where a branch is randomly chosen for data reception when no acceptable branch is found, SECps selects the branch with the highest SNR among all unacceptable branches.

4.6.2 Statistics of the Combined SNR

Joint CDF and PDF

The joint CDF of SEC is written as

$$F(x) = \begin{cases} \Pr[\gamma_T \leq \gamma_1 < x] + \Pr[\max\{\gamma_1, \cdots, \gamma_L\} < \gamma_T] \\ \quad + \sum_{i=2}^{L} \Pr[\max\{\gamma_1, \cdots, \gamma_{i-1}\} < \gamma_T, \gamma_T \leq \gamma_i < x], & x \geq \gamma_T \\ \Pr[\max\{\gamma_1, \cdots, \gamma_L\} < x], & x < \gamma_T \end{cases} \tag{4.71}$$

where $F_\gamma(x)$ and $f_\gamma(x)$ are the CDF and PDF of a single branch evaluated at x, respectively. For i.i.d. channels, (4.71) can be written as

$$F(x) = \begin{cases} 1 - \sum_{i=0}^{L-1} [F_\gamma(\gamma_T)]^i \{1 - F_\gamma(x)\}, & x \geq \gamma_T \\ [F_\gamma(x)]^L, & x < \gamma_T \end{cases} \tag{4.72}$$

Differentiating (4.72) with respect to x, the PDF of combined SNR is given as

$$f(x) = \begin{cases} \sum_{i=0}^{L-1} [F_\gamma(\gamma_T)]^i f_\gamma(x), & x \geq \gamma_T \\ L[F_\gamma(x)]^{L-1} f_\gamma(x), & x < \gamma_T \end{cases} \tag{4.73}$$

MGF

The MGF of SEC is given by

$$\mathcal{M}(s) = L \sum_{i=0}^{L-1} \binom{L-1}{i} \frac{(-1)^i}{i+1-s\overline{\gamma}} (1 - e^{-\frac{(i+1-s\overline{\gamma})\gamma_T}{\overline{\gamma}}}) + \frac{e^{s\gamma_T}}{1-s\overline{\gamma}} \{1 - (1 - e^{-\frac{\gamma_T}{\overline{\gamma}}})^L\} \tag{4.74}$$

4.6.3 Performance Analysis

Number of Branch Estimation

SEC or SECps provides complexity reduction compared to SC that can be quantified by the number of branch estimation. Using the probability that i branches are estimated multiplied by i and taking summation of them, the number of branch estimation is given by

$$\overline{N}_e = 1 + \sum_{i=1}^{L-1} [F_\gamma(\gamma_T)]^i = \frac{1 - [F_\gamma(\gamma_T)]^L}{1 - F_\gamma(\gamma_T)} \tag{4.75}$$

For i.i.d. Rayleigh channels, (4.75) can be written as

$$\overline{N}_e = e^{\frac{\gamma_T}{\overline{\gamma}}}\{1-(1-e^{-\frac{\gamma_T}{\overline{\gamma}}})^L\} \tag{4.76}$$

Outage Probability

Using (4.72), the outage probability of SECps with the outage threshold γ_{min} is easily given as

$$P_{out} = (1-e^{-\frac{\gamma_{min}}{\overline{\gamma}}})^L + e^{-\frac{\gamma_T}{\overline{\gamma}}}\sum_{i=1}^{L-1}\{(1-e^{-\frac{\gamma_{min}}{\overline{\gamma}}})^i - (1-e^{-\frac{\gamma_T}{\overline{\gamma}}})^i\}\mathcal{U}(\gamma_{min}-\gamma_T) \tag{4.77}$$

where $\mathcal{U}(\cdot)$ is the unitstep function.

Average Error Rate

Based on the MGF in (4.74), the average BER for SECps with BPSK over i.i.d. Rayleigh channels is given by

$$\begin{aligned} P_b = L\sum_{i=0}^{L-1}\binom{L-1}{i}\frac{(-1)^i}{i+1}\left\{\frac{1}{2}\left(1-\sqrt{\frac{\overline{\gamma}g}{i+1+\overline{\gamma}g}}\right) - \mathcal{I}_1(\frac{\overline{\gamma}g}{i+1}, \frac{(i+1)\gamma_T}{\overline{\gamma}})\right\} \\ + \{1-(1-e^{-\frac{\gamma_T}{\overline{\gamma}}})^L\}e^{\frac{\gamma_T}{\overline{\gamma}}}\mathcal{I}_1(\overline{\gamma}g, \frac{\gamma_T}{\overline{\gamma}}), \end{aligned} \tag{4.78}$$

where $\mathcal{I}_1(a,b)$ is given in (B.10).

4.7 Minimum Estimation and Combining GSC (MEC-GSC)

Although MS-GSC provides the best performance out of low-complexity schemes introduced in Chapter 4, it necessitates the channel estimation and monitoring of the instantaneous SNR of all available branches so as to select a subset

based on the magnitude. In an attempt at simplifying the channel estimation complexity of the system, an alternative combing scheme called MEC-GSC is recently proposed in [59].

4.7.1 Combining Strategy

As defined previously, let γ_T be the target SNR threshold that may be set for a satisfactory communications. MEC-GSC starts from the first channel and estimating sequentially through the L available branches until it finds a branch whose SNR exceeds the threshold γ_T. As soon as a branch is found, it stops estimating the rest of the branches. In this first stage, the operation is the same as that of SEC or SECps, which is described in Chapter 4.6. If no acceptable branch is found, then the second stage starts where the receiver attempts to apply the MS-GSC scheme since all available branches have been estimated during the first stage.

4.7.2 Statistics of the Combined SNR

Joint PDF

The joint PDF of the combined SNR and number of combined branches is given by

$$f(\gamma, L_c) = \begin{cases} \dfrac{1-[F_\gamma(\gamma_T)]^L}{1-F_\gamma(\gamma_T)} f_\gamma(\gamma), & \gamma_T \le \gamma \le \infty,\ L_c = 1, \\ f^*(\gamma, L_c), & \gamma_T \le \gamma < \frac{L_c}{L_c-1}\gamma_T,\ L_c = 2, \cdots, L, \\ f_{MRC}(\gamma), & 0 \le \gamma < \gamma_T,\ L_c = L, \end{cases} \tag{4.79}$$

where $f^*(\gamma, L_c)$ for i.i.d. Rayleigh channels is provided in (4.44).

MGF

The MGF of MEC-GSC can be derived as

$$\begin{aligned}\mathcal{M}(s) = &\frac{1-[F_\gamma(\gamma_T)]^L}{1-F_\gamma(\gamma_T)}\int_{\gamma_T}^{\infty} e^{s\gamma} f_\gamma(\gamma)d\gamma \\ &+ \sum_{L_c=2}^{L}\int_{\gamma_T}^{\frac{L_c\gamma_T}{L_c-1}} e^{s\gamma} f^*(\gamma, L_c)d\gamma + \int_0^{\gamma_T} e^{s\gamma} f_{MRC}(\gamma)d\gamma.\end{aligned} \tag{4.80}$$

Substituting (4.79) into (4.80) and some mathematical manipulation, the MGF for i.i.d. Rayleigh channels can be derived in a closed-form.

4.7.3 Performance Analysis

Number of Branch Estimations

Since the MEC-GSC scheme has the same strategy as that of SECps until all the branches are estimated, the number of branch estimation is the same as that of SECps, that is

$$\overline{N}_e = \frac{1-[F_\gamma(\gamma_T)]^L}{1-F_\gamma(\gamma_T)}. \tag{4.81}$$

Number of Combined Branches

Once all the branches are estimated, the MEC-GSC operates the same as MS-GSC. Thus, the number of combined branches is the same as that of MS-GSC, which is given by

$$\overline{L}_c = 1 + \sum_{i=1}^{L_c-1} F_{(i)}(\gamma_T) \tag{4.82}$$

where $F_{(i)}(x)$ is the CDF of GSC when i branches are selected, which is available in closed-form in [41].

Outage Probability

The outage probability of MEC-GSC is given by

$$\mathrm{P_{out}} = \begin{cases} F_{(L)}(\gamma_T), & 0 \le \gamma < \gamma_T \\ \dfrac{1-[F_\gamma(\gamma_T)]^L}{1-F_\gamma(\gamma_T)}\{F_\gamma(\gamma)-F_\gamma(\gamma_T)\} + \left\{\displaystyle\sum_{l=2}^{L} F^*(\gamma;l) + F_{(L)}(\gamma_T)\right\}, & \gamma \ge \gamma_T \end{cases} \tag{4.83}$$

where $F^*(\gamma;l) = \Pr[\sum_{j=1}^{l-1}\gamma_{(j)} < \gamma_T, \gamma_T \le \sum_{j=1}^{l} < \gamma]$ is provided in a general form in (4.37) and in a closed-form for i.i.d. Rayleigh fading channels in [69].

Average Error Rate

Using the MGF approach, the average BER of MEC-GSC for BPSK over i.i.d. Rayleigh channels is given by

$$P_b = \{1-(1-e^{-\frac{\gamma_T}{\overline{\gamma}}})^L\}e^{\frac{\gamma_T}{\overline{\gamma}}}\mathcal{I}_1\left[1,\overline{\gamma}g,\frac{\gamma_T}{\overline{\gamma}}\right] + \mathcal{J}\left[\overline{\gamma}g,L\right] - \mathcal{J}_1\left[L,\overline{\gamma}g,\frac{\gamma_T}{\overline{\gamma}}\right] + P_b^* \tag{4.84}$$

where P_b^* is derived in (4.57).

4.8 Performance Comparison

In this Section, the low-complexity schemes listed above are compared in terms of BER performance, the number of combined branches, and the number of branch estimation.

Using the closed-form expressions introduced in the previous Sections, Fig. 4.2 shows the BER performance of the low-complexity diversity schemes described above when ten diversity branches are available and the target threshold is set to 6dB in i.i.d. Rayleigh fading channel environment. For comparison, the BER curves for no diversity case and MRC are also plotted. Among the low-diversity combining schemes, it is easy to see that MS-GSC

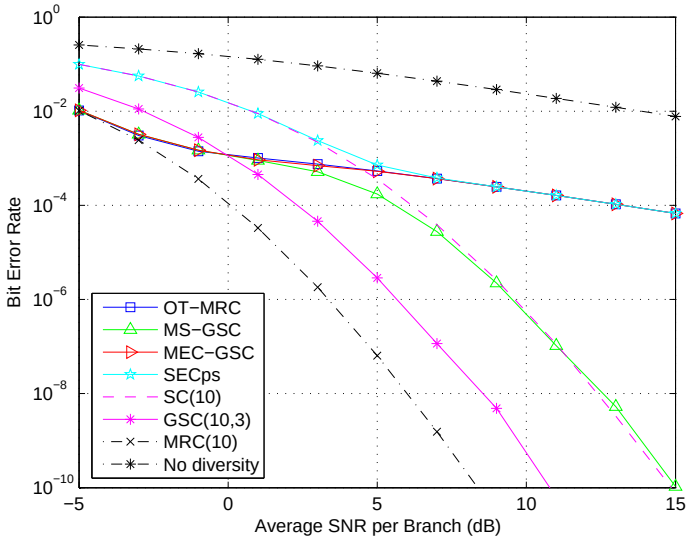

Figure 4.2: Bit error rate performance of the low-complexity diversity combining schemes when L=10 and γ_T=6dB

performs the best since it operates as MRC for low SNR region but gradually moves to SC as the average branch SNR increases. Interestingly, OT-MRC shows almost the same BER performance as that of MEC-GSC.

The MS-GSC also outperforms the OT-MRC scheme in terms of average number of combined branches as shown in Fig. 4.3. The performance superiority of MS-GSC comes from the fact that it requires channel estimation from all available branches in order to select the strong branches, which is illustrated in Fig. 4.4. On the other hand, the MEC-GSC scheme requires the same number of combined branches as that of MS-GSC, but it needs less number of channel estimation as depicted in Fig. 4.4. Since OT-MRC does not need to order branches in terms of the magnitude, the channel estimation of a branch is necessary only when the branch is combined. Thus, the number of branch estimation is the same as the number of combined branches, which can be seen from the figures. Compared to MS-GSC and MEC-GSC, the OT-MRC scheme is located in the middle.

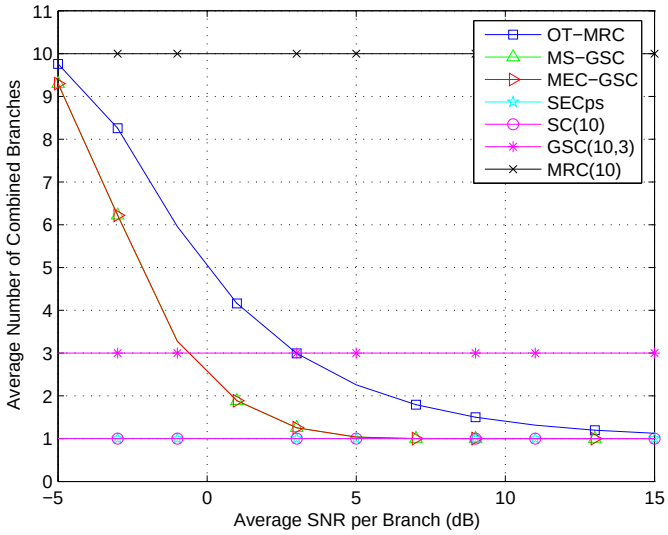

Figure 4.3: Average number of combined branches of the low-complexity diversity combining schemes when L=10 and γ_T=6dB

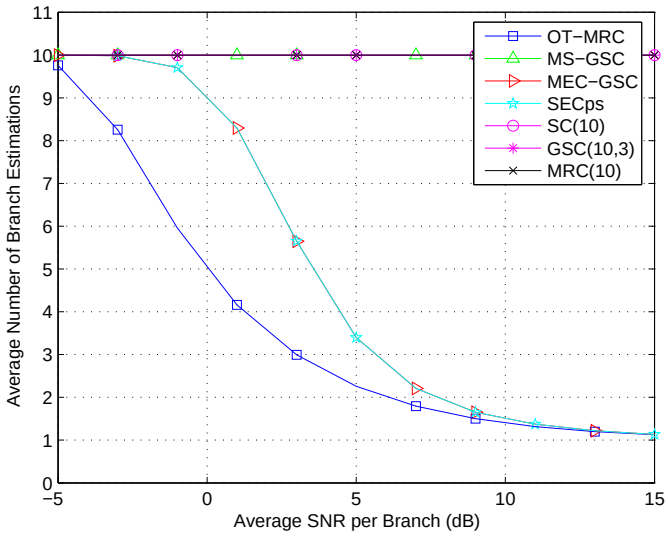

Figure 4.4: Average number of branch estimations of the low-complexity diversity combining schemes when L=10 and γ_T=6dB

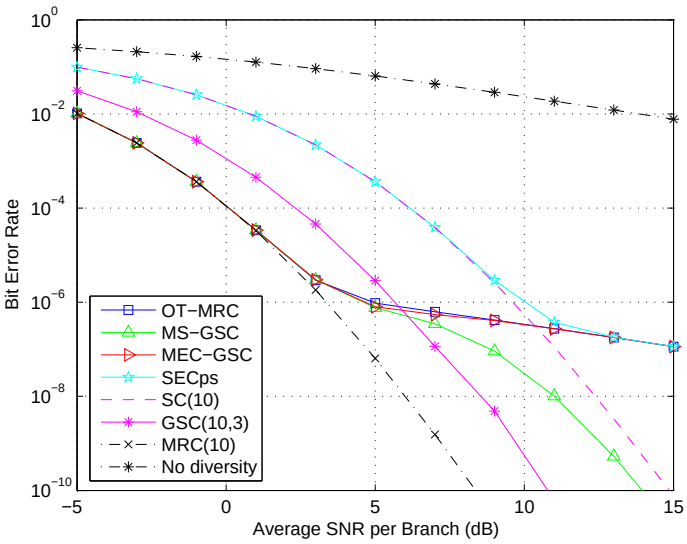

Figure 4.5: Bit error rate performance of the low-complexity diversity combining schemes when L=10 and γ_T=10dB

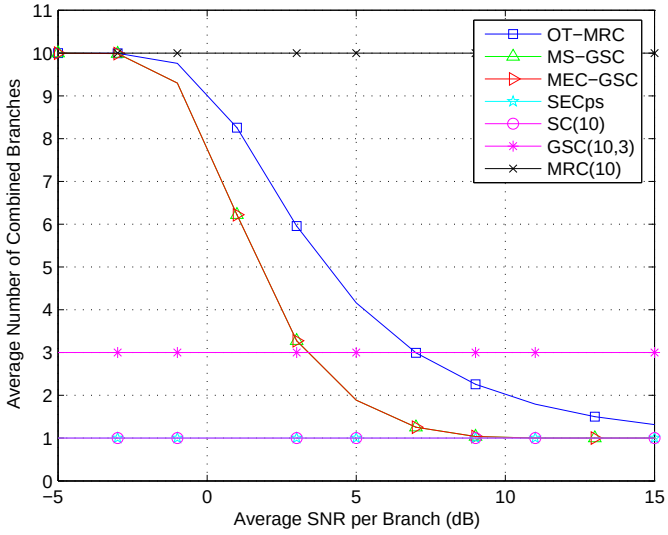

Figure 4.6: Average number of combined branches of the low-complexity diversity combining schemes when L=10 and γ_T=10dB

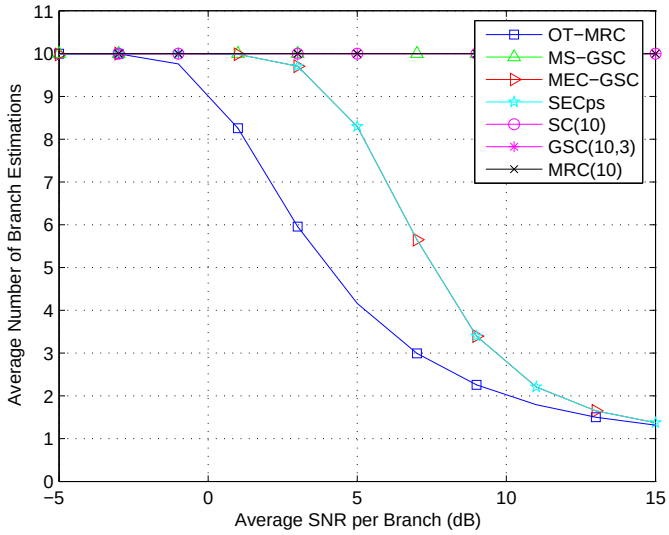

Figure 4.7: Average number of branch estimations of the low-complexity diversity combining schemes when L=10 and γ_T=10dB

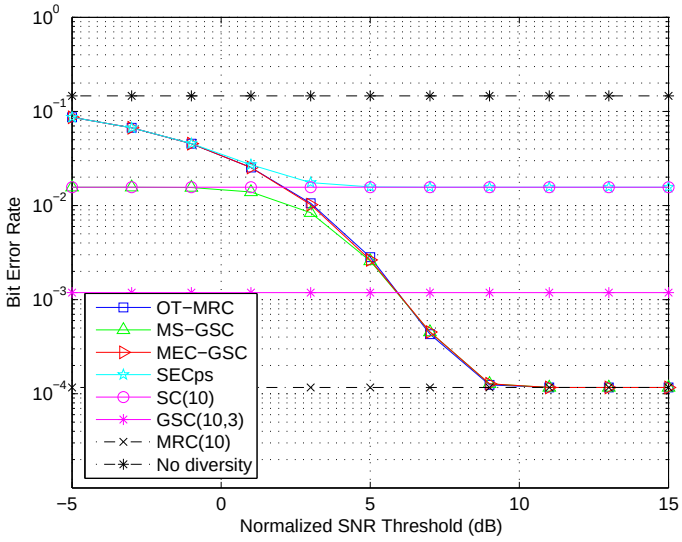

Figure 4.8: Bit error rate performance versus normalized SNR threshold ($\frac{\gamma_T}{\overline{\gamma}}$) of the low-complexity diversity combining schemes when L=10

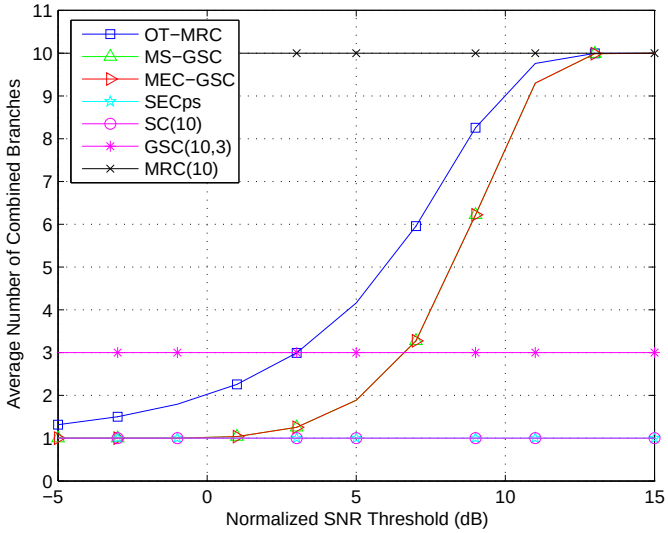

Figure 4.9: Average number of combined branches versus normalized SNR threshold ($\frac{\gamma_T}{\overline{\gamma}}$) of the low-complexity diversity combining schemes when L=10

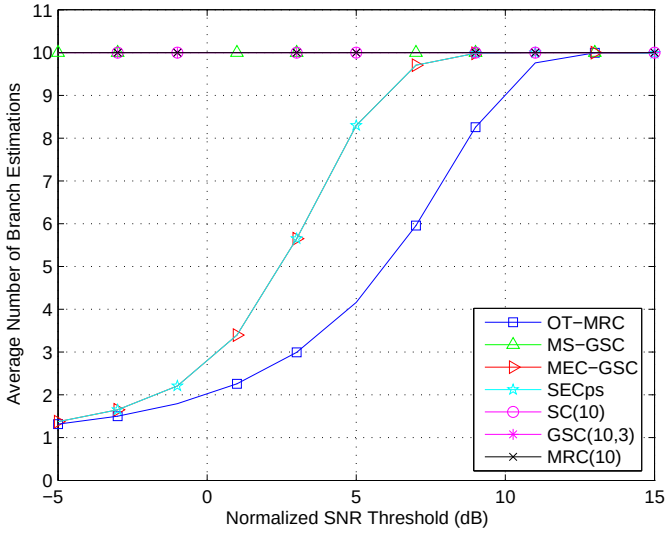

Figure 4.10: Average number of branch estimations versus normalized SNR threshold ($\frac{\gamma_T}{\overline{\gamma}}$) of the low-complexity diversity combining schemes when L=10

Fig. 4.5, 4.6, and 4.7 shows the BER, number of combined branches, and number of branch estimations when γ_T=10dB. Compared to the case of γ_T=6dB, the BER performance follows that of MRC over wider region of average SNR per branch and more branches are combined to satisfy the higher performance requirement. Thus, we can find out that the target threshold should be well determined based on the QoS requirement.

4.9 Effect of Channel Fading Correlation

Independent fading is a common assumption in studying the performance of diversity schemes. However, independent fading is not always realized in practice [70]. Especially for small-size mobile terminals equipped with multiple antennas, they may have insufficient antenna spacing to obtain independent fading in each branch. Additionally, they might not have enough space to place more than two antennas due to the size requirements. Under these restrictions and limitations, investigating the performance of dual branch diversity schemes in a correlated fading channel environment has some practical meanings. Thus, we consider the dual branch OT-MRC and MEC-GSC schemes, which may be better applicable to the mobile terminal thanks to their low complexity[4], over correlated Nakagami-m fading channels and compare their performance to see the effect of the correlation.

4.9.1 Statistics of OT-MRC and MEC-GSC

OT-MRC

Let γ_1 and γ_2 denotes the instantaneous SNR of the first and second branch, respectively. When γ_1 and γ_2 are jointly correlated Nakagami-m random vari-

[4]The low complexity may be interpreted as the low power consumption

ables, the joint PDF of γ_1 and γ_2 is given by [17, eq. (126)]

$$f(\gamma_1,\gamma_2)=\left(\frac{1}{\sqrt{\sigma_1\sigma_2}}\right)^{m+1}\frac{(\gamma_1\gamma_2)^{\frac{m-1}{2}}}{\Gamma(m)\rho^{\frac{m-1}{2}}(1-\rho)}e^{-\frac{1}{1-\rho}(\frac{\gamma_1}{\sigma_1}+\frac{\gamma_2}{\sigma_2})}I_{m-1}\left(\frac{2\sqrt{\rho\gamma_1\gamma_2}}{\sqrt{\sigma_1\sigma_2}(1-\rho)}\right), \tag{4.85}$$

where $\sigma_1=\overline{\gamma}_1/m$, $\sigma_2=\overline{\gamma}_2/m$, $\overline{\gamma}_l$ is the average SNR of the lth branch (l=1,2), m is the Nakagami fading parameter ($m\geq 0.5$), ρ is the correlation coefficient between γ_1 and γ_2, $\Gamma(\cdot)$ is the gamma function, and $I_v(\cdot)$ is the modified Bessel function of the first kind of order v.

Substituting (4.85) into (4.16) for $L_c=2$ and using the PDF of Nakagami-m fading channel model [17, eq. (3)] and the PDF of MRC output over two correlated Nakagami-m branches given in [17, eq. (142)], we can write the joint PDF of Γ and L_c as

$$f_{\gamma_{\rm OM}}(\gamma,L_c)=\begin{cases}e^{-\frac{\gamma}{\sigma_1}}\dfrac{\gamma^{m-1}}{\Gamma(m){\sigma_1}^m}, & \gamma_T\leq\gamma<\infty, L_c=1,\\ f^*(\gamma), & \gamma_T\leq\gamma<\infty, L_c=2,\\ \dfrac{\sqrt{\pi}e^{-\alpha\gamma}\xi^m}{\Gamma(m)}(\dfrac{\gamma}{2\beta})^{m-\frac{1}{2}}I_{m-\frac{1}{2}}(\beta\gamma), & 0\leq\gamma<\gamma_T, L_c=2,\end{cases} \tag{4.86}$$

where

$$\alpha=\frac{\sigma_1+\sigma_2}{2\sigma_1\sigma_2(1-\rho)},\quad \beta^2=\frac{(\sigma_1-\sigma_2)^2+4\sigma_1\sigma_2\rho}{4\sigma_1^2\sigma_2^2(1-\rho)^2},\quad \xi=\frac{1}{\sigma_1\sigma_2(1-\rho)}. \tag{4.87}$$

Using the series expansion of the Bessel function [63, eq. (8.445)] and the binomial expansion, $f^*(\gamma)$ is derived as

$$f^*(\gamma)=\int_0^{\gamma_T}f(\gamma_1,\gamma-\gamma_1)d\gamma_1=$$
$$\sum_{k=0}^{\infty}\sum_{i=0}^{m+k-1}\binom{m+k-1}{i}\frac{\rho^k\xi^{m+k}(-1)^i(1-\rho)^{-k}}{k!\Gamma(m+k)\Gamma(m)\chi^{m+k+i}}\gamma^{m+k-i-1}e^{-\sigma_1\xi\gamma}\gamma(m+k+i,\chi\gamma_T), \tag{4.88}$$

where

$$\chi = \frac{\sigma_2 - \sigma_1}{\sigma_1 \sigma_2 (1-\rho)}. \tag{4.89}$$

For identically distributed fading channels, i.e., $\sigma_1 = \sigma_2 = \sigma$, (4.88) is simplified with the help of the L'Hospital's rule as

$$f^*(\gamma) \;=\; \sum_{k=0}^{\infty} \frac{\rho^k \xi^{m+k} e^{-\sigma\xi\gamma} \gamma^{2m+2k-1}}{k!\Gamma(m+k)\Gamma(m)(1-\rho)^k} B\left(\frac{\gamma_T}{\gamma}, m+k, m+k\right), \tag{4.90}$$

where $B(x,p,q)$is the incomplete beta function [63, eq. (8.391)]. As a special case, for independent and identically distributed fading channels, i.e., $\rho = 0$, (4.90) can be further reduced to

$$f^*(\gamma) = e^{-\frac{\gamma}{\sigma}} \frac{\gamma^{2m-1}}{\sigma^{2m}[\Gamma(m)]^2} B\left(\frac{\gamma_T}{\gamma}, m, m\right), \tag{4.91}$$

which agrees with [57, eq. (9)].

MEC-GSC

We can write the PDF of the MEC-GSC output SNR, γ_{MEC}, as
(i) for $\gamma_T \leq \gamma < \infty$, and $L_c = 1$,

$$f_{\gamma_{\text{MEC}}}(\gamma, L_c) = f_1(\gamma) + \int_0^{\gamma_T} f(\gamma_1, \gamma) d\gamma_1 \tag{4.92}$$

(ii) for $\gamma_T \leq \gamma < 2\gamma_T$, and $L_c = 2$,

$$f_{\gamma_{\text{MEC}}}(\gamma, L_c) = \int_0^{\frac{\gamma}{2}} f(\gamma - \gamma_2, \gamma_2) d\gamma_2 - \int_{\gamma_T}^{\gamma} f(\gamma_1, \gamma - \gamma_1) d\gamma_1, \tag{4.93}$$

(iii) for $0 \leq \gamma < \gamma_T$, and $L_c = 2$,

$$f_{\gamma_{\text{MEC}}}(\gamma, L_c) = f_{\text{MRC}}(\gamma), \tag{4.94}$$

where $f_1(\gamma)$ is the PDF of γ_1 and $f_{\text{MRC}}(\gamma)$ is the PDF of the MRC output SNR. Substituting (4.85) into (4.92)-(4.94) , we have the joint PDF given as

$$f_{\gamma_{\text{MEC}}}(\gamma, L_c) =$$
$$\begin{cases} \frac{\gamma^{m-1}e^{-\frac{\gamma}{\sigma_1}}}{\Gamma(m){\sigma_1}^m} + \frac{\gamma^{m-1}e^{-\frac{\gamma}{\sigma_2}}}{\Gamma(m){\sigma_2}^m}\left\{1 - Q_m(\sqrt{2\sigma_1\xi\rho\gamma}, \sqrt{2\sigma_2\xi\gamma_T})\right\}, & \gamma_T \leq \gamma < \infty, L_c = 1 \\ 2f^*(\gamma) - \dfrac{\sqrt{\pi}e^{-\alpha\gamma}\xi^m}{\Gamma(m)}\left(\dfrac{\gamma}{2\beta}\right)^{m-\frac{1}{2}} I_{m-\frac{1}{2}}(\beta\gamma), & \gamma_T \leq \gamma < \infty, L_c = 2 \\ \dfrac{\sqrt{\pi}e^{-\alpha\gamma}\xi^m}{\Gamma(m)}\left(\dfrac{\gamma}{2\beta}\right)^{m-\frac{1}{2}} I_{m-\frac{1}{2}}(\beta\gamma), & 0 \leq \gamma < \gamma_T, L_c = 2 \end{cases} \tag{4.95}$$

where $f^*(\gamma)$ is defined in (4.88) and $Q_m(\cdot,\cdot)$ is the generalized (mth order) Marcum Q function [66].

4.9.2 Performance Analysis

Average combined SNR

The average combined SNR of dual diversity systems is given by

$$\overline{\gamma} = \sum_{L_c=1}^{2} \int_0^\infty \gamma f(\gamma, L_c) d\gamma. \tag{4.96}$$

Substituting (4.86) or (4.95) into (4.96), the average combined SNR for OT-MRC or MEC-GSC over correlated Nakagami-m channels is derived as a closed-form.

Average number of branches

The average number of branches is given by

$$\overline{L_c} = \sum_{L_c=1}^{2} L_c \int_0^\infty f(\gamma, L_c) d\gamma, \tag{4.97}$$

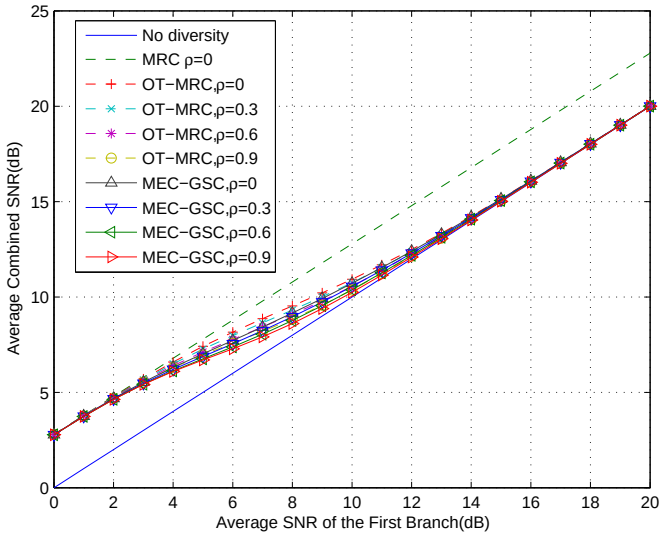

Figure 4.11: Average combined SNR of dual OT-MRC and MEC-GSC over correlated Nakagami-m fading channels for $\gamma_T = 7$ dB

where $f(\gamma, L_c)$ is given in (4.86) for OT-MRC or in (4.95) for MEC-GSC.

Average bit error rate

The bit error rate (BER), denoted by $P_b(E)$, for BPSK is obtained as [2]

$$P_b(E) = \sum_{L_c=1}^{2} \int_0^\infty Q(\sqrt{2\gamma}) f(\gamma, L_c) d\gamma \tag{4.98}$$

we can calculate the average BER of BPSK with OT-MRC or MEC-GSC over correlated Nakagami fading channels by using (4.86) or (4.95) in (4.98).

4.9.3 Numerical Results

As numerical examples we consider the nonidentical distributions with a linear relation between two SNRs of diversity paths such as $\overline{\gamma}_2 = q\overline{\gamma}_1$ and set $q = 0.9$. The target SNR and the Nakagami parameter are also fixed as $\gamma_T = 7$

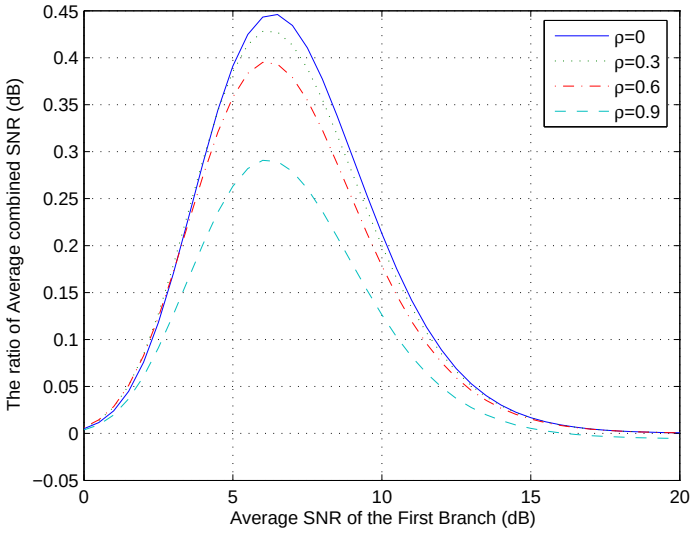

Figure 4.12: The ratio of average combined SNR of dual OT-MRC to that of MEC-GSC over correlated Nakagami-m fading channels for $\gamma_T = 7$ dB

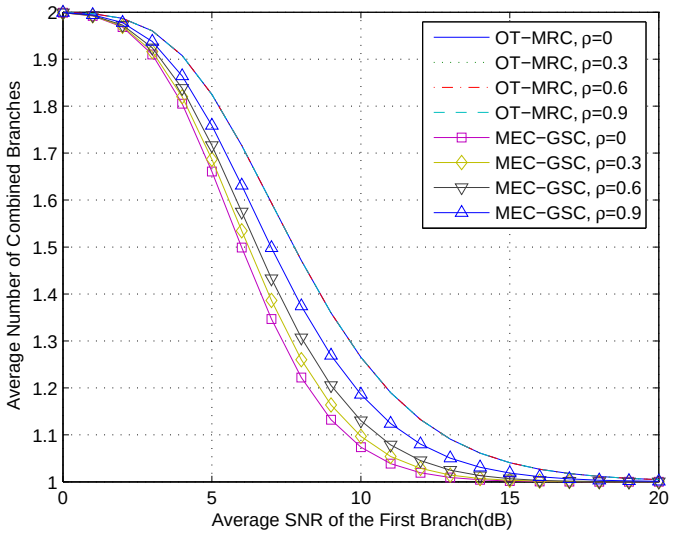

Figure 4.13: Average number of combined branches of dual OT-MRC and MEC-GSC over correlated Nakagami-m fading channels for $\gamma_T = 7$ dB

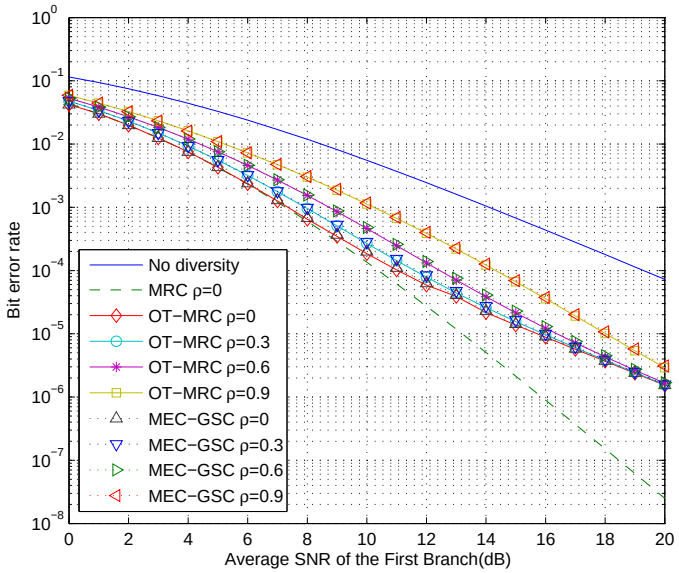

Figure 4.14: Bit error rate of dual OT-MRC and MEC-GSC over correlated Nakagami-m fading channels for $\gamma_T = 7$ dB

dB and $m = 2$, respectively. Fig. 4.11 shows the average combined SNR for dual OT-MRC and MEC-GSC, when $\rho = 0$, 0.3, 0.6, and 0.9, and compared with the performance of no diversity (single branch) and dual MRC. It can be seen that the average combined SNR of both OT-MRC and MEC-GSC follows the combined SNR of dual MRC with $\rho = 0$ when the average branch SNR approaches zero and gradually steps onto the SNR of a single branch with no diversity as expected. Fig. 4.12 shows the ratio of average combined SNR of dual OT-MRC to that of MEC-GSC, when $\rho = 0$, 0.3, 0.6, and 0.9. As shown in this figure, OT-MRC scheme slightly outperforms MEC-GSC around the pre-selected target threshold γ_T by $0 \sim 0.45$dB depending on the degree of correlation. Fig. 4.13 shows the average number of branches for dual OT-MRC and MEC-GSC when $\rho = 0$, 0.3, 0.6, and 0.9. Note that the average number of combined branches of OT-MRC is not affected by the correlation coefficient. For any value of the correlation coefficient the MEC-GSC requires smaller average number of combined branches than the OT-MRC, while the

difference of BER performance between OT-MRC and MEC-GSC is negligible over the correlation coefficient as shown in Fig. 4.14. Therefore we can conclude that the OT-MRC is more efficient in terms of the power-consumption, while satisfying the required target threshold.

4.10 Practical Aspects

In this Section, we evaluate the performance of the adaptive diversity combining schemes in a practical scenario in a cellular system environment. Among the adaptive diversity combining schemes, OT-MRC and MEC-GSC are considered in what follows.

4.10.1 Cellular Environment

Performance of OT-MRC in a cellular environment

We first assume that users are equipped with OT-MRC and are distributed uniformly over the cell that has a circular shape. To evaluate the performance of OT-MRC in a cellular environment more accurately, we consider a combination of both shadowing and small scale fading where the local mean of the small scale fading signal amplitude is log-normal distributed.

Averaging over the distribution of the average fading SNR $\overline{\gamma}$, the PDF of OT-MRC over the composite log-normal shadowing-Rayleigh fading distributions is obtained by

$$f_{\gamma_s}(\gamma) = \int_0^\infty f_{\gamma_s|\overline{\gamma}}(\gamma)\ f_{ln}(\overline{\gamma}) d\overline{\gamma} \tag{4.99}$$

where $f_{\gamma_s}(\gamma)$ is the PDF of OT-MRC over Rayleigh fading channels in (4.23) when $m = 1$ and $f_{ln}(x)$ is the log-normal distribution evaluated at x given by

$$f_{ln}(x) = \frac{10\ \log_{10} e}{x\sqrt{2\pi\sigma_n^2}}\ \exp\left[- \frac{(10\ \log_{10}(x) - m_n)^2}{2\sigma_n^2} \right]. \tag{4.100}$$

Note that m_n and σ_n are the mean and standard deviation of the log-normal distribution respectively and are represented in dBs.

Since users are uniformly distributed over the cell, the PDF of OT-MRC spatially averaged over the cell is obtained by

$$f_{\text{cell}}(\gamma) = \int_0^R \int_0^{\theta_s} f_{\gamma_s|r,\theta}(\gamma) \ \frac{2\ r}{R^2\ \theta_s}\ d\theta_s\ dr \tag{4.101}$$

where r is the distance between the base station and the user and θ_s is the sectorization angle in radians. R is the cell radius and $f_{\gamma_s}(\gamma)$ is in (4.99).

The goal of the adaptive diversity combining schemes is to achieve the reduction of both average processing power for combining branches and the number of channel estimation, which are quantified by the average number of combined branches and the average number of branch estimation, respectively. Since OT-MRC estimates branches only when it needs to be combined, the number of combined branches and branch estimation are the same.

Using the average number of combined branches of OT-MRC over i.i.d. Rayleigh fading channels given in (4.23) when $m = 1$ and the PDF of OT-MRC in a cellular environment given in (4.101), the average number of combined branches of OT-MRC in a cellular environment is given by

$$\begin{aligned}\overline{L}_{\text{cell}} =& L - \sum_{L_c=1}^{L-1} \frac{10\ \log_{10} e}{\Gamma(L_c)\sqrt{2\pi\sigma_n^2}} \\ &\times \int_0^{\infty} \int_0^{R} \Gamma(L_c, \frac{\gamma_T}{x})\ \exp\Big[- \frac{(10\ \log_{10}(x) - m_n)^2}{2\sigma_n^2} \Big] \frac{2\ r}{xR^2} dr dx\end{aligned} \tag{4.102}$$

where $m_n = \text{SNR}_{\text{tx}} - 10\log_{10} C - 10\alpha \log_{10}(r)$ is the mean and σ_n is the standard deviation of the log-normal shadowing, and SNR_{tx} is the transmission SNR.

The outage probability, P_{out}, is an important performance measure for wireless communication systems. It is defined as the probability that the output SNR falls below a threshold value, denoted by γ_{min}. Based on the PDF of OT-MRC in a cellular environment given in (4.101), the average output

probability of OT-MRC over the cell is represented by

$$P_{\text{out}}^{\text{cell}} = \frac{10\ \log_{10}e}{\sqrt{2\pi\sigma_n^2}} \int_0^{\infty} \int_0^{R} P_{\text{out}}(\gamma_{\min}|x)\ \exp\left[- \frac{(10\ \log_{10}(x) - m_n)^2}{2\sigma_n^2} \right] \frac{2\ r}{xR^2}\ drdx \tag{4.103}$$

where $P_{\text{out}}(\gamma_{\min}|\overline{\gamma} = x)$ is the outage probability of OT-MRC over i.i.d. Rayleigh fading channels given in (4.25) when $m = 1$.

Performance of MEC-GSC in a cellular environment

Similarly, the PDF of MEC-GSC spatially averaged over the cell is obtained by

$$f_{\text{cell}}(\gamma) = \int_0^{\infty} \int_0^{R} f_{\gamma_s|r,x}(\gamma)\ f_{ln|r}(x) \frac{2\ r}{R^2}\ drdx \tag{4.104}$$

where $f_{\gamma_s|r,x}(\gamma)$ is the PDF of MEC-GSC over i.i.d. Rayleigh fading channels in (4.79) and $f_{ln}(x)$ is in (4.100).

Unlike MS-GSC, MEC-GSC tries not to estimate all the branches, but only the branches that need to be combined. Therefore, the average number of of combined branches is always less than or equal to the average number of branch estimation.

Using the PDF of MEC-GSC in a cellular environment in (4.104), the average number of combined branches of OT-MRC in a cellular environment is given by

$$\overline{L}_{\text{cell}} = \frac{10\ \log_{10}e}{\sqrt{2\pi\sigma_n^2}} \int_0^{\infty} \int_0^{R} \overline{L}_{c|x}\ \exp\left[- \frac{(10\ \log_{10}(x) - m_n)^2}{2\sigma_n^2} \right] \frac{2\ r}{xR^2}\ drdx \tag{4.105}$$

where $\overline{L}_{c|x}$ is the average number of combined branches of MEC-GSC over i.i.d. Rayleigh fading channels given the average SNR $\overline{\gamma} = x$, which is shown in (4.82).

Similarly, the average outage probability of MEC-GSC in a cellular

Cell radius	1 km
Carrier frequency	2.0 GHz
Propagation model	128.1 + 37.6 $\log_{10}$ (r)
Standard deviation of shadowing	8 dB
Transmission SNR	128.1 dB
User mobility	3 or 30 km/h
Doppler frequency	5.7 or 56.7 Hz
Coherence time	31.5 or 3.2 ms
Transmission time interval	2 ms
Fast fading model	Rayleigh fading

Table 4.1: HSDPA simulation parameters

environment is given by

$$\mathrm{P}_{\mathrm{out}}^{\mathrm{cell}} = \frac{10\ \log_{10} e}{\sqrt{2\pi\sigma_n^2}} \int_0^{\infty} \int_0^{R} \mathrm{P}_{\mathrm{out}}(\gamma_{\min}|x)\ \exp\left[-\frac{(10\ \log_{10}(x) - m_n)^2}{2\sigma_n^2} \right] \frac{2\ r}{xR^2}\ drdx \tag{4.106}$$

where $\mathrm{P}_{\mathrm{out}}$ is the outage probability of MEC-GSC over i.i.d. Rayleigh fading channels shown in (4.83).

4.10.2 Simulation in an HSDPA Environment

Although the aforementioned adaptive diversity combining schemes provide a considerable reduction of complexity or power consumption, true adaptive selection of the number of active antennas over small scale fading such as Rayleigh channels may not be practical. For instance, activating and deactivating an antenna with the associated RF chain are nontrivial tasks, which may require non-negligible amount of time.

Simulation parameters

In time-division multiplexing systems such as evolution data only (EV-DO) and high speed downlink packet access (HSDPA), channel estimation and data

transmission are performed in a slot by slot basis [71]. Therefore, the time slot duration needs to be designed to have the channel stationary over the duration.

Every time slot has a guard period followed by data burst. Since adaptive antenna selections take place during a guard period in the adaptive diversity combining schemes, the power on or off ramp time of RF transceivers is a crucial factor in the design. According to the data sheets of some wireless LAN RF transceivers, the power on or off ramp time is around 5 μs or less [72–74]. Thus, an adaptive selection of a subset of antennas by turning on and off RF chains within a guard period is presumably feasible.

Table 4.1 summarizes the parameters used in the simulation. Based on common assumptions for HSDPA simulation in [75], we adopt the following propagation model:

$$PL(r) = 128.1 + 37.6\log_{10}(r) \quad [\text{dB}] \tag{4.107}$$

where r is the distance between the base station and the user in the unit of killometers. According to the user mobility distribution in [75], we consider two different speeds, i.e., 3 and 30 km/h, where the maximum doppler frequency for those speeds is given by 5.6 and 56.7 Hz, respectively. The coherence time is approximated by

$$T_c \approx \frac{9}{16\pi f_d} \tag{4.108}$$

where f_d is the maximum doppler frequency. Thus, an approximate coherence time associated with the speeds is calculated as 31.5 and 3.2 ms, respectively. Considering the coherence time calculated as above, we observe that the HSDPA system was designed to have the transmission time interval of 2 ms [76]. In addition, we assume the transmission SNR to be 128.1 dB such that the SNR in the cell edge is simply 0 dB.

Fig. 4.15 compares the average number of combined branches of OT-MRC and that of MEC-GSC in a cellular environment when $L = 4$. Simulation results are also plotted to verify the analysis. Fig. 4.16 shows the outage probability of OT-MRC and that of MEC-GSC in a cellular environment. For

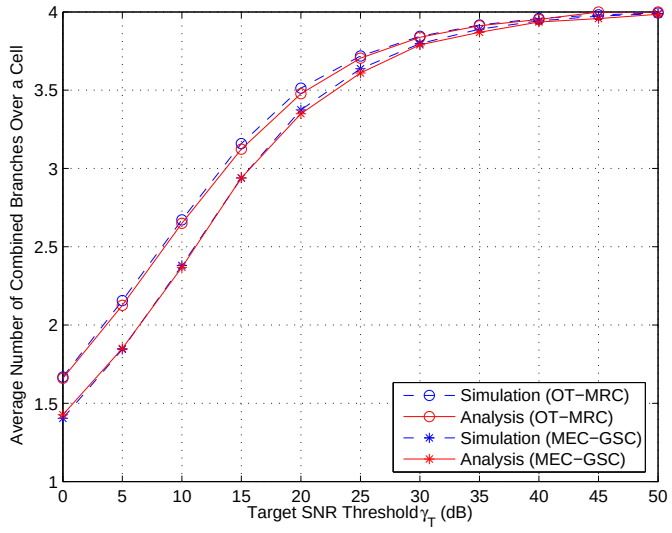

Figure 4.15: Average number of combined branches of OT-MRC and MEC-GSC in a cellular environment when $L = 4$

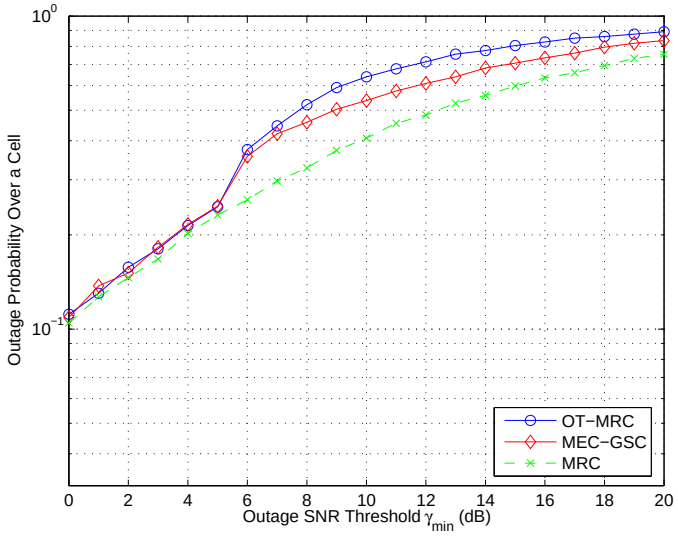

Figure 4.16: Average outage probability of OT-MRC and MEC-GSC in a cellular environment when $L = 4$

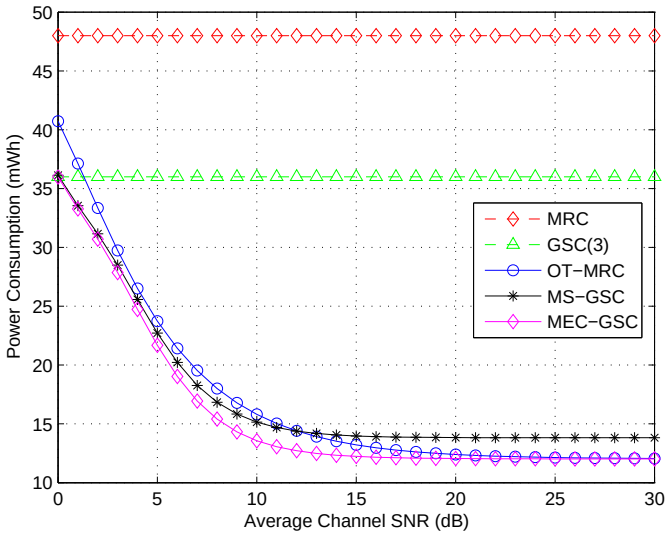

Figure 4.17: Average power consumption of OT-MRC, MS-GSC, and MEC-GSC when $L = 4$

comparison purposes, the outage probability of MRC in a cellular environment is also plotted.

Power consumption

If we assume $p\%$ guard period overhead (for instance, 5% in HSDPA means a guard period of 100 μs), the power consumption of the traditional diversity system may be calculated as follows.

$$\mathcal{P}_{\text{conv}} = L \times \mathcal{P}_{\text{txrx}} \text{ [mWh]} \tag{4.109}$$

where L is the number of available antennas, $\mathcal{P}_{\text{txrx}}$ is the power consumption of a transceiver in transmit or receive mode. On the other hand, the power consumption of OT-MRC can be written as

$$\mathcal{P}_{\text{OM}} = \sum_{n=1}^{L} \Pr_{\text{OM}}[n]\{n\mathcal{P}_{\text{txrx}} + (L-n)\mathcal{P}_{\text{down}}\} \text{ [mWh]} \tag{4.110}$$

where $\Pr_{\text{OM}}[n] = \int_0^\infty f(\gamma, n)d\gamma$ is the probability of n antennas being combined for OT-MRC, which can be easily obtained using (4.16), and $\mathcal{P}_{\text{down}}$ is the power consumption of a transceiver in shutdown mode. Since MS-GSC estimates all available branches to select the best ones, no power saving is achieved during a guard period. The power consumption of MS-GSC can be written as

$$\mathcal{P}_{\text{MG}} = \frac{p}{100} L\mathcal{P}_{\text{txrx}} + \left(1 - \frac{p}{100}\right) \sum_{n=1}^{L} \Pr_{\text{MG}}[n]\{n\mathcal{P}_{\text{txrx}} + (L-n)\mathcal{P}_{\text{down}}\} \text{ [mWh]} \tag{4.111}$$

where $\Pr_{\text{MG}}[n] = \int_0^\infty f(\gamma, n)d\gamma$ is the probability of n antennas being combined for MS-GSC, which can be obtained using (4.38). However, since MEC-GSC attempts to select an acceptable branch, not the best branch as in MS-GSC, until all branches are estimated, some additional power saving over MS-GSC is expected. The power consumption of MEC-GSC can be written as

$$\mathcal{P}_{\text{ME}} = \frac{p}{100} \overline{N}_e \mathcal{P}_{\text{txrx}} + \left(1 - \frac{p}{100}\right) \sum_{n=1}^{L} \Pr_{\text{MG}}[n]\{n\mathcal{P}_{\text{txrx}} + (L-n)\mathcal{P}_{\text{down}}\} \text{ [mWh]} \tag{4.112}$$

where $\overline{N}_e$ is the average number of channel estimation in (4.81).

Just to get the picture of the effectiveness of the adaptive diversity combining schemes, we referred to the data sheet of a 802.11b transceiver and found some real values of the power consumption for various modes: $\mathcal{P}_{\text{txrx}} \approx 360$ [mWh], $\mathcal{P}_{\text{down}} \approx 180$ [μWh] [77]. Based on these values, we illustrate the average power consumption of OT-MRC, MS-GSC, and MEC-GSC in Fig. 4.17 when $L = 4$. The power consumption of MRC and GSC are also plotted for comparison. It can be seen from the figure that the adaptive diversity combining schemes achieve about 75% reduction of power consumption compared to MRC in this example. Notice that this is a very simplified example where none of the values above represents actual power consumption measured from real hardware chipsets.

Chapter 5

Spectral Efficiency Enhancement in Multicarrier Systems

5.1 Introduction

Along with users' needs for higher data rates, multi-carrier systems have received a great deal of interest where lots of narrow-band channels are used in parallel instead of wide-band [78]. The orthogonal frequency division multiplexing (OFDM) is the most well-known and popular multi-carrier system where simple transceivers based on fast Fourier transform (FFT) and inverse FFT (I-FFT) are possible, thanks to the cyclic structure of channel matrix. The fourth generation (4G) wireless system standards, such as WiMAX [79] or 3GPP LTE [80], and some WLAN standards, such as 802.11a/g, are adopting OFDM as a primary physical layer solution [81].

In a multiuser cellular environment, some users are located in proximity to the base station (BS), whereas other users can suffer inter-cell interference in the cell edge [82]. Some mobile devices can be equipped with four antennas with sophisticated schemes, while other mobile handsets provide a conven-

tional single antenna functionality. Not only do various types of mobile device hardware exist, but applications running in the devices also have their own QoS requirements. Some users might want to enjoy real-time video streaming service while travelling, whereas a number of other users will generate sporadic data traffic by checking emails or web-surfing. Based on different requirements and limitations, wireless systems using the well known trade-off between multiplexing and diversity can achieve robustness as well as high data rates. In [83], a fundamental trade-off between diversity and multiplexing is discussed. Adaptive switching between diversity and spatial multiplexing provides a significant gain and increased link robustness [84–86].

Besides multiplexing systems, adaptive modulation has been shown as an effective technique to increase the spectral efficiency [4,5,9,10,87–90]. In the adaptive modulation, the modulation level is adaptively adjusted contingent upon the channel status.

Multi-channel systems require a scheme to associate information bits efficiently with each channel. In traditional multi-channel systems, adaptive modulation is used in each channel independently. Therefore, transmission is avoided over deeply faded channels and high level/high rate constellations are used over channels experiencing good channel conditions. More specifically, when the quality of a channel falls below a specified cutoff threshold, denoted by γ_T, adaptive modulation precludes any signal from being transmitted through that channel. This blockage of transmission may result in lowering the spectral efficiency of systems when the majority of channels undergo extreme fading conditions.

We introduce a multi-channel system that uses a diversity combining technique in conjunction with adaptive modulation to increase the overall spectral efficiency. This system transmits the same information redundantly over a subset of the total number of channels, which are optimally combined at the receiver to improve the SNR and thus provide a higher data rate. It allows all the channels to be used in a more effective way at the small expense of computational complexity at both the transmitter and receiver.

An ideal multi-channel system with adaptive modulation and a diversity combining technique, which we call a benchmark scheme, first measures the quality of all available channels and makes an exhaustive search of all the possible ways of using a diversity combining technique among the multiple channels in order to find the one that provides the maximum overall spectral efficiency. Although a diversity combining technique and adaptive modulation are merged optimally in this ideal system, it is too computationally complex to be implemented in practice.

In this chapter, a hybrid scheme is proposed, which is suboptimal in the sense that only the channels whose SNR is below the cutoff threshold are considered to be diversity combined. We call such channels as cutoff channels. In the proposed scheme, the same information bearing signal is transmitted redundantly through a subset of channels whose SNR is below γ_T, denoted by cutoff channels, and a diversity combining technique is utilized at the receiver to improve the overall output SNR. This system adaptively changes the number of channels to be combined depending on the quality of the channels, resulting in a considerable spectral efficiency gain over the conventional multi-channel system especially in desperate channel conditions. In our study of the proposed scheme, we carry out a thorough performance evaluation by considering the average spectral efficiency, the outage probability, and the average BER and comparing them with ones of the conventional scheme and the optimal (benchmark) scheme in terms of maximum average spectral efficiency. In these performance comparisons it is illustrated that the proposed scheme considerably outperforms the conventional scheme and is as good as the benchmark scheme in performance but with much reduction of complexity.

5.2 System Model

Consider a system with a total of L independent orthogonal channels, each of which undergoes slow flat fading such that the channel remains almost constant over tens of symbol times. We assume that perfect channel state

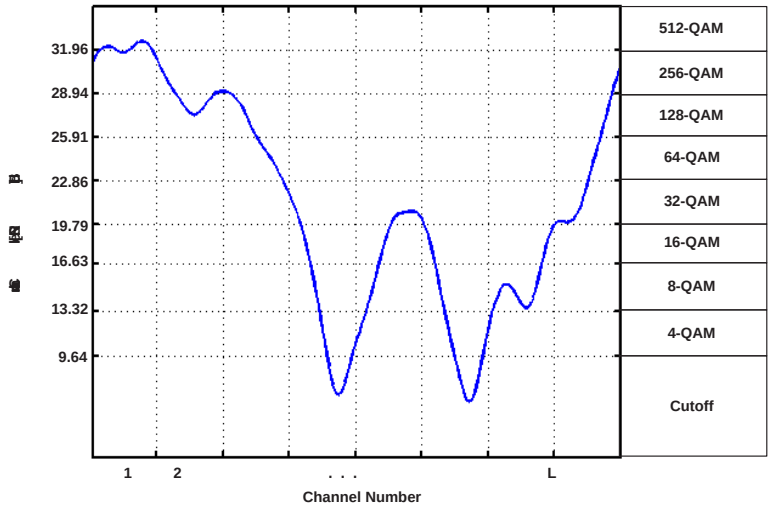

Figure 5.1: Conventional adaptive modulation for multi-channel systems.

information is available in both transmitter and receiver. Each channel assigns a different number of bits to transmit based on its channel quality as shown in Fig. 5.1. We also assume an on-off type of power allocation per channel as when we assume equal power transmission over all the channels. It is known that the on-off power control alleviates the linearity requirement of the power amplifier [91]. Note that adaptive power loading is often considered to further increase the spectral efficiency, but regulatory concerns and the peak-to-average power ratio problem usually inhibit adaptive power loading from being used in practice. In addition, it is known that rate adaptation is the key to achieving high link spectral efficiency and that variable-power variable-rate systems provide a small spectral efficiency gain over constant-power variable-rate systems while the latter simplifies hardware complexity significantly [11, 92].

5.3 Proposed Adaptive Scheme

In the conventional multi-channel adaptive modulation scheme, each channel applies adaptive modulation independently. Therefore, it is possible that no transmission occurs in a channel where another channel takes advantage of very high-order modulation simultaneously. There are cases, however, that a majority of channels have no transmission at all. In such cases, it is straightforward that joint diversity combining and adaptive modulation will help to increase the overall performance.

5.3.1 Optimal Scheme

The maximum spectral efficiency of diversity-assisted multi-channel systems can be found by exhaustive search over all possible channel combinations. Let us denote K as the number of independent and different data streams. For instance, if all the channels are carrying independent data and no channel is combined, then $K = L$. On the other hand, if there are, for example, three dual diversity combined channels, then six channels are involved with the diversity combining and the others are individual channels. In this case, $K = L - 6 + 3 = L - 3$. In what follows, we call multiple channels delivering the same data stream as a combined channel.

Let $\mathbb{S}_L$ be a set of vectors given as $\mathbb{S}_L = \{\mathbf{s}_1, \mathbf{s}_2, \cdots \mathbf{s}_n, \cdots, \mathbf{s}_N\}$, where $\mathbf{s}_n$ is a vector whose element indicates the number of channels to be used for an independent data stream and N is a total number of possible channel combinations. For example, for four channel systems, (i.e. L=4), we have $N = 5$ and $\mathbb{S}_4 = \{\{4\}, \{3,1\}, \{2,2\}, \{2,1,1\}, \{1,1,1,1\}\}$. In this case, we know from $\mathbf{s}_1 = \{4\}$ that only one data stream is used via all the channels combined while $\mathbf{s}_4 = \{2,1,1\}$ indicates three independent channels including one dual combined channel and two individual channels. For each of $\mathbf{s}_n$, consider a set of possible combinations of assigning channels and denote the set as $\mathbb{V}_n$. For $\mathbf{s}_4$ from above example, we have $\mathbb{V}_4 = \{\mathbf{v}_1, ..., \mathbf{v}_4\} = \{\{\gamma_1+\gamma_2, \gamma_3, \gamma_4\}, \{\gamma_1+\gamma_3, \gamma_2, \gamma_4\}, \{\gamma_1+\gamma_4, \gamma_2, \gamma_3\}, \{\gamma_2+\gamma_3, \gamma_1, \gamma_4\}\}$ where γ_l is

the instantaneous received SNR of the lth channel. The optimal scheme performs a full search over all the vectors $\mathbf{s}_n$, each with all the possible combinations $\mathbb{V}_n$, to find out the vector that provides the maximum spectral efficiency, which can be written as

$$SE^{\text{opt}} = \max_{\mathbf{s}_i \in \mathbb{S}_L, \mathbf{v}_j \in \mathbb{V}_i} \sum_{k=1}^{K} \mathcal{C}(v_{j,k}) \tag{5.1}$$

where $v_{j,k}$ is the kth element of the $\mathbf{v}_j$ vector and $\mathcal{C}(\gamma)$ is the number of bits associated with the SNR, γ, from the adaptive modulation.

5.3.2 Hybrid Scheme

In the proposed scheme, only the channels whose SNR falls below the cutoff threshold, denoted by γ_T, are considered to be combined to increase the spectral efficiency. No data is transmitted through those channels in the conventional system. The other channels whose individual SNR is above γ_T use the adaptive modulation independently as the conventional system does. Suppose there are m channels where the SNR of each channel is below γ_T, and we denote the SNRs of those m channels as $\{\underline{\gamma_i}\}_{i=1}^{m}$, and the rest of the channels whose SNR is higher than γ_T are mapped onto $\{\overline{\gamma_i}\}_{i=1}^{L-m}$. Similar to the optimal scheme, the maximum spectral efficiency of the proposed scheme can be written as

$$SE^{\text{hyb}} = \sum_{i=1}^{L-m} \mathcal{C}(\overline{\gamma_i}) + \max_{\mathbf{s}_i \in \mathbb{S}_m, \underline{\mathbf{v}_j} \in \underline{\mathbb{V}_i}} \sum_{k=1}^{K} \mathcal{C}(\underline{v_{j,k}}) \tag{5.2}$$

where $\underline{\mathbb{V}_k}$ is a set of possible vectors consisting of $\{\underline{\gamma_i}\}_{i=1}^{m}$ for $\mathbf{s}_k$, $\underline{\mathbf{v}_j}$ is the jth vector in $\underline{\mathbb{V}_k}$, and $\underline{v_{j,k}}$ is the kth element of the $\underline{\mathbf{v}_j}$ vector. For instance, when $m = 3$, $\mathbb{S}_3 = \{\{3\}, \{2,1\}, \{1,1,1\}\}$, $\mathbf{s}_2 = \{2,1\}$ has $\underline{\mathbb{V}_2} = \{\underline{\mathbf{v}_1}, \underline{\mathbf{v}_2}, \underline{\mathbf{v}_3}\} = \{\{\underline{\gamma_1} + \underline{\gamma_2}, \underline{\gamma_3}\}, \{\underline{\gamma_1} + \underline{\gamma_3}, \underline{\gamma_2}\}, \{\underline{\gamma_2} + \underline{\gamma_3}, \underline{\gamma_1}\}\}$. Whereas the optimal scheme introduced previously uses the full channel information, the hybrid scheme attempts to maximize the overall spectral efficiency only with the cutoff channels, which offers considerable complexity reduction.

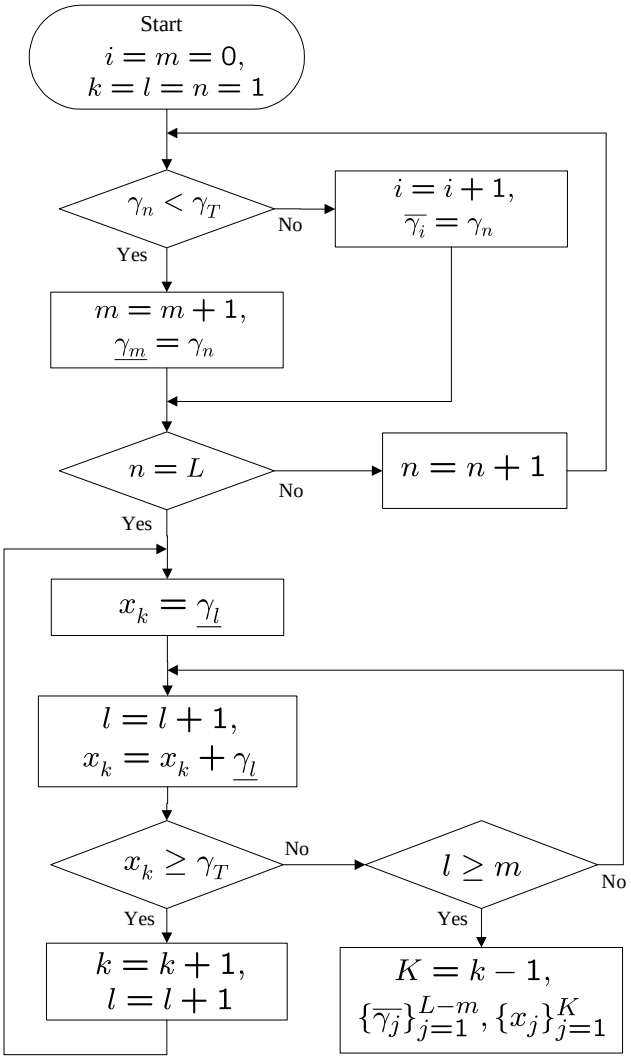

Figure 5.2: Flow chart for the algorithm of the proposed scheme

For solving the discrete optimization problem above, a simple incremental algorithm is proposed as follows.

- Step 1: First, select the first cutoff channel $\underline{\gamma_1}$, which are arbitrarily ordered. Then keep adding the number of cutoff channels until we find n_1 satisfying $\sum_{i=1}^{n_1} \underline{\gamma_i} \geq \gamma_T$ and $\sum_{i=1}^{n_1-1} \underline{\gamma_i} < \gamma_T$. The minimum number of cutoff channels are selected such that the combined SNR becomes higher than γ_T, where this group of cutoff channels $\underline{v_{1,1}} = \underline{\gamma_1} + \underline{\gamma_2} + \cdots + \underline{\gamma_{n_1}}$ is now usable and is denoted as a qualified combined channel.

- Step 2: Second, repeat the first step by increasing the number of combined channels starting from $\underline{\gamma_{n_1+1}}$ until we find n_2 that satisfies $\sum_{i=n_1+1}^{n_1+n_2} \underline{\gamma_i} \geq \gamma_T$ and $\sum_{i=n_1+1}^{n_1+n_2-1} \underline{\gamma_i} < \gamma_T$. The second qualified combined channel shows $\underline{v_{1,2}} = \underline{\gamma_{n_1+1}} + \cdots + \underline{\gamma_{n_1+n_2}}$. Repeat the same procedure until we find no more qualified combined channels.

We summarize the proposed hybrid scheme as a flow chart in Fig. 5.2.

5.4 Average Spectral Efficiency

5.4.1 Conventional Scheme

It can be shown that the BER of M-QAM with Gray coding over an AWGN channel can be approximated by [93]

$$\mathrm{BER}(M_j, \gamma) \approx 0.1 \exp\left(- \frac{3\gamma}{2(2^{j+1} - 1)} \right) \tag{5.3}$$

for all values of M and for BER $< 10^{-3}$. Based on (A.19), the switching thresholds can be obtained as

$$\gamma_{T_j} = \frac{2(1 - 2^{j+1}) \ln(10\mathrm{BER})}{3} \tag{5.4}$$

where BER $\leq 10^{-3}$ and $j = 1, 2, 3, \cdots, K$. Table 1.1 shows the switching thresholds of M-QAM for a target BER 10^{-3}.

In conventional multi-channel systems with the adaptive modulation, transmission is avoided if the SNR of a channel falls below the cutoff threshold. The average spectral efficiency for the L-channel systems can be written as

$$SE^{\text{con}} = \sum_{i=1}^{L} \frac{\sum_{j=1}^{K} R_j^{(i)} P_j^{(i)}}{W} \tag{5.5}$$

where W is the total bandwidth used by the system, $R_j^{(i)}$ is the rate of the ith channel given that the size of the constellation is chosen to be $M = 2^{j+1}$ for $j = 1, \cdots, K$, and $P_j^{(i)}$ is the probability for the ith channel to choose the constellation size $M = 2^{j+1}$ and can be calculated by

$$P_j^{(i)} = F^{(i)}(\gamma_{T_{j+1}}) - F^{(i)}(\gamma_{T_j}). \tag{5.6}$$

$F^{(i)}(x) = \Pr[\gamma_i < x]$ is the outage probability of the ith channel evaluated at x and γ_{T_j} is a threshold for 2^{j+1}-QAM modulation. Note that the cutoff threshold γ_T is the same as γ_{T_1} in Table 1.1. The outage probability is available for various fading channels from the literature so the average spectral efficiency in (5.6) can be easily found for various fading channels.

5.4.2 Hybrid Scheme

The spectral efficiency for L-channel systems with the proposed hybrid scheme can be written as

$$SE^{\text{hyb}} = \sum_{m=0}^{L} \frac{P_{L,m} \cdot SE_{L,m}}{W} \tag{5.7}$$

where $P_{L,m}$ and $SE_{L,m}$ are the probability and the spectral efficiency of the case that m out of L channels have an extreme fading such that their SNR values fall below γ_T, respectively. For i.i.d. fading channels, $P_{L,m}$ and $SE_{L,m}$ in (5.7) can be expressed as

$$P_{L,m} = {}_L C_m \cdot {P_{\text{out}}}^m (1 - P_{\text{out}})^{L-m} \tag{5.8}$$

and

$$SE_{L,m} = \sum_{k=0}^{\lfloor \frac{m}{2} \rfloor} \sum_{\mathbf{n}_k \in \mathbb{N}_k} P_m(k, \mathbf{n}_k) SE_{L,m}(k, \mathbf{n}_k), \tag{5.9}$$

where $P_m(k, \mathbf{n}_k)$ and $SE_{L,m}(k, \mathbf{n}_k)$ are the probability and the spectral efficiency when k qualified combined channels are newly generated under the condition that m out of L channels are cutoff, respectively. In (5.9), we denote $\mathbf{n}_k$ as a vector of which element is the number of actual channels that belongs to each qualified combined channel, $\mathbb{N}_k$ as the set containing all the possible $\mathbf{n}_k$ vectors as its elements, and $\lfloor \cdot \rfloor$ as the floor function. For example, let us suppose that a total of eight channels are available and five channels among them are cutoff ($L = 8, m = 5$). Assuming two qualified combined channels are generated (k=2) due to a diversity combining technique, we easily find that there exist three different $\mathbf{n}_k$s depending on the quality of cutoff channels. Then it can be seen that $\mathbb{N}_k = \{\{2, 3\}, \{3, 2\}, \{2, 2\}\}$, where $\{2, 3\}$ means that the first qualified combined channel consists of two actual cutoff channels and the second comprises three actual cutoff channels. $\{3, 2\}$ and $\{2, 2\}$ can be interpreted in the same way. If $\mathbf{n}_k = \{2, 2\}$, one cutoff channel is left over and will be combined with one of non-cutoff channels, which creates a possibility of achieving a level higher modulation order than the non-cutoff channel by itself.

In the proposed hybrid scheme, we employ MRC over the cutoff channels in order to obtain the combined SNR higher than γ_T instead of dropping them as in the conventional scheme. The number of qualified combined channels generated by means of MRC becomes a random variable depending on the received SNRs of m cutoff channels. Based on the mode of operation, the probability that k qualified combined channels are generated given m cutoff

channels can be written as

$$\begin{aligned} P_m(k,\mathbf{n}_k) =& \Pr\Bigg[\sum_{i=1}^{n_1}\gamma_i \geq \gamma_T, \sum_{i=n_1+1}^{n_1+n_2}\gamma_i \geq \gamma_T, \cdots, \sum_{i=N(k-1)+1}^{N(k)}\gamma_i \geq \gamma_T, \\ & \sum_{i=N(k)+1}^{m}\gamma_i < \gamma_T, \sum_{i=1}^{n_1-1}\gamma_i < \gamma_T, \sum_{i=n_1+1}^{n_1+n_2-1}\gamma_i < \gamma_T, \cdots, \\ & \sum_{i=N(k-1)+1}^{N(k)-1}\gamma_i < \gamma_T \Big| \gamma_1 < \gamma_T, \cdots, \gamma_m < \gamma_T\Bigg], \end{aligned} \tag{5.10}$$

where n_i for $2 \leq n_i \leq m$ is denoted as the number of actual channels for the ith combined channel, $\mathbf{n}_k = \{n_1, \cdots, n_k\}$, and $N(k) = \sum_{i=1}^{k} n_i$. To represent the spectral efficiency in a structural manner, we define

$$\begin{aligned} P_n^- &= \Pr[\sum_{i=1}^{n}\gamma_i < \gamma_T \Big| \gamma_1 < \gamma_T, \cdots, \gamma_n < \gamma_T], \\ P_n^+ &= \Pr[\sum_{i=1}^{n}\gamma_i \geq \gamma_T, \sum_{i=1}^{n-1}\gamma_i < \gamma_T \Big| \gamma_1 < \gamma_T, \cdots, \gamma_n < \gamma_T], \end{aligned} \tag{5.11}$$

where $P_1^- = 1$ and $P_1^+ = 0$. It is easy to see that, for independent channels, P_n^- can be represented as

$$P_n^- = \frac{F_n(\gamma_T)}{\{F(\gamma_T)\}^n}, \tag{5.12}$$

where $F_n(x)$ is the CDF of output SNR of n-branch MRC evaluated at x and $F(x)$ is the CDF of a single channel output SNR evaluated at x. For Rayleigh fading channels, $F(x)$ and $F_n(x)$ are given in Table 2.1 and Table 3.1, respectively. On the other hand, P_n^+ can be written as

$$P_n^+ = \frac{F_{n-1}(\gamma_T)}{\{F(\gamma_T)\}^{n-1}} - \frac{F_n(\gamma_T)}{\{F(\gamma_T)\}^n}. \tag{5.13}$$

Notice that P_n^- and P_n^+ are easily calculated for various fading channels. Using

P_n^+ and P_n^- defined in (5.11), (5.10) can be simplified as

$$P_m(k, \mathbf{n}_k) = P_{n_1}^+ P_{n_2}^+ \cdots P_{n_k}^+ P_{m-N(k)}^-. \tag{5.14}$$

Also note that

$$\sum_{k=0}^{\lfloor \frac{m}{2} \rfloor} \sum_{\mathbf{n}_k \in \mathbb{N}_k} P_m(k, \mathbf{n}_k) = 1, \tag{5.15}$$

which can be rewritten as

$$P_m^- + \sum_{k=1}^{\lfloor \frac{m}{2} \rfloor} \sum_{n_1=2}^{m} \sum_{n_2=2}^{m-n_1} \cdots \sum_{n_k=2}^{m-N(k-1)} P_{n_1}^+ \cdots P_{n_k}^+ P_{m-N(k)}^- = 1, \tag{5.16}$$

where $\lfloor \frac{m}{2} \rfloor$ is the number of maximum possible qualified combined channels, each of which combines two cutoff channels in such cases. (5.16) can be proved using the following expression recursively: $\Pr[\gamma_i < \gamma_T]\Pr[\gamma_j < \gamma_T] = \Pr[\gamma_i + \gamma_j < \gamma_T] + \Pr[\gamma_i + \gamma_j \geq \gamma_T, \gamma_i < \gamma_T, \gamma_j < \gamma_T]$.

On the other hand, the spectral efficiency when k qualified combined channels are generated among m cutoff channels can be written as

$$SE_{L,m}(k, \mathbf{n}_k) = \begin{cases} \sum_{j=1}^{k} SE_{n_j}^- + SE_{m-N(k)+1}^+ (L - m - 1) SE_1, & 0 \leq m < L, \\ \sum_{j=1}^{k} SE_{n_j}^- & m = L, \end{cases} \tag{5.17}$$

where SE_1 is the spectral efficiency of a single channel, which is simply obtained by substituting $L = 1$ into (5.5). The two conditional spectral efficiency expressions, SE_i^+ and SE_i^- in (5.17), are derived in closed-forms as shown in Appendix A.1. Therefore, we can obtain the spectral efficiency of the proposed hybrid system for m cutoff channels as

$$SE_{L,m} = \sum_{k=1}^{\lfloor \frac{m}{2} \rfloor} \sum_{n_1=2}^{m} \sum_{n_2=2}^{m-n_1} \cdots \sum_{n_k=2}^{m-N(k-1)} P_m(k, \mathbf{n}_k) SE_{L,m}(k, \mathbf{n}_k) \tag{5.18}$$

where $P_m(k, \mathbf{n}_k)$ and $SE_{L,m}(k, \mathbf{n}_k)$ are given in (5.14) and (5.17), respectively. In result, the spectral efficiency for the hybrid scheme with L channels can be attained by substituting (5.8) and (5.18) into (5.7).

5.5 Outage Probability

5.5.1 Conventional Scheme

An outage occurs when all the channel SNR values fall into no-transmission region and can be expressed as

$$P^{\text{con}} = \{F(\gamma_T)\}^L, \tag{5.19}$$

where γ_T is the cutoff threshold.

5.5.2 Hybrid Scheme

The outage of the hybrid scheme occurs if all the channels are combined together to get the maximum possible SNR but the combined SNR is below the threshold, that is, $\gamma_1 + \cdots + \gamma_L < \gamma_T$. Thus, the outage probability of the hybrid scheme can be written as

$$P^{\text{hyb}} = F_L(\gamma_T). \tag{5.20}$$

Note that this is the same as the outage probability of the optimal scheme.

5.6 Average Bit Error Rate

5.6.1 Conventional Scheme

The average BER of the traditional scheme, based on the adaptive modulation, can be given as

$$\mathrm{BER}^{\mathrm{con}} = \frac{1}{L}\sum_{i=1}^{L}\sum_{j=1}^{K}\frac{\overline{\mathrm{BER}_{\mathrm{j}}}^{(i)}}{1-F^{(i)}(\gamma_{T_1})} \tag{5.21}$$

where

$$\overline{\mathrm{BER}_{\mathrm{j}}}^{(i)} = \int_{\gamma_{T_j}}^{\gamma_{T_{j+1}}} \mathrm{BER}(M_j,\gamma) f^{(i)}(\gamma) d\gamma, \tag{5.22}$$

where $f^{(i)}(x)$ is the PDF of output SNR of the ith channel evaluated at x. Using the BER approximation in (A.19), we can rewrite (5.22) for i.i.d. Rayleigh fading channels simply as

$$\overline{\mathrm{BER}_{\mathrm{j}}}^{(i)} = \frac{0.1(e^{-b_j\gamma_{T_j}} - e^{-b_j\gamma_{T_{j+1}}})}{b_j\overline{\gamma}} \tag{5.23}$$

where $b_j = \frac{1}{\overline{\gamma}} + \frac{3}{2(2^{j+1}-1)}, j = 1, \cdots, K$.

5.6.2 Hybrid Scheme

The similar approach introduced for deriving the spectral efficiency can also be used for the evaluation of the BER performance. The average BER of the proposed hybrid scheme can be written as

$$\mathrm{BER}^{\mathrm{hyb}} = \sum_{m=0}^{L} P_{L,m} \cdot \mathrm{BER}_{L,m} \tag{5.24}$$

where $P_{L,m}$ is given in (5.8). The average BER when m channels are cutoff out of L available channels is written as

$$\mathrm{BER}_{L,m} = \sum_{k=0}^{\lfloor \frac{m}{2} \rfloor} \sum_{\mathbf{n}_k \in \mathbb{N}_k} P_m(k, \mathbf{n}_k) \mathrm{BER}_{L,m}(k, \mathbf{n}_k). \tag{5.25}$$

where $P_m(k, \mathbf{n}_k)$ is given in (5.14) and

$$\mathrm{BER}_{L,m}(k, \mathbf{n}_k) = \frac{1}{N_{\mathrm{ch}}} \begin{cases} \displaystyle\sum_{j=1}^{k} \mathrm{BER}_{n_j}^{-} + \mathrm{BER}_{m-N(k)+1}^{+} + (L-m-1)\mathrm{BER}_1, & m < L, \\ \displaystyle\sum_{j=1}^{k} \mathrm{BER}_{n_j}^{-}, & m = L, \end{cases} \tag{5.26}$$

where $N_{\mathrm{ch}} = L + k - m$ and $\mathrm{BER}_1 = \sum_{j=1}^{K} \overline{\mathrm{BER}}_k$ is BER of a single channel. Notice that k represents the number of newly generated qualified combined channels and $\mathbf{n}_k = \{n_1, \cdots, n_k\}$ is a vector where n_j is the number of actual channels in the jth qualified combined channels. Two conditional BER expressions introduced above are given as

$$\begin{aligned} \mathrm{BER}_i^{+} &= \sum_{j=1}^{K} \frac{\overline{\mathrm{BER}}_{i,j}^{+}}{1 - F_i(\gamma_{T_1})} \\ \mathrm{BER}_i^{-} &= \sum_{j=1}^{K} \frac{\overline{\mathrm{BER}}_{i,j}^{-}}{1 - F_i(\gamma_{T_1})} \end{aligned} \tag{5.27}$$

where $F_i(x)$ is the CDF of i-branch MRC evaluated at x,

$$\overline{\mathrm{BER}}_{i,j}^{+} = \int_{\gamma_{T_j}}^{\gamma_{T_{j+1}}} \mathrm{BER}(M_j, \gamma) f_i^{+}(\gamma) d\gamma, \tag{5.28}$$

and

$$\overline{\mathrm{BER}}_{i,j}^{-} = \int_{\gamma_{T_j}}^{\gamma_{T_{j+1}}} \mathrm{BER}(M_j, \gamma) f_i^{-}(\gamma) d\gamma. \tag{5.29}$$

Closed-form expressions for $\overline{\text{BER}}_{i,j}^{+}$ and $\overline{\text{BER}}_{i,j}^{-}$ are given in Appendix A.2. Using (5.14) and (5.26), (5.25) can be rewritten as

$$\text{BER}_{L,m} = \sum_{k=1}^{\lfloor \frac{m}{2} \rfloor} \sum_{n_1=2}^{m} \sum_{n_2=2}^{m-n_1} \cdots \sum_{n_k=2}^{m-N(k-1)} P_m(k, \mathbf{n}_k) \text{BER}_{L,m}(k, \mathbf{n}_k). \tag{5.30}$$

Consequently, substituting (5.8) and (5.30) into (5.24), the average BER for the hybrid scheme can be obtained.

5.7 Complexity Analysis

Compared to the conventional system, the diversity-assisted system proposed in this paper needs to make additional efforts in order to find the configuration of channels that provides the maximum spectral efficiency. Therefore, the complexity of these systems is quantified in terms of the maximum number of search required to find the best channel configuration in the worst cases.

5.7.1 Optimal Scheme

Since all the possible chances of combining channels among all available channels are considered, the number of search that needs to be conducted for the configuration of channels with the maximum spectral efficiency is the sum of a number of multinomial coefficients without knowledge of order. Thus, the complexity of the optimal scheme can be written as

$$N^{\text{opt}} = \sum_{\substack{n_1, n_2, \cdots, n_L \geq 0 \\ n_1+n_2+\cdots+n_L=L \\ n_1 \geq n_2 \geq \cdots \geq n_L}} \frac{L!}{n_1! n_2! \cdots n_L!} \frac{1}{d_1! \cdots d_K!} \tag{5.31}$$

where $d_1, \cdots, d_K$ are the number of duplicated positive integers in $\{n_i\}_{i=1}^{L}$, each of which is equivalent to the number of channels in each combined channel. For instance, for $L = 6$, $\{n_1, n_2, n_3, n_4, n_5, n_6\} = \{2, 1, 1, 1, 1, 0\}$ and $\{1, 0, 1, 2, 1, 1\}$ are equivalent and in this case $d_1 = 4$. For a large L, with

the help of Stirling's approximation for the factorial function, logarithm of the complexity can be approximated simply as

$$\log N^{\text{opt}} \approx \frac{L}{2} \log L. \tag{5.32}$$

5.7.2 Hybrid Scheme

The hybrid scheme reduces considerably the amount of complexity compared to the optimal scheme due to two facts. First, only the cutoff channels are considered for combining. Second, the number of channels to be combined in the combined channels $\{n_i\}_{i=1}^{K}$ are sequentially determined. It is the same as a binary tree where a branch is selected in each level and the other is pruned. Since a comparison occurs every level in the binary tree, the number of levels required to reach the conclusion can be considered as the complexity. Thus, the complexity of the hybrid scheme can simply be derived as

$$\log N^{\text{hyb}} = \log L. \tag{5.33}$$

5.8 Numerical Results

Fig. 5.3 shows the average spectral efficiency of the conventional scheme, the hybrid scheme, and the optimal scheme with six orthogonal channels as a function of average channel SNR. The spectral efficiency of the continuous rate system is also plotted. Continuous rate means that the number of bits per symbol is not restricted to integer values. Although continuous rate M-QAM is possible [94], discrete rate M-QAM is more practical, where the constellation size is limited to 2^n for a positive integer number n [92]. For the verification of our analytic results, the spectral efficiency of both the conventional scheme and the hybrid scheme are simulated and presented in the figure. The simulated spectral efficiency of the optimal scheme is also plotted for a comparison with the hybrid scheme. As clearly seen in the figure, both optimal and hybrid

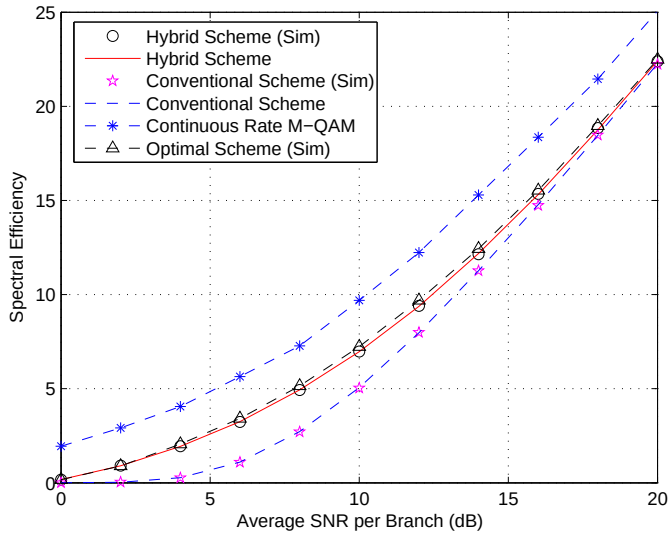

Figure 5.3: Average spectral efficiency of the optimal scheme and hybrid scheme ($L = 6$)

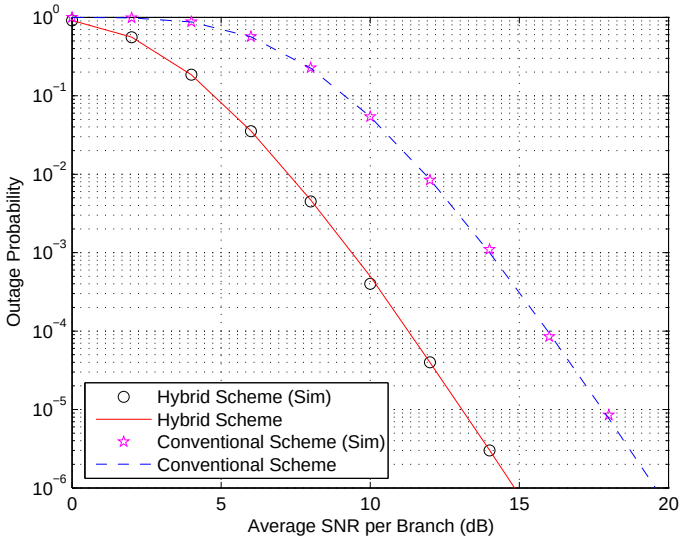

Figure 5.4: Outage probability of the optimal scheme and hybrid scheme ($L = 6$).

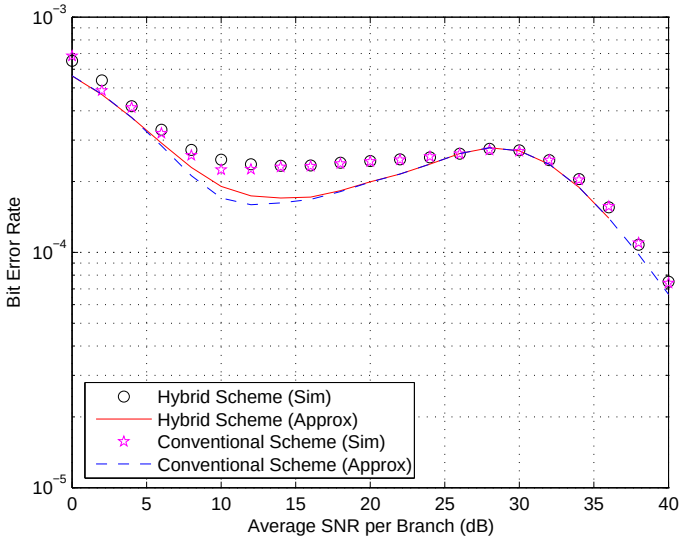

Figure 5.5: Average bit error probability of the optimal scheme and hybrid scheme ($L = 6$).

scheme provide noticeable spectral efficiency gain over the conventional scheme in the low average SNR region. This is due to the fact that both schemes take advantage of a diversity combining technique, whereas the conventional scheme avoids transmission over cutoff channels. Hence, the hybrid scheme exploits tradeoff between diversity among channels and overall data rate with little complexity overhead. We can also see from this figure that the performance of the hybrid scheme is very close to that of the optimal scheme.

Fig. 5.4 compares the outage probability of the hybrid scheme with that of conventional scheme. Simulation results are also plotted to verify the analytical results. As shown in this figure, the hybrid scheme offers almost 5dB gain over the conventional scheme for $L = 6$, which is easily understood by the fact that the hybrid scheme can attain some spectral efficiency gain owing to a diversity combining technique even though all the channels are cutoff.

The BER performance of the hybrid scheme for a target BER of 10^{-3} is illustrated in Fig. 5.5 along with that of the conventional scheme for compar-

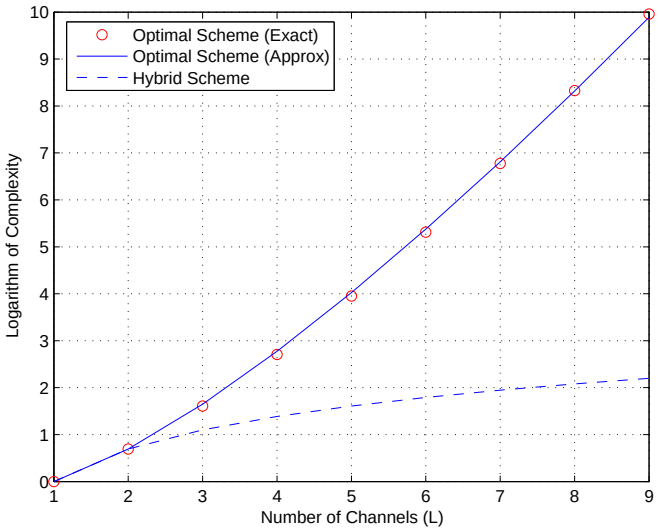

Figure 5.6: Comparison of the complexity of the optimal scheme and hybrid scheme.

ison. The BER results based on the approximation are plotted together with simulation results for verification. Since the BER approximation for M-QAM, which is shown in (A.19), is tight at high SNR region, the analytical BER calculation shows an exact match with simulation result, although a small difference is found at low SNR region due to the approximation. Since the hybrid scheme combines cutoff channels to make combined SNR to meet γ_T, which is set for BER of 10^{-3}, the hybrid scheme achieves extra spectral efficiency with no additional BER degradation.

The optimal scheme and the hybrid scheme achieve the spectral efficiency gain over the conventional scheme at the cost of additional complexity, which involves examination of the quality of cutoff channels. Fig. 5.6 compares the complexity of the optimal scheme and the proposed hybrid scheme. Since the optimal scheme performs an exhaustive search over all the channels, its complexity is prohibitive, whereas the hybrid scheme shows a linear function between complexity and the number of channels due to its sequential operation. Therefore, the difference between the optimal scheme and the

Cell radius	1 km	
Carrier frequency	2.3 GHz	
Propagation model	129.68 + 30 $\log_{10}$ (r)	
Transmission SNR	134.68 dB	
Interference model	Log-normal	
Standard deviation of shadowing	8 dB	
Number of cells	18 (6 1st tier cells & 12 2nd tier cells)	
Subcarrier bandwidth	11.16 kHz	
Coding	No coding	
Modulation	BPSK, QPSK, 16-QAM, 64-QAM	
System bandwidth	1.25 MHz	5 MHz
FFT size	128	512
Number of data subcarriers	96	384

Table 5.1: WiMAX simulation parameters

hybrid scheme is significant because of the two facts described previously. It also shows that (5.32) is a very tight approximation to (5.31). As the number of channels increases, the optimal scheme requires an exponential complexity whereas the hybrid scheme shows a linear function.

5.9 Simulation in a Practical Scenario

In order to evaluate the proposed scheme in a realistic scenario, the hybrid scheme is integrated with a practical system for simulation.

5.9.1 802.16 WiMAX System Environment

Table 5.1 summarizes the parameters used in the simulation, where some of them are adopted from a WiMAX standard [95]. Interference from other cells is modelled by log-normal distribution, which is a common assumption in a multi-cellular environment. First tier as well as second tier cells are considered for interference, where 18 cells exist in the simulation. WiMAX

j	modulation	γ_{T_j} [dB]
1	BPSK	6.80
2	QPSK	9.64
3	16-QAM	16.63
4	64-QAM	22.86

Table 5.2: Constellation and switching thresholds for simulation

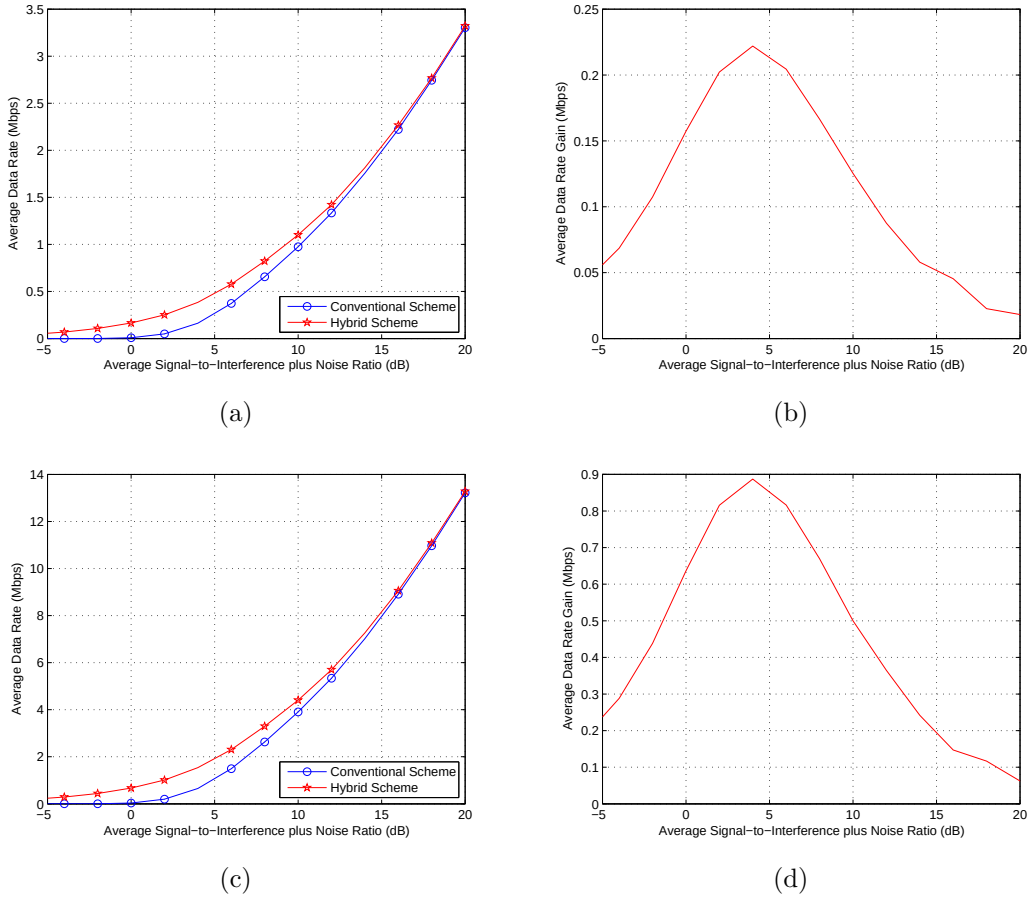

Figure 5.7: (a) Average data rate and (b) average data rate gain of the hybrid scheme over the conventional scheme in a WiMAX system environment with 1.25 MHz system bandwidth, and (c) average data rate and (d) average data rate gain in a WiMAX system environment with 5 MHz system bandwidth.

provides a scalable system bandwidth of $1.25 \sim 20$ MHz, but in this simulation we only consider 1.25 and 5 MHz system bandwidths. Simulation with other system banwidth can be easily performed by a simple parameter change. Table 5.2 shows the constellation and switching thresholds used in the simulation.

Fig. 5.7(a) compares the average data rate of the hybrid scheme and the conventional scheme in a WiMAX system environment with system bandwidth of 1.25 MHz. The average data rate gain of the hybrid scheme over that of the conventional scheme is illustrated in Fig. 5.7(b). Similarly, Fig. 5.7(c) and Fig. 5.7(d) show the average data rate and average data rate gain of the hybrid scheme for WiMAX with system bandwidth of 5 MHz. As described previously, the hybrid scheme shows a considerable gain in terms of the average data rate in low SNR region and, therefore, improves cell-edge link budget if used in a cellular environment. Interestingly, it is observed that the gain has a peak at average SNR around 5dB. The reason of this phenomenon can be simply explained as follows. The main idea of the hybrid scheme is to use diversity combining among subcarriers if necessary, which can offer higher spectral efficiency compared to the conventional scheme where each subcarrier transmits independent information. For an extremely low SNR (ex. -5 dB), however, even though multiple subcarriers are all combined together, the combined SNR may not be able to meet γ_T^1, which is the lowest SNR threshold in the adaptive modulation, and is thus still in the outage SNR region with a high probability. Therefore, we can see that the hybrid scheme performs best for a fairly low SNR (around 5dB).

Fig. 5.8 shows spatially averaged data rate gain of the hybrid scheme over the conventional scheme as a function of cell radius. As the cell radius increases, interference power from other cells decreases, which becomes noise-limited channel. On the other hand, as the cell radius decreases, interference power is dominant and noise power can be ignored, which is interference-limited. From the figure, it is clear that the proposed scheme provides a considerable data rate gain on average. Furthermore, the proposed system performs more effectively in an interference-limited channel environment.

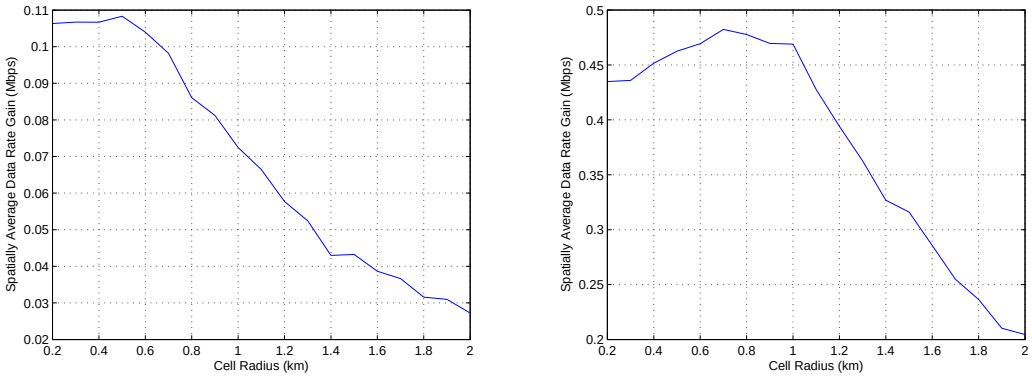

(a) (b)

Figure 5.8: Average data rate gain of the hybrid scheme over the conventional scheme in a multi-cellular WiMAX environment with (a) 1.25 MHz system bandwidth, and (b) 5 MHz system bandwidth.

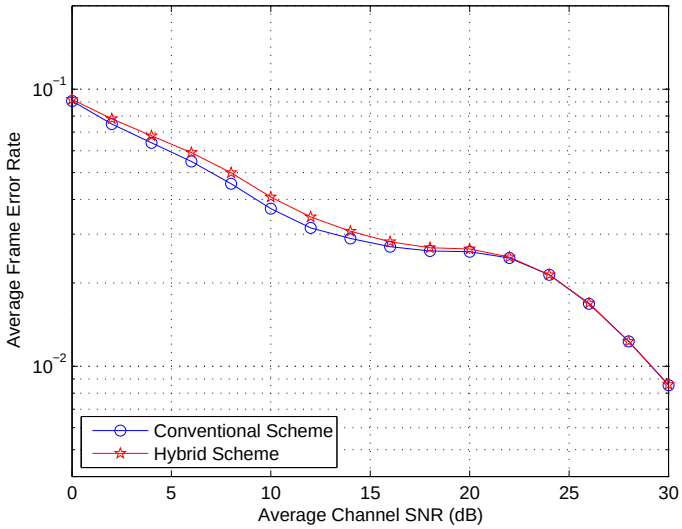

Figure 5.9: Average Frame Error Rate of the hybrid scheme and the conventional scheme in a WiMAX system environment with 1.25 MHz system bandwidth.

Fig. 5.9 depicts the average frame error rate of both the hybrid scheme and the conventional scheme for WiMAX with system bandwidth of 1.25 MHz, where a frame consists of 200 bits.

5.10 Conclusion

Multi-channel systems with joint adaptive modulation and diversity combining are studied in this paper. First an optimal scheme (in the spectral efficiency sense) is studied and discussed. In addition, a sub-optimal hybrid scheme is proposed and analyzed in terms of average spectral efficiency and average BER performance. Numerical results show that the hybrid scheme delivers almost the same spectral efficiency as that of the optimal scheme with a significant reduction in complexity. In addition, the hybrid scheme delivers considerable spectral efficiency gain at the cost of a small amount of complexity. Negligible difference is observed between the hybrid scheme and the conventional scheme in terms of BER and PER performance.

Chapter 6

Joint Switched Diversity and Adaptive Modulation

6.1 Introduction

An unprecedented hunger for high data rate is not only a phenomenon that is occuring in wireless cellular networks. Indeed due to an overwhelming number of high quality videos, audios, and pictures, and a variety of personal portable devices for them, connectivity with reliability and high data rate is even more important in WPAN applications. A WPAN interconnects devices centered around an individual person's workspace over wireless connection. The technology for WPAN is still in its infancy and is undergoing rapid development. Ultra wideband (UWB) and millimeter wave communications are the physical layer candidates for the IEEE 802.15 task group 3 (TG3) WPAN standard.

For such WPAN applications, reliability of the connection is a crucial requirement. In this regard, multiple antennas with diversity transmission are a must-have technology for WPAN system designers. However, multiple antennas with multiple RF chains require high complexity in hardware as well as an increased processing power budget. Since the WPAN is optimized for low-cost and low-power consumption, multiple RF chains may not be a

good choice although an optimum performance can be achieved. Therefore, an antenna selection scheme with multiple antennas and a single RF chain is highly desirable.

Among the various antenna selection algorithms, a switched diversity scheme with adaptive modulation offers a good performance and complexity tradeoff. As described in Chapter 3, a switched diversity combining scheme is a good cadidate for systems in which multiple RF chains are too expensive. It is equipped with multiple antennas but a single RF chain such that an antenna with an acceptable channel quality is selected for signal reception. If the signal quality of the current antenna falls below a per-determined fixed threshold, then another antenna with its channel quality higher than the threshold is sought. Furthermore, wireless channel always has some time correlation, which can be characterized by Doppler frequency. In other words, it is sometimes very likely the current antenna will again be selected in the next antenna selection process due to the channel time correlation. How often antenna selection occurs depends on the channel coherence time and, thus, time slot duration and switching threshold need to be designed properly based on the channel coherence time and characteristics. Given non-zero time correlation, switched diversity schemes can provide reduced channel estimation overhead as well as low-processing complexity, compared to the case of selecting the best antenna in every time slot, which incurs channel quality measurement of all antennas.

In addition, discrete modulation levels in adaptive modulation allow for some degree of freedom in antenna selection. It is clear from the viewpoint of overall spectral efficiency that the spectral efficiency acquired by the antenna with the highest channel quality is the same as the spectral efficiency acquired by selecting any antenna that belongs to the modulation level for the best antenna. Motivated by this, we show in this chapter how a switched diversity scheme can be jointly used with adaptive modulation depending on several optimization goals. The beauty of this scheme is that a simple change of the switching threshold allows the receiver to adaptively adjust its mode of

operation contingent upon the goal and availability of resources.

The idea of a switched diversity scheme can be readily extended to a multiuser scheduling, where the scheduler selects a single user for data transmission based on the users' channel quality in a time-division multiplexing fashion to achieve multiuser diversity [15, 96, 97]. In a multiuser scenario, one of the major impacts on performance is the feedback load and feedback rate. To be able to take advantage of maximum multiuser diversity, a base station needs feedback from all the users. Since each user does not know the channel quality of other users, a current system like Qualcomm's High Data Rate (HDR) requires a base station to collect feedbacks from all the users [71].

Various scheduling schemes aiming at reducing feedback load while exploiting multiuser diversity gain are discussed in the literature [98–104]. A popular way to reduce the number of feedbacks is by using a channel SNR threshold, where only the users who have a channel quality higher than the threshold send feedback to the scheduler. The selective multiuser diversity (SMUD) algorithm in [105] shows that the feedback load is significantly reduced by using such a threshold. Later in this chapter, we show how the switched diversity scheme with adaptive modulation analyzed previously can also be used in a multiuser scenario.

6.2 Switched Diversity Systems with Adaptive Modulation

Suppose a user has diversity branches numbered $1 \sim L$ in an arbitrary order. Each of the diversity branches may correspond to a receive antenna that captures a replica of the transmitted signal. We assume i.i.d. fading channels.

The switched diversity schemes can be combined with adaptive modulation in multiple ways. Depending on the primary goal, the switched diversity scheme can change its mode of operation from a bandwidth efficient scheme to a power efficient scheme, or vice versa, by a simple change of the switching

threshold. The system can even adaptively change its mode of operation over time based on the channel state or available resources, such as battery power.

6.2.1 Spectral Efficiency Maximizing Scheme

The spectral efficiency maximizing scheme aims at maximizing performance with less complexity or switching overhead. Note that the number of switching in this system is equivalent to the number of channel estimation.

Mode of operation

The mode of operation is as follows. The user first estimates the first antenna. If the signal quality of the first antenna exceeds the highest SNR threshold for adaptive modulation, denoted by γ_T^N, then the first antenna is selected for signal reception. Otherwise, it switches to the second antenna and sees if its signal quality can support the highest modulation order. If so, the second antenna is selected, or it again switches to the third antenna. It continues switching until it finds an antenna where the highest modulation can be assigned. If all the antennas do not satisfy γ_T^N, then the best antenna compared to others is selected and the modulation order it can support is chosen for transmission. As long as an antenna that supports the highest modulation is found during this selection process, this antenna is selected for signal reception and the estimation of the rest of the antennas is not performed and thus no further switching occurs. By doing this, the number of estimation can be reduced while the maximum possible spectral efficiency is still achieved if compared to the selection diversity scheme where all the antennas are measured prior to user selection.

Statistics

Based on the mode of operation described above, we found that its operation becomes the same as the SECps scheme [58] with γ_T^N as its SNR threshold.

The CDF of output SNR is written as

$$F(x) = \begin{cases} \Pr[\gamma_T^N \leq \gamma_1 < x] + \Pr[\max\{\gamma_1, \cdots, \gamma_L\} < \gamma_T^N] \\ \quad + \sum_{i=2}^{L} \Pr[\max\{\gamma_1, \cdots, \gamma_{i-1}\} < \gamma_T^N, \gamma_T^N \leq \gamma_i < x], & x \geq \gamma_T^N \\ \Pr[\max\{\gamma_1, \cdots, \gamma_L\} < x], & x < \gamma_T^N. \end{cases} \tag{6.1}$$

For i.i.d. channels, (6.1) can be written as

$$F(x) = \begin{cases} 1 - \dfrac{1 - (F_\gamma(\gamma_T^N))^L}{1 - F_\gamma(\gamma_T^N)}\{1 - F_\gamma(x)\}, & x \geq \gamma_T^N \\ [F_\gamma(x)]^L, & x < \gamma_T^N, \end{cases} \tag{6.2}$$

where $F_\gamma(x)$ and $f_\gamma(x)$ are the CDF and PDF of the output SNR in a single receive antenna evaluated at x, respectively. Differentiating (6.2) with respect to x, the PDF of combined SNR is given by

$$f(x) = \begin{cases} \dfrac{1 - (F_\gamma(\gamma_T^N))^L}{1 - F_\gamma(\gamma_T^N)} f_\gamma(x), & x \geq \gamma_T^N \\ L[F_\gamma(x)]^{L-1} f_\gamma(x), & x < \gamma_T^N. \end{cases} \tag{6.3}$$

Average Spectral Efficiency

Switched diversity scheme can achieve as much spectral efficiency as seletion diversity scheme offers owing to the discreteness inherent to adaptive modulation. Notice that the selection diversity scheme is a switched diversity scheme with an optimum threshold. From the standpoint of output spectral efficiency, it does not make any difference which antenna is selected as long as the selected antenna has its received SNR higher than γ_T^N such that the highest modulation order can be adopted. Higher received SNR in general brings a lower BER, but this is not necessary since adaptive modulation already guarantees the target BER. Hence, discreteness of adaptive modulation provides certain degree of freedom allowing to tradeoff the spectral efficiency and switching overhead or

power consumption. The average output spectral efficiency is written as

$$\text{ASE} = \sum_{n=1}^{N} SE_n \int_{\gamma_T^n}^{\gamma_T^{n+1}} f(x)dx, \tag{6.4}$$

where $\gamma_T^0 = 0$, $\gamma_T^{N+1} = \infty$, and SE_n is the spectral efficiency of the nth SNR region in the adaptive modulation. Substituting (6.3) into (6.4), the average spectral efficiency is simply represented with a closed-form as

$$\text{ASE} = SE_N\{1 - (F_\gamma(\gamma_T^N))^L\} + \sum_{n=1}^{N-1} SE_n\{[F_\gamma(\gamma_T^{n+1})]^L - [F_\gamma(\gamma_T^n)]^L\} \tag{6.5}$$

Average Bit Error Performance

The bit error rate of M-QAM modulation with Gray encoding at high SNR region is tightly approximated by [11].

$$\text{BER}_n(x) \approx a_n Q(\sqrt{b_n x}), \tag{6.6}$$

where $n = \log_2 M$. For M-QAM modulations, a_n and b_n are simply given by [24]

$$a_n = \frac{2(\sqrt{2^n} - 1)}{n\sqrt{2^n}}, \quad b_n = \frac{3}{2^n - 1}. \tag{6.7}$$

The average bit error rate of the spectral efficiency maximizing scheme can be written as

$$\text{ABER} = \frac{1}{1 - (F(\gamma_T^1))^L} \sum_{n=1}^{N} \int_{\gamma_T^n}^{\gamma_T^{n+1}} \text{BER}_{n+1}(x) f(x) dx. \tag{6.8}$$

Using (6.3) and (6.6), we can rewrite (6.8) as

$$\begin{aligned}\text{ABER} =& \frac{1}{1-(F_\gamma(\gamma_T^1))^L}\Bigg\{\frac{1-(F_\gamma(\gamma_T^N))^L}{1-F_\gamma(\gamma_T^N)}a_{N+1}\int_{\gamma_T^N}^{\infty} Q(\sqrt{b_{N+1}x})f_\gamma(x)dx \\ &+ L\sum_{n=1}^{N-1} a_{n+1}\int_{\gamma_T^n}^{\gamma_T^{n+1}} Q(\sqrt{b_{n+1}x})[F_\gamma(x)]^{L-1}f_\gamma(x)dx\Bigg\}.\end{aligned} \tag{6.9}$$

Average Antenna Switching Overhead

The average antenna switching overhead is simply written as

$$\begin{aligned}\text{ASO} &= \sum_{i=0}^{L-1}(i+1)(F(\gamma_T^N))^i\{1-F(\gamma_T^N)\} + L(F(\gamma_T^N))^L \\ &= \frac{1-(F(\gamma_T^N))^L}{1-F(\gamma_T^N)}.\end{aligned} \tag{6.10}$$

6.2.2 Antenna Switching Minimizing Scheme

The antenna switching minimizing scheme intends to minimize the antenna switching overhead, or equivalently the number of channel estimation.

Mode of operation

The mode of operation is similar to the previous scheme. The first antenna is estimated and used with the highest modulation level it can support. If the first antenna has the received SNR lower than γ_T^1, which is an outage case, then switching to the next antenna occurs. The second antenna is then estimated and used with its highest modulation level. If another outage takes place, then this procedure continues with the third antenna until total outage over all the antennas occurs. Based on the mode of operation, its operation is identical to SECps with γ_T^1 as SNR threshold.

Statistics

The CDF is written as

$$F(x) = \begin{cases} \Pr[\gamma_T^1 \le \gamma_1 < x] + \Pr[\max\{\gamma_1, \cdots, \gamma_L\} < \gamma_T^1] \\ \quad + \sum_{i=2}^{L} \Pr[\max\{\gamma_1, \cdots, \gamma_{i-1}\} < \gamma_T^1, \gamma_T^1 \le \gamma_i < x], & x \ge \gamma_T^1 \\ \Pr[\max\{\gamma_1, \cdots, \gamma_L\} < x], & x < \gamma_T^1. \end{cases} \tag{6.11}$$

For i.i.d. channels, (6.11) can be written as

$$F(x) = \begin{cases} 1 - \dfrac{1 - (F_\gamma(\gamma_T^1))^L}{1 - F_\gamma(\gamma_T^1)}\{1 - F_\gamma(x)\}, & x \ge \gamma_T^1 \\ [F_\gamma(x)]^L, & x < \gamma_T^1 \end{cases} \tag{6.12}$$

where $F_\gamma(x)$ and $f_\gamma(x)$ are the CDF and PDF of the output SNR in a single receive antenna evaluated at x, respectively. Differentiating (6.12) with respect to x, the PDF of the combined SNR is given as

$$f(x) = \begin{cases} \dfrac{1 - (F_\gamma(\gamma_T^1))^L}{1 - F_\gamma(\gamma_T^1)} f_\gamma(x), & x \ge \gamma_T^1 \\ L[F_\gamma(x)]^{L-1} f_\gamma(x), & x < \gamma_T^1 \end{cases} \tag{6.13}$$

Average Spectral Efficiency

Similarly, using (6.4) and (6.13), the average spectral efficiency is simply represented with the closed-form expression given by

$$\text{ASE} = \frac{1 - (F_\gamma(\gamma_T^1))^L}{1 - F_\gamma(\gamma_T^1)} \sum_{n=1}^{N} SE_n\{F_\gamma(\gamma_T^{n+1}) - F_\gamma(\gamma_T^n)\}. \tag{6.14}$$

Average Error Performance

The average symbol error rate of the scheme can be written as

$$\text{ABER} = \frac{1}{1 - F(\gamma_T^1)} \left\{ \sum_{n=1}^{N} a_{n+1} \int_{\gamma_T^n}^{\gamma_T^{n+1}} Q(\sqrt{b_{n+1} x}) f_\gamma(x) dx \right\}. \tag{6.15}$$

Average Antenna Switching Overhead

The average antenna switching overhead is simply written as

$$\text{ASO} = \frac{1 - (F(\gamma_T^1))^L}{1 - F(\gamma_T^1)}. \tag{6.16}$$

6.2.3 Adaptive Scheme with Optimum Threshold

For switched diversity schemes, care must be taken for determining the switching threshold, which is an important system design issue. For instance, a high threshold results in an undesirably increased number of antenna switching, whereas a poor diversity gain is obtained for a low threshold. Therefore, this Section introduces an adaptive scheme where the switching threshold is adaptively adjusted according to the average channel quality.

Optimum Threshold

Unlike switch and stay combining (SSC), switched combining with post-examining selection (SECps) does not have a finite optimum threshold for minimizing BER performance since it operates as selection combining when none of the antennas meet the switching threshold. To manageably approach this problem, we introduce a value, denoted by ϵ, to represent the closeness to the optimum value. Consequently, the optimum threshold, denoted by γ_T^{opt}, for

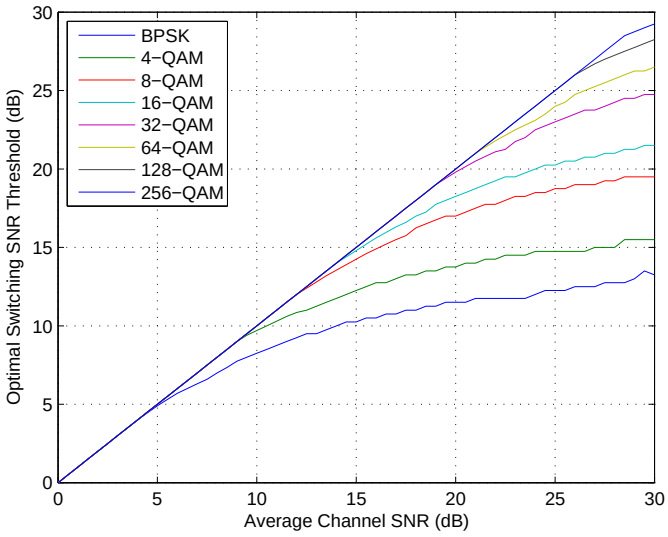

Figure 6.1: Optimum switching threshold for SECps with multiple modulation levels

minimizing the BER performance is defined in this case by

$$\begin{aligned}&\int_0^{\gamma_T^{\text{opt}}} f_{SC}(x)\text{BER}(x)dx + \frac{1-(F_\gamma(\gamma_T^{\text{opt}}))^L}{1-F_\gamma(\gamma_T^{\text{opt}})}\int_{\gamma_T^{\text{opt}}}^{\infty} f_\gamma(x)\text{BER}(x)dx \\ &= (1+\epsilon)\int_0^{\infty} f_{SC}(x)\text{BER}(x)dx,\end{aligned} \tag{6.17}$$

where $f_{SC}(x)$ is the PDF of SC evaluated at x. Fig. 6.1 depicts optimum threshold values for SECps with various modulation levels as a function of average channel SNR when $\epsilon = 2 \cdot 10^{-2}$. For each modulation level, the optimal threshold is represented as a log-like function over average channel SNR. However, it is not surprising that optimum threshold is proportional to average channel SNR when multiple modulation levels are taken in consideration.

After some numerical calculation, we found that optimal threshold for SECps with multiple modulation levels can be simply approximated as

$$\gamma_T^{\text{opt}} \approx \overline{\gamma}, \tag{6.18}$$

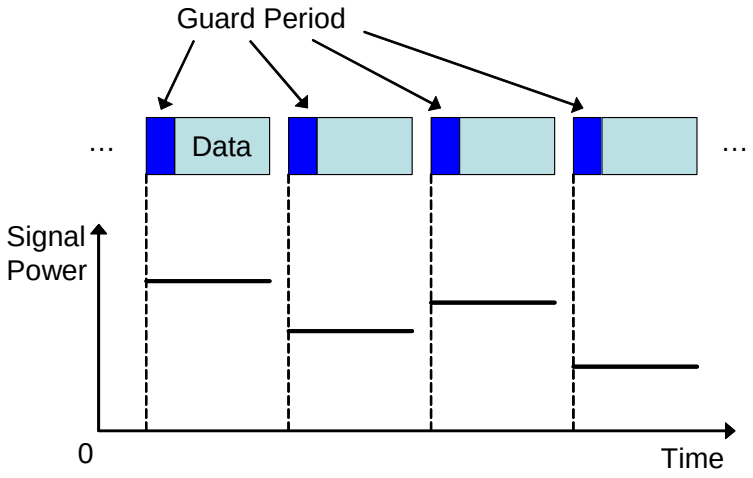

Figure 6.2: A discrete time division multiplexing system over block fading channels.

which can be seen in Fig. 6.1. The average spectral efficiency, average number of channel estimation, and average BER performance of this adaptive scheme with optimum threshold are illustrated in Section 6.6.1.

6.3 Switch-based Multiuser Scheduling

6.3.1 System Model

We consider a discrete time division multiple access system for multiuser communications as shown in Fig. 6.2. In every time slot, only one user is selected by the base station or access point and the given power budget is fully used for the selected user in the time slot. Every time slot has a short guard band followed by a data burst. The proper design of the duration of time slot based on the channel coherence time and a scheduling algorithm will enjoy high multiuser diversity order and offer a high overall performance. Each user uses either the spectral efficiency maximizing scheme or the antenna switching minimizing scheme that we described previously. Suppose a transmitter with a single antenna and K users each with multiple antennas. Let L_k denote the

total number of receive antennas for the kth user. In addition to the efficient usage of bandwidth and power for each user, multiuser scenario involves user scheduling strategies. We also assume a backlogged model, where each user always has data to transmit. Consequently, the scheduler can make a decision only based on the channel quality of the users.

In this Section, we take a switch-based scheduling scheme in consideration, where any user whose received SNR is higher than the given SNR threshold is selected. A switch-based scheduling scheme along with the adaptive modulation offers some degrees of freedom in user selection, resulting in the efficient use of bandwidth or power resources. In a similar fashion as in the switched diversity with adaptive modulation in a single user case, any user who falls in the channel SNR region that the best user belongs to can be selected while achieving the same overall spectral efficiency. By doing this, some reduced complexity in the scheduler can be obtained.

6.3.2 Switch-based Scheduling

The maximum overall system spectral efficiency can be achieved by the opportunistic scheme where the user with the highest signal quality is always selected for every time slot. It is straightforward to see that the opportunistic scheme in this scenario is identical to the user scheduling based on the selection diversity used in every time slot.

When the adaptive modulation with discrete modulation levels is used, multiple users possibly belong to the same modulation level. In such cases, it does not make any difference from the viewpoint of the spectral efficiency if the scheduler selects any user among since they will all adopt the highest modulation level. This approach can even offer reduced processing complexity for the scheduler and, more importantly, reduced feedback load.

The switch-based scheme selects any user who meets the given condition among the randomly ordered users. When a user is found, it no longer investigates other users. The users are shuffled in a randomly basis every time

the selection is carried out. Since it stops measuring the rest of the user's signal as soon as a qualified user is found, the number of estimation is much less than that of the opportunistic scheme. Since the channel estimation involves in general an increase in the bandwidth as well as in the amount of feedback, it is highly desirable to minimize the number of channel estimation in closed-loop wireless systems.

Depending on the optimization goal, we can tradeoff the overall spectral efficiency and feedback load, or equivalently processing complexity, in switch-based schemes by a simple change of the switching threshold, which are introduced in what follows.

6.3.3 Overall System Spectral Efficiency Maximizing Scheme

This scheme can also be called as the bandwidth efficient scheme or the performance maximing scheme. This scheme aims at maximizing the overall system spectral efficiency with less switching overhead in a multiuser environment.

Mode of operation

The overall system spectral efficiency maximizing scheme (OSSEMax) operates as follows. The users are ordered in an arbitrary fashion. First, the BS probes the first user. If the first user can support the highest modulation order, then the first user is selected for the current time slot. Otherwise, the BS switches to the second user and check if the second user can support the highest modulation. If so, then the second user is serviced. If not, the BS switches again this time to the third user. The BS keeps switching between users until it finds a user who can support the highest modulation and assigns the current time slot to this user. Every user sends a single bit feedback notifying whether or not it can support the highest modulation. If none of the users can adopt the highest modulation, then the BS requests the users another type of feedback that contains the highest modulation each user can support. Based on the feedback from all the users, the BS selects a user who

can support the highest modulation compared to other users.

Average System Spectral Efficiency

Based on the mode of operation, the average system spectral efficiency for the OSSEMax scheme with K users, where the ith user is equipped with L_i antennas, is written as

$$\text{ASE} = \sum_{n=1}^{N} SE_n \sum_{k=1}^{K} \binom{K}{k} \prod_{i=1}^{k} \{F_i(\gamma_T^{n+1}) - F_i(\gamma_T^n)\} \prod_{j=k+1}^{K} F_j(\gamma_T^n) \tag{6.19}$$

where $F_i(x)$ is the CDF of output SNR for the ith user evaluated at x. Since all the users perform the spectral efficiency maximizing scheme, the average system spectral efficiency is obtained by substituting (6.2) into (6.19).

$$\text{ASE} = \sum_{n=1}^{N} SE_n \sum_{k=1}^{K} \binom{K}{k} \prod_{i=1}^{k} \{[F_{\gamma_i}(\gamma_T^{n+1})]^{L_i} - [F_{\gamma_i}(\gamma_T^n)]^{L_i}\} \prod_{j=k+1}^{K} [F_{\gamma_j}(\gamma_T^n)]^{L_j} \tag{6.20}$$

where $F_{\gamma_i}(x)$ and $f_{\gamma_i}(x)$ are the CDF and PDF of a single channel of the ith user evaluated at x. If all the users have the same number of receive antennas, i.e., $L_k = L$ for $k = 1, \cdots, K$, then (6.20) can be simplified as

$$\text{ASE} = \sum_{n=1}^{N} SE_n \sum_{k=1}^{K} \binom{K}{k} \{[F_\gamma(\gamma_T^{n+1})]^L - [F_\gamma(\gamma_T^n)]^L\}^k [F_\gamma(\gamma_T^n)]^{L(K-k)}. \tag{6.21}$$

Using the binomial distribution, We can rewrite (6.21) as

$$\text{ASE} = \sum_{n=1}^{N} SE_n \{[F_\gamma(\gamma_T^{n+1})]^{LK} - [F_\gamma(\gamma_T^n)]^{LK}\}. \tag{6.22}$$

It is interesting to note from the mathematical standpoint that this scheme can be viewed as a single user applying SECps with KL antennas and γ_T^N as its SNR threshold.

6.3.4 Feedback Load and Antenna Switching Minimizing Scheme

Another extreme case is considered to serve as the lower bound on performance with the highest processing complexity savings. This scheme can also be called as the energy efficient scheme, since it aims at minimizing both feedback load and antenna switching overhead for a user in a multiuser environment.

Mode of operation

The feedback load and antenna switching minimizing scheme (FLASMin) schedules a random user yielding any modulation level for transmission. First, the scheduler selects a random user. The selected user even chooses a random antenna for signal reception. If this antenna undergoes an outage, then the user selects another antenna unless the received SNR is below the outage SNR threshold. If this selected user suffers from an total outage over all its available antennas, then another randomly selected user, excluding the previously selected user(s), is investigated and this user SNR is checked against the outage threshold. The same procedure continues until the scheduler finds any user who can support any modulation order.

Average System Spectral Efficiency

According to the mode of operation, the average system spectral efficiency for the FLASMin scheme is written as

$$\text{ASE} = \sum_{n=1}^{N} SE_n \sum_{k=0}^{K-1} \prod_{i=1}^{k} F_i(\gamma_T^1)\{F_{k+1}(\gamma_T^{n+1}) - F_{k+1}(\gamma_T^n)\}. \tag{6.23}$$

If all the users have the same number of receive antennas, then the average system spectral efficiency is derived by substituting (6.12) into (6.23) as

$$\text{ASE} = \sum_{n=1}^{N} SE_n \frac{1 - [F_\gamma(\gamma_T^1)]^{LK}}{1 - F_\gamma(\gamma_T^1)}\{F_\gamma(\gamma_T^{n+1}) - F_\gamma(\gamma_T^n)\}. \tag{6.24}$$

Again, this scheme can be viewed as a single user applying SECps with KL antennas and γ_T^1 as its SNR threshold.

6.3.5 Trade-off Scheme

Some mobile devices may be equipped with four antennas and have powerful processor(s), whereas other devices may only have a single antenna with limited processing power. Some devices may support high quality video applications, while others only allow low data rate applications. Those powerful devices sometimes may require a power saving mode to maintain a long operating hour. Under these variety of different circumstances, each user may set or adaptively change its operating mode based on the availability of the given resource budget. Additionally, the scheduler can set a user-specific threshold for each user such that a fairness based on each user's condition and requirement can be obtained. However, this user-specific threshold requires an extensive knowledge of each user's channel statistics.

In this Section, we consider a simple and practical scheduler that has a common switching threshold for all the users. Only the users who have a higher received SNR than the threshold send a feedback to the scheduler. Furthermore, for simplicity we assume that all the users belong to the same service class and take a spectral efficiency maximizing scheme as their mode of operation. Let γ_T^{ψ} denote the SNR threshold determined by the scheduler, where ψ is an integer satisfying $1 \leq \psi \leq N$. This threshold may need to be optimized and updated according to the users' channel variation.

Mode of operation

The trade-off scheme (TOSch) operates as follows. The scheduler first selects a random user who performs the spectral efficiency maximizing scheme introduced in Section 6.2.1. The selected user investigates if the highest modulation level can be adopted for transmission. If any antenna supporting the highest modulation level is found, then this antenna is used for signal reception. If

none of the antennas support the highest modulation level, then the antenna with the highest channel SNR compared to others is selected for signal reception and its modulation level is reported to the scheduler. Now the scheduler examines whether the reported modulation level is higher than the modulation level defined by its switching threshold γ_T^{ψ}. If so, then this user qualifies and the scheduler selects this user for data transmission and stops the user selection process. If not, the scheduler selects another user excluding the previous user(s) in random and investigates if this user qualifies. If the scheduler set γ_T^{ψ} to γ_T^N, then the operation is exactly the same as the overall system spectral efficiency maximizing scheme introduced in Section 6.3.3. On the other hand, setting γ_T^{ψ} to γ_T^1 provides the other extreme scheme called a feedback load minimizing scheme. In this scheme, a user qualifies as long as this user can adopt any modulation level excluding an outage and the scheduler finds any qualified user, which offers a greatly reduced feedback load.

Average System Spectral Efficiency

Based on the mode of operation described above, the average system spectral efficiency is given by

$$\begin{aligned}\text{ASE} = &\sum_{n=1}^{\psi-1} SE_n \sum_{k=1}^{K} \binom{K}{k} \prod_{i=1}^{k} \{[F_{\gamma_i}(\gamma_T^{n+1})]^{L_i} - [F_{\gamma_i}(\gamma_T^{n})]^{L_i}\} \prod_{j=k+1}^{K} [F_{\gamma_j}(\gamma_T^{n})]^{L_j} \\ &+ \sum_{n=\psi}^{N} SE_n \sum_{k=0}^{K-1} \prod_{i=1}^{k} [F_{\gamma_i}(\gamma_T^{\psi})]^{L_i} \{[F_{\gamma_{k+1}}(\gamma_T^{n+1})]^{L_{k+1}} - [F_{\gamma_{k+1}}(\gamma_T^{n})]^{L_{k+1}}\}.\end{aligned} \tag{6.25}$$

The detailed derivation of (6.25) is given in Appendix A.3. If all the users have the same number of receive antennas, then (6.25) can be rewritten as

$$\begin{aligned}\text{ASE} = &\sum_{n=1}^{\psi-1} SE_n\{[F_\gamma(\gamma_T^{n+1})]^{LK} - F_\gamma(\gamma_T^n)]^{LK}\} \\ &+ \sum_{n=\psi}^{N} SE_n \frac{1-[F_\gamma(\gamma_T^{\psi})]^{LK}}{1-[F_\gamma(\gamma_T^{\psi})]^{L}}\{[F_\gamma(\gamma_T^{n+1})]^{L} - [F_\gamma(\gamma_T^n)]^{L}\}.\end{aligned} \tag{6.26}$$

6.4 User Scheduling with Fairness

Needless to say, fairness is always an important factor in multiuser scheduling, since high level of fairness in general sacrifices the overall performance. Fairness can be defined in multiple ways. A first possibility is to assign the same rate to all users, which seems fair at a first sight. However, in a cellular networks, some users are in the proximity of the base station, but others are in the cell edge. Under this heterogeneity of users' channel condition, the proportional fairness rule provides a better notion of fairness with enhanced performance.

In order to improve the fairness among users, we combine the switch-based schemes introduced previously with the idea of enhanced equal access scheduling policy to guarantee high probability of access for each user. For comparison, the opportunistic policy is firstly reviewed where the best user is always selected among all users in every time slot.

6.4.1 Opportunistic Scheduling Policy

The opportunistic scheduling policy is a so-called greedy scheduling algorithm, since the user with the highest channel quality is always selected among all users in every selection process. In the switch-based schemes, the scheduler performs user selection as soon as any user under the given condition is found without testing all the users. Therefore, the rest of the users in the user pool after the user selection do not even have a chance to request to get a channel

access. In order to give all the users a fair chance to compete for time slots in a probabilistic manner, the user number is randomly shuffled and user switching starts from user number 1 in the numerical order. Since the best user is always scheduled, the user selected in the previous slot can also be selected for the next slot. Therefore, fairness in terms of performance or throughput may not be guaranteed in this scheme. However, random shuffling will provide each user a fair chance to compete for a channel access. The average system spectral efficiency for the opportunistic scheduling policy for the switch-based schemes is written as

$$\mathrm{ASE}_{\mathrm{op}} = \frac{1}{K}\sum_{k=1}^{K}\mathrm{ASE}(K) \tag{6.27}$$

where $\mathrm{ASE}(K)$ is the average system spectral efficiency for K users given in (6.22), (6.24), and (6.26) for the OSSEMax scheme, the FLASMin scheme, and the TOSch scheme, respectively.

6.4.2 Equal Access Scheduling Policy

In the time division multiple access scheme, the fairness may be quantified by the number of channel access or the number of time slots assigned to each user. A simple alternative scheduling called equal access scheme is proposed in [106] to improve fairness, where the selected user in the current time slot is removed from the user pool for the following time slots until all the users are scheduled. Therefore, it is guaranteed that every user has a maximum inter-access time of $2K-1$ time slots, which is necessary especially for delay-sensitive services such as video or audio. Since the number of users in the user pool is decremented everytime a scheduling occurs, the average multiuser diversity order is represented as $\frac{K+1}{2}$. The average system spectral efficiency for the equal access scheduling policy for the switch-based schemes is written as

$$\mathrm{ASE}_{\mathrm{eq}} = \frac{1}{K}\sum_{k=1}^{K}\mathrm{ASE}(k) \tag{6.28}$$

where ASE(k) is the average system spectral efficiency for k users given in (6.22), (6.24), and (6.26) for the OSSEMax scheme, the FLASMin scheme, and the TOSch scheme, respectively. Notice that the number of users in the user pool k is a variable in (6.28), whereas it is a constant K in (6.27).

6.5 Feedback Load and Rate

Feedback load is defined as the number of feedbacks required for the scheduler to perform a user selection. Normalized average feedback load can be defined as the ratio of the average feedback load per time slot by the total number of users [105]. On the other hand, feedback rate is defined as the number of bits in a feedback. Feedback load and rate in general show an interesting tradeoff relationship. If a feedback is allowed to have enough number of bits for channel quality information, then the average feedback load in general will be lower than the case of 1 bit feedback.

6.5.1 Overall System Spectral Efficiency Maximizing Scheme

Based on the mode of operation described in Section 6.3.3, each user sends a feedback only if its receive SNR meets the highest modulation level, and this requires just 1 bit. If all the users fail to meet the highest modulation level, then the scheduler may request a full feedback from each user. Users then report the highest modulation level they can support to the scheduler ($\log_2 N$ bits are needed for N modulation levels). If multiple users belong to a same modulation level, a random selection breaks the tie.

Assuming i.i.d. channels over users, the average feedback load is given by

$$\begin{aligned}\overline{F}_L &= \sum_{k=1}^{K-1} k(1-F(\gamma_T^N))F(\gamma_T^N)^{k-1} + K(F(\gamma_T^N))^{K-1} + K(F(\gamma_T^N))^K \\ &= \frac{1-(F(\gamma_T^N))^K}{1-F(\gamma_T^N)} + K(F(\gamma_T^N))^K\end{aligned} \tag{6.29}$$

where $F(x)$ is the CDF of the channel statistics of a user evaluated at x.

If none of the users can adopt the highest modulation level, a full feedback with $\log_2 N$ bits is necessary from each user and this may be a non-negligible overhead. The average feedback rate is written as

$$\overline{F}_R = 1 - (\lceil \log_2(N+1) \rceil - 1)(F(\gamma_T^N))^K, \tag{6.30}$$

where $\lceil x \rceil$ is the ceiling function.

6.5.2 Feedback Load and Antenna Switching Minimizing Scheme

Based on the mode of operation in Section 6.3.4, the feedback load and antenna switching minimizing scheme schedules a random user with any modulation level excluding an outage. In order for the selected user to report the highest modulation level it can afford, a $\lceil \log_2(N+1) \rceil$ bit feedback is required for a total of N modulation levels. Since the lowest SNR threshold, which is an outage threshold, is used as the switching threshold for the scheduler, no feedback rate saving is offered, i.e., $\overline{F}_R = \lceil \log_2(N+1) \rceil$. However, the average feedback load is apparently minimized and so is the antenna switching in a user. The average feedback load is given by

$$\begin{aligned} \overline{F}_L &= \sum_{k=1}^{K-1} k(1 - F(\gamma_T^1))F(\gamma_T^1)^{k-1} + K(F(\gamma_T^1))^{K-1} \\ &= \frac{1 - (F(\gamma_T^1))^K}{1 - F(\gamma_T^1)} \end{aligned} \tag{6.31}$$

6.5.3 Trade-off Scheme

Similar to the previous schemes, each user send a feedback containing its highest modulation level only if its receive SNR meets the switching threshold γ_T^ψ. If all the users fail to have the received SNR higher than γ_T^ψ, then the

scheduler may request an additional feedback. Each user then reports the highest modulation level it can support to the scheduler given the fact that the received SNR is lower than γ_T^{ψ} (a feedback needs $\log_2\psi$ bits to represent $\phi - 1$ modulation levels and an outage). If multiple users belong to a same modulation level, a random selection breaks the tie. The average feedback load is given by

$$\overline{F}_L = \frac{1 - (F(\gamma_T^{\psi}))^K}{1 - F(\gamma_T^{\psi})} + K(F(\gamma_T^{\psi}))^K \tag{6.32}$$

Since γ_T^{ψ} is used for the switching threshold, each user needs $\lceil \log_2(N - \psi + 2) \rceil$ bits for a feedback, which represents the highest modulation the user can use among the modulation levels higher than γ_T^{ψ}. The average feedback rate is given as

$$\overline{F}_R = \lceil \log_2(N - \psi + 2) \rceil (1 - (F(\gamma_T^{\psi}))^K) + \lceil \log_2(\phi) \rceil (F(\gamma_T^{\psi}))^K, \tag{6.33}$$

6.6 Numerical Results and Simulation

6.6.1 Joint Switched Diversity and Adaptive Modulation

Fig. 6.3 depicts the average spectral efficiency of the spectral efficiency maximizing scheme (SWC_N), the antenna switching minimization scheme (SWC_1), and the adaptive scheme with optimal threshold (SWC_opt) introduced in Section 6.2.1, 6.2.2, and 6.2.3, respectively, when $L = 4$. Note that the simulation results verifies the analysis in the sense that all the schemes provide indentical average output spectral efficiency for an average channel SNR lower than γ_T^1, whereas the SWC_1 scheme shows a noticeable difference for an average channel SNR above γ_T^1 as can be anticipated from its mode of operation. The adaptive modulation with no diversity gain is also plotted for bench mark comparison. Interestingly, the SWC_opt scheme represents a near-optimal average output

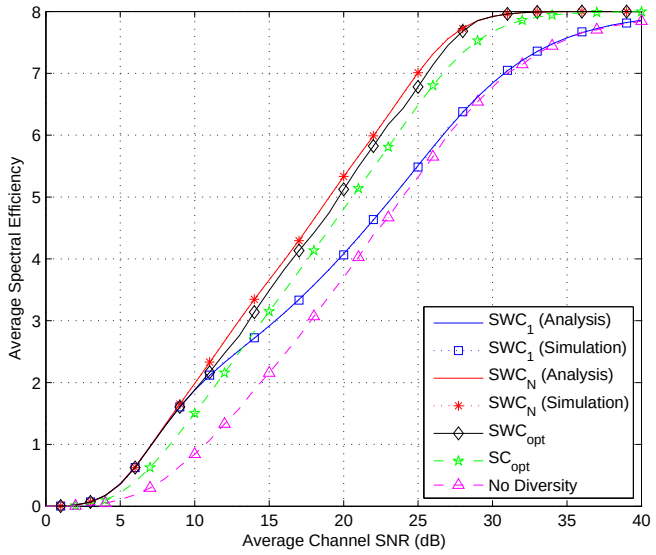

Figure 6.3: Average spectral efficiency of various schemes

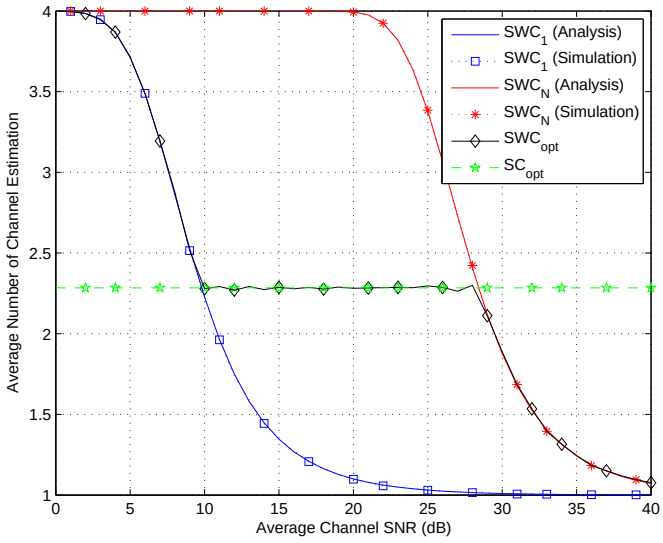

Figure 6.4: Average number of channel estimation (antenna switching) of the various schemes

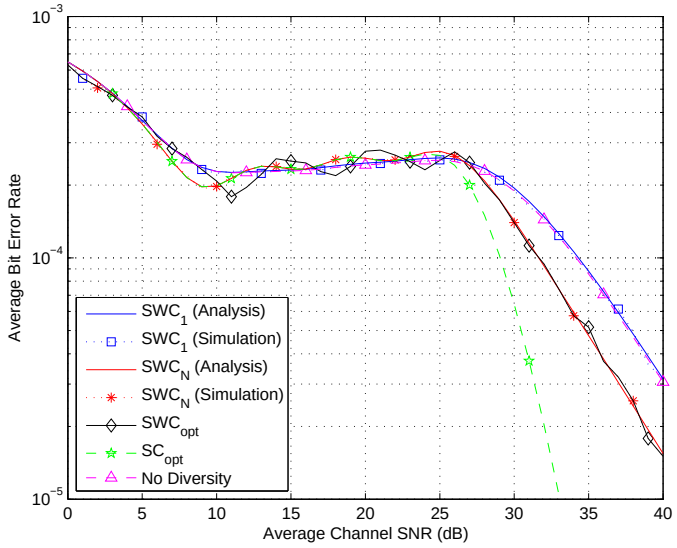

Figure 6.5: Average bit error rate of the various schemes

spectral efficiency over the channel SNR region between γ_T^1 and γ_T^N. As expected from its mode of operation, $\mathrm{SWC_{opt}}$ behaves in the similar fashion as $\mathrm{SWC_1}$, when the channel SNR is lower than γ_T^1 and $\mathrm{SWC_N}$ when the channel SNR higher than γ_T^N. For comparison, a selection diversity, denoted by $\mathrm{SC_{opt}}$, that requires the same number of channel estimation as in the $\mathrm{SWC_{opt}}$ scheme is also plotted. Since a selection diversity in general estimates all available antennas to select the best channel quality among them, it can be said that $\mathrm{SC_{opt}}$ has less number of antennas[1] than $\mathrm{SWC_{opt}}$. Therefore, $\mathrm{SWC_{opt}}$ outperforms $\mathrm{SC_{opt}}$ while maintaining the same number of channel estimation overhead as illustrated in Fig. 6.4, which shows an excellent trade-off between the output spectral efficiency and the number of channel estimation as visualized in the figures. The average number of channel estimation in this Section is analyzed and simulated under the assumption of block fading channels, in which the

[1]The number of antennas for $\mathrm{SC_{opt}}$ is a fractional number. Notice that, however, $\mathrm{SC_{opt}}$ is introduced only for comparison with the switched diversity schemes given the same number of channel estimation.

channel is stationary over a block and is independent from block to block. Also the time slot duration is assumed to be the block length, which allows us to transparently analyze the performance of the systems without considering Doppler frequency. However, in practice, the wireless channel is neither constant over the channel coherence time nor independent from block to block. Therefore, the time slot duration is typically designed less than the channel coherence time in order to reduce performance degradation due to the channel variation during the time slot. Consequently, the channel sometimes can stay with a similar value over several time slots, which may require less number of channel estimation. However, it is meaningful to evaluate the performance under the assumption of the block fading channels, because the block fading is the worst case in the sense that the channel independently varies every time slot, which requires the highest channel estimation overhead. Finally, the average BER performance for all the schemes is shown in Fig. 6.5. Similar to the BER behavior exhibited by the other adaptive modulation systems, an almost flat region between γ_T^1 and γ_T^N is observed.

6.6.2 Multiuser Diversity with Switch-based Scheduling

Suppose a frequency division duplexing (FDD) system where uplink and downlink channels are separated by frequency. Let T_m be the mini-slot duration, which may be set as the processing time required for the scheduler to deal with a single user. Let T_s be the time-slot duration that can be defined as a multiple of T_m, i.e., $T_s = \alpha T_m$, where $\alpha = 600$ in this simulation. We assume that the guard period is variable and is consists of feedback load multiplied by T_m. Therefore, the average guard period can be written as $\overline{T}_g = \overline{F}_L \cdot T_m$.

Considering the average feedback load, the average overall spectral efficiency is given by

$$\text{AOSE} = \text{ASE} \times \frac{T_s - \overline{T}_g}{T_s} = \text{ASE} \times \left(1 - \frac{\overline{F}_L}{\alpha}\right). \tag{6.34}$$

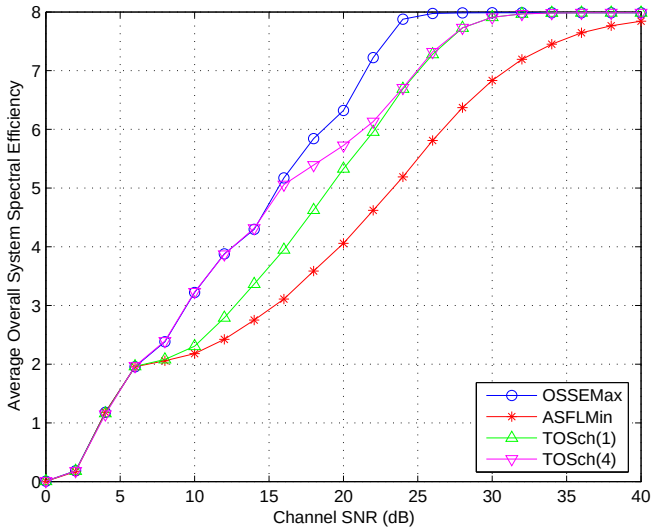

Figure 6.6: Average overall spectral efficiency for the switch-based multiuser access scheme with various parameters for the number of user $K = 10$

Notice that the average overall spectral efficiency is reduced by a factor $\frac{T_s - \overline{T}_g}{T_s}$ and, thus a long guard period decreases the output spectral efficiency.
Fig. 6.6 shows the average overall spectral efficiency with respect to the average channel SNR. In this figure, the TOSch scheme with its switching threshold γ_T^n is denoted by TOSch(n). A more interesting fact is found when the average overall spectral efficiency is plotted as a function of the number of users as shown in Fig. 6.7. As the number of users increases, the OSSEMax scheme shows worse spectral efficiency performance than the TOSch scheme with the switching threshold of γ_T^5. This can be simply explained by the average feedback load illustrated in Fig. 6.8. Since the OSSEMax scheme requires a large number of feedback requests, the average overall spectral efficiency is trimmed due to the long guard period. Fig. 6.9 illustrates the normalized average feedback load of the OSSEMax, ASFLMin, and TOSch with the switching threshold of γ_T^5 when the number of users is $K = 10$. As anticipated, the normalized average feedback load decreases as the average channel SNR in-

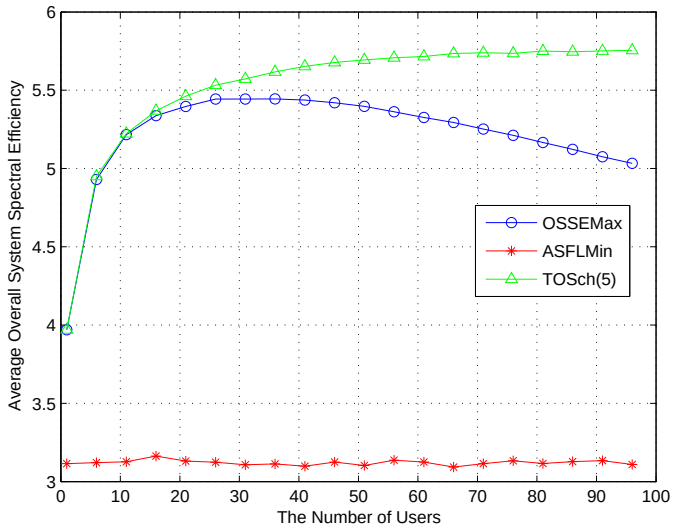

Figure 6.7: Average overall spectral efficiency for the switch-based multiuser access scheme with various parameters as a function of the number of users for average channel SNR $\overline{\gamma}$=18dB

creases. From this figure, we can see that it is possible to adaptively adjust the switching threshold of TOSch so as to limit the normalized feedback load into a certain level. This has also some practical value, since the guard period needs to be limited into a certain value in practical systems. This adaptive switch-based multiuser scheme can be simply implemented and wil provide a reduced guard period without sacrificing much of the average overall spectral efficiency. Fig. 6.10 shows that the TOSch scheme provides a significant reduction of the normalized average feedback as the number of users increases. This figure also demonstrates the effectiveness of the TOSch scheme.

6.7 Conclusion and Future Work

The joint use of switched diversity and adaptive modulation provides a reduction of average number of channel estimation without spectral efficiency loss. By a simple change of the switching threshold, the switched diversity

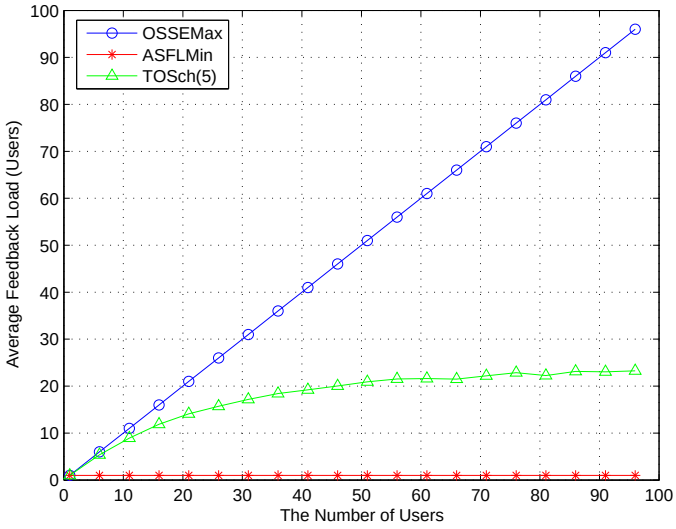

Figure 6.8: Average feedback load for the switch-based multiuser access scheme with various parameters as a function of the number of users for average channel SNR $\overline{\gamma}$=16dB

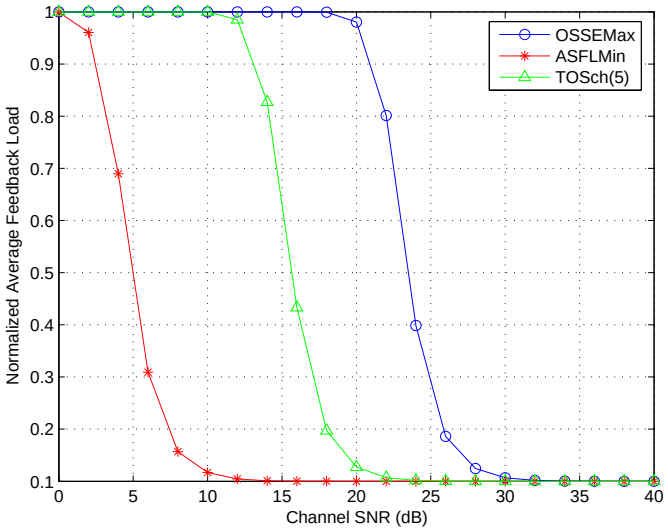

Figure 6.9: Average feedback load for the switch-based multiuser access scheme with various parameters for the number of user $K = 10$

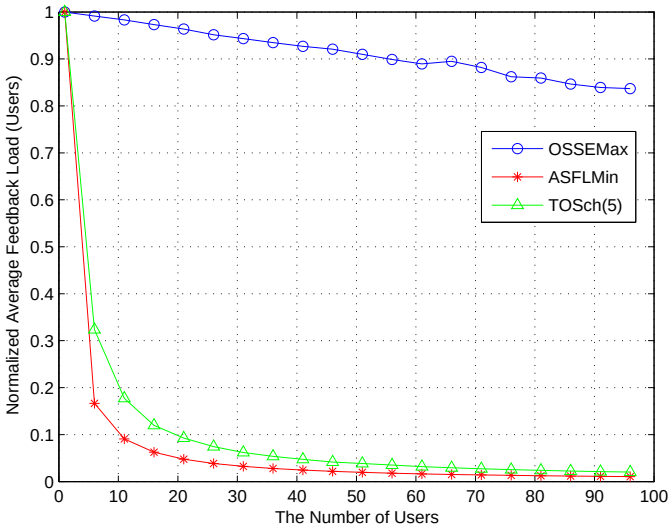

Figure 6.10: Normalized average feedback load for the switch-based multiuser access scheme with various parameters as a function of the number of users for average channel SNR $\overline{\gamma}$=20dB

scheme can easily change its mode of operation from spectral efficiency maximization to power consumption minimization. Switch-based multiuser access schemes are also presented and their performance analyzed. Numerical results quantifying the trade-off between average overall spectral efficiency and feedback load show that the average feedback load can be significantly reduced compared to the optimal overall system spectral efficiency maximizing scheme without having a considerable output spectral efficiency loss. As part of future work, we plan to investigate an adaptive trade-off scheme with an adjustable switching threshold that is set according to the average channel conditions.

Chapter 7

Conclusions

7.1 Summary and Contributions

Previous work on diversity combining techniques shows that a much improved SNR is obtained in a receiver when combining multiple diversity branches. Most straight forward examples are multiple antenna systems and code-division multiple access (CDMA) rake receivers that take advantage of spatial diversity channels or multipath diversity channels. In addition, OFDM systems use frequency diversity over subcarriers whereas slotted time-division multiplexing systems can achieve multiuser diversity in addition to time diversity. Although these various diversity resources provide high reliability over a wireless link, sometimes diversity resources are overused such that an excessive SNR is obtained when the channel state is favorable.

This additional SNR gain due to diversity techniques may contribute to nothing on the spectral efficiency performance when used with discrete-rate adaptive modulation if the output SNR from a diversity receiver falls into the same SNR region as the output SNR from a receiver with no diversity. In such cases, the additional SNR gain provides only a lower BER than the BER for a no diversity receiver, which is not necessary in terms of QoS because the adaptive modulation already guarantees the targeting BER. Therefore, in order to make an efficient use of diversity resources, the number of active

diversity branches can be adaptively selected. Adaptive diversity combining schemes described in this dissertation attempt to select the minimum number of diversity branches required to meet the SNR threshold pre-determined for the QoS. Several different ways of adaptive diversity branch selection are presented in Chapter 4 with a detailed performance analysis. Contributions in Chapter 4 include the proposal of the OT-MRC scheme, which was independently proposed in [56], with a detailed analysis over generalized fading channel models. We also proposed the MS-GSC scheme and investigated its performance, independently from [52], but our approach involves multiple integrals and, thus, is difficult to calculate. However, our approach is more general since no assumption was made for analysis, whereas the approach in [52] is applicable only to i.i.d. Rayleigh fading channels. Since the adaptive diversity combining schemes have the knowledge of the target SNR threshold, some definite integral equations having an exponential function with its exponent of the target SNR threshold, which were known to have no closed-forms, need to be calculated to figure out BER performance. Another contribution in this chapter lies in the derivation of useful exact closed-forms for BER performance of the adaptive diversity combining schemes.

A multi-carrier system with joint diversity combining and adaptive modulation is proposed and studied in Chapter 5. This proposed system improves the output spectral efficiency in the low SNR region at the cost of a small complexity and, thus, can be used in mobile devices in order to obtain enhanced data rate at the cell edge. The analytical expression for the spectral efficiency is derived and is verified by simulation for various different parameters. The BER performance and complexity analysis of the proposed schemes are also presented.

The WPAN applications are the leading technologies for so-called "Digital Convergence", which is expected to be a huge market for telecommunication companies as well as personal computer manufacturers in near future. Since power and cost effectiveness are main factors for such systems to survive, a simple architecture with high reliability and data rate is crucial for the design

of WPAN devices. Considering this goal, we introduced in Chapter 6 a system framework that incorporates a switched diversity scheme with adaptive modulation. This idea is later extended to a time-division multiplexing system in a multiuser scenario where overall spectral efficiency and feedback overhead show an intriguing trade-off relationship.

7.2 Future Work

7.2.1 Extensions of Adaptive Diversity Techniques to MIMO

The idea in adaptive diversity combining schemes introduced in Chapter 4 can also be extended to a multiple transmit antenna case or MIMO case [107]. Considering practical wireless systems, the Alamouti scheme is the most popular and feasible diversity technique used in multiple antenna systems due to its simple structure and full diversity gain [108]. Therefore, it is meaningful to investigate the performance gain of antenna selection (or switching) diversity when used with the Alamouti scheme in a MIMO environment. Closed-form expressions can be derived for achievable spectral efficiency, bit error rate, and outage probabilty of this system.

7.2.2 Efficient Feedback Schemes in a Multiuser Scenario

Reducing the number of feedbacks is an active research area since the next generation wireless standards adopt wireless systems based on multiple channels, such as MIMO or OFDM, as a key technology. The amount of feedback in such systems is abundant due to the number of subchannels and, thus, needs to be reduced without sacrificing much spectral efficiency or capacity.

Similarly, a time-division multiplexing system in a multiuser scenario also incurs feedback problems. Various scheduling schemes that are aimed

at reducing feedback load while achieving multiuser diversity gain based on a threshold are discussed in the literature. For some of the schemes, the following assumptions are often made: 1) users are able to detect feedback collisions and 2) channel statistics are known a priori to users. However, the above assumptions often lack some practical meaning. For instance, in a cellular network, since users are spatially distributed over a cell, there would be hidden regions that exist in the other side of the cell such that a user is not able to detect a feedback signal from other users located in the hidden regions. Apparently channel statistics is difficult to know a priori and it may not be possible for each user to know its channel statistics until measured. Sensor networks provide another good example that the above assumptions may not apply.

Considering the limitations listed above, we propose a simple and practical feedback scheme based on switched multiuser access without assuming knowledge of channel statistics and collision detection capability. The basic principle behind this scheme is to find any one among the users who belong to the SNR region for the best user, where SNR regions are defined by adaptive modulation. The performance of the proposed feedback scheme will be derived as analytical expressions and compared with other feedback schemes.

Appendix A

Some Derivations

In this appendix, we provide some detailed derivation of some equations presented previously.

A.1 Derivation of SE_i^+ and SE_i^-

Two conditional spectral efficiency expressions are defined as

$$\begin{aligned} SE_i^+ &= \sum_{j=1}^{K} R_{i,j} \cdot P_{i,j}^+ \\ SE_i^- &= \sum_{j=1}^{K} R_{i,j} \cdot P_{i,j}^- \end{aligned} \tag{A.1}$$

where $R_{i,j}$ is introduced in Eq. (5.5) and

$$\begin{aligned} P_{i,j}^+ &= F_i^+(\gamma_{T_{j+1}}) - F_i^+(\gamma_{T_j}), \\ P_{i,j}^- &= F_i^-(\gamma_{T_{j+1}}) - F_i^-(\gamma_{T_j}), \end{aligned} \tag{A.2}$$

where

$$F_i^+(x) = \Pr\left[\sum_{n=1}^{i-1}\gamma_n + \gamma_i < x \middle| \sum_{n=1}^{i-1}\gamma_n < \gamma_T,\ \gamma_i \geq \gamma_T\right] \tag{A.3}$$

and

$$F_i^-(x) = \Pr\left[\sum_{n=1}^{i-1}\gamma_n + \gamma_i < x \middle| \sum_{n=1}^{i-1}\gamma_n + \gamma_i \geq \gamma_T,\ \sum_{n=1}^{i-1}\gamma_n < \gamma_T,\ \gamma_i < \gamma_T\right]. \tag{A.4}$$

Let $\tau = \sum_{n=1}^{i-1}\gamma_n$ and $\eta = \gamma_i$. Using the variable substitution, Eq. (A.3) is rewritten as

$$F_i^+(x) = \Pr[\tau + \eta < x | \tau < \gamma_T, \eta \geq \gamma_T], \tag{A.5}$$

which can be represented with an integral form as

$$F_i^+(x) = \frac{1}{\widetilde{P}_i^+}\begin{cases} 0, & x < \gamma_T \\ \displaystyle\int_0^{x-\gamma_T}\int_{\gamma_T}^{x-\tau} f(\eta)f_{i-1}(\tau)d\eta d\tau, & \gamma_T \leq x < 2\gamma_T \\ \displaystyle\int_0^{\gamma_T}\int_{\gamma_T}^{x-\tau} f(\eta)f_{i-1}(\tau)d\eta d\tau, & x \geq 2\gamma_T \end{cases} \tag{A.6}$$

where

$$\widetilde{P}_i^+ = \Pr[\tau < \gamma_T, \eta \geq \gamma_T] = F_{i-1}(\gamma_T)\{1 - F(\gamma_T)\}. \tag{A.7}$$

$f(x)$ and $F(x)$ are the PDF and CDF of a single channel output SNR evaluated at x, respectively, whereas $f_i(x)$ and $F_i(x)$ are the PDF and CDF of the output SNR for the MRC combining scheme with i branches evaluated at x, respectively.

Note that the PDF and CDF of MRC output SNR are available for various fading channels in the literature. Similarly, Eq. (A.4) is rewritten as

$$\begin{aligned} F_i^-(x) &= \Pr[\tau + \eta < x | \tau + \eta \geq \gamma_T, \tau < \gamma_T, \eta < \gamma_T] \\ &= \begin{cases} 0, & x < \gamma_T, \\ 1 - \dfrac{1}{\widetilde{P}_i^-}\displaystyle\int_{x-\gamma_T}^{\gamma_T}\int_{x-\tau}^{\gamma_T} f(\eta)f_{i-1}(\tau)d\eta d\tau, & \gamma_T \leq x < 2\gamma_T \\ 1, & x \geq 2\gamma_T, \end{cases} \end{aligned} \tag{A.8}$$

where

$$\begin{aligned}\widetilde{P}_i^- &= \Pr[\tau+\eta \geq \gamma_T, \tau < \gamma_T, \eta < \gamma_T] \\ &= F(\gamma_T)F_{i-1}(\gamma_T) - F_i(\gamma_T).\end{aligned} \tag{A.9}$$

Based on the switching thresholds for the adaptive modulation shown in the Table 1.1, it is worth noting that $x \geq 2\gamma_T$ is the region of our interest. Therefore, $P_{i,j}^+$ for Rayleigh fading channels can be derived, by substituting the PDF of a single branch in Table 2.1 and the PDF of MRC(L) over Rayleigh channels in Table 3.1 into Eq. (A.6) and further into Eq. (A.2), as

$$P_{i,j}^+ = \left\{ e^{-\frac{\gamma_{T_j}}{\overline{\gamma}}} - e^{-\frac{\gamma_{T_{j+1}}}{\overline{\gamma}}} \right\} e^{\frac{\gamma_T}{\overline{\gamma}}} \frac{(\frac{\gamma_T}{\overline{\gamma}})^{i-1}}{(i-1)!} \left\{ 1 - \frac{\Gamma(i-1, \frac{\gamma_T}{\overline{\gamma}})}{\Gamma(i-1)} \right\}^{-1}. \tag{A.10}$$

According to the region of interest in Eq. (A.8), $P_{i,j}^-$ is simply written as

$$P_{i,j}^- = \begin{cases} 1, & j = 1 \\ 0, & j \geq 2 \end{cases}. \tag{A.11}$$

Thus, substituting Eq. (A.10) and Eq. (A.11) into Eq. (A.1), we reach the conditional spectral efficiency expressions for Rayleigh channels as

$$\begin{aligned} SE_i^+ =& \sum_{j=1}^{K} (j+1) \left\{ e^{-\frac{\gamma_{T_j}}{\overline{\gamma}}} - e^{-\frac{\gamma_{T_{j+1}}}{\overline{\gamma}}} \right\} e^{\frac{\gamma_T}{\overline{\gamma}}} \frac{(\frac{\gamma_T}{\overline{\gamma}})^{i-1}}{(i-1)!} \left\{ 1 - \frac{\Gamma(i-1, \frac{\gamma_T}{\overline{\gamma}})}{\Gamma(i-1)} \right\}^{-1} \\ SE_i^- =& 2 \end{aligned} \tag{A.12}$$

A.2 Derivation of $\overline{\mathrm{BER}}_{i,j}^+$ and $\overline{\mathrm{BER}}_{i,j}^-$

Define $\overline{\mathrm{BER}}_{i,\{\alpha,\beta\}}^+$ and $\overline{\mathrm{BER}}_{i,\{\alpha,\beta\}}^-$ as

$$\overline{\mathrm{BER}}_{i,\{\alpha,\beta\}}^+ = \int_\alpha^\beta \mathrm{BER}(M_j, \gamma) f_i^+(\gamma) d\gamma \tag{A.13}$$

and

$$\overline{\mathrm{BER}}^{-}_{i,\{\alpha,\beta\}} = \int_{\alpha}^{\beta} \mathrm{BER}(M_j,\gamma) f_i^{-}(\gamma) d\gamma, \tag{A.14}$$

where $\gamma_{T_j} \leq \alpha \leq \beta < \gamma_{T_{j+1}}$. Note that $\overline{\mathrm{BER}}^{+}_{i,j} = \overline{\mathrm{BER}}^{+}_{\{\alpha=\gamma_{T_j},\beta=\gamma_{T_{j+1}}\}}$ and $\overline{\mathrm{BER}}^{-}_{i,j} = \overline{\mathrm{BER}}^{-}_{\{\alpha=\gamma_{T_j},\beta=\gamma_{T_{j+1}}\}}$. By differentiating the conditional CDFs in Eq. (A.6) and Eq. (A.8), the conditional PDFs are given as

$$f_i^{+}(x) = \frac{1}{\widetilde{P}_i^{+}} \begin{cases} \displaystyle\int_0^{x-\gamma_T} f(x-\tau) f_{i-1}(\tau) d\tau, & \gamma_T \leq x < 2\gamma_T \\ \displaystyle\int_0^{\gamma_T} f(x-\tau) f_{i-1}(\tau) d\tau, & x \geq 2\gamma_T \end{cases} \tag{A.15}$$

and

$$f_i^{-}(x) = \frac{1}{\widetilde{P}_i^{-}} \int_{x-\gamma_T}^{\gamma_T} f(x-\tau) f_{i-1}(\tau) d\tau, \quad \gamma_T \leq x < 2\gamma_T. \tag{A.16}$$

For Rayleigh fading channels, Eq. (A.15) and Eq. (A.16) are given as

$$f_i^{+}(x) = \frac{1}{\widetilde{P}_i^{+}} \begin{cases} \dfrac{(x-\gamma_T)^{i-1}}{(i-1)!\overline{\gamma}^i} e^{-\frac{x}{\overline{\gamma}}}, & \gamma_T \leq x < 2\gamma_T \\ \dfrac{\gamma_T^{i-1}}{(i-1)!\overline{\gamma}^i} e^{-\frac{x}{\overline{\gamma}}}, & x \geq 2\gamma_T \end{cases} \tag{A.17}$$

and

$$f_i^{-}(x) = \frac{1}{\widetilde{P}_i^{-}} \frac{\gamma_T^{i-1} - (x-\gamma_T)^{i-1}}{(i-1)!\overline{\gamma}^i} e^{-\frac{x}{\overline{\gamma}}}, \gamma_T \leq x < 2\gamma_T. \tag{A.18}$$

It can be shown that the BER of M-QAM with Gray coding over an AWGN channel can be approximated by [93]

$$\mathrm{BER}(M,\gamma) \approx 0.1 \exp\left(- \frac{3\gamma}{2(2^{j+1}-1)} \right) \tag{A.19}$$

for $M = 2^{j+1}$ and $\mathrm{BER} < 10^{-3}$. Using Eq. (A.19) and substituting Eq. (A.17) and Eq. (A.18) into Eq. (A.13) and Eq. (A.14), respectively, it can be shown

that $\overline{\mathrm{BER}}^{+}_{i,\{\alpha,\beta\}}$ and $\overline{\mathrm{BER}}^{-}_{i,\{\alpha,\beta\}}$ for Rayleigh channels are derived as

$$\overline{\mathrm{BER}}^{+}_{i,\{\alpha,\beta\}} = \frac{0.1}{b_j\overline{\gamma}} \begin{cases} \dfrac{\exp[-b_j\gamma_T]}{(b_j\overline{\gamma})^{i-1}} \left[\dfrac{\Gamma[i, b_j(\alpha-\gamma_T)] - \Gamma[i, b_j(\beta-\gamma_T)]}{\Gamma[i]} \right], & \gamma_T \le \alpha \le \beta < 2\gamma_T \\ \dfrac{1}{(i-1)!}\left(\dfrac{\gamma_T}{\overline{\gamma}}\right)^{i-1} \Big[\exp[-b_j\alpha] - \exp[-b_j\beta] \Big], & 2\gamma_T \le \alpha \le \beta \end{cases} \tag{A.20}$$

and

$$\begin{aligned} \overline{\mathrm{BER}}^{-}_{i,\{\alpha,\beta\}} =& \frac{0.1}{b_j\overline{\gamma}} \Bigg\{ \frac{1}{(i-1)!}\left(\frac{\gamma_T}{\overline{\gamma}}\right)^{i-1} \Big[\exp[-b_j\alpha] - \exp[-b_j\beta] \Big] \\ & - \frac{\exp[-b_j\gamma_T]}{(b_j\overline{\gamma})^{i-1}} \left[\frac{\Gamma[i, b_j(\alpha-\gamma_T)] - \Gamma[i, b_j(\beta-\gamma_T)]}{\Gamma[i]} \right] \Bigg\}, \quad \gamma_T \le \alpha \le \beta < 2\gamma_T. \end{aligned} \tag{A.21}$$

A.3 Derivation of Eq. (6.25)

Assume K users are competing for channel access where each user is assumed to have infinite backlogged data. Suppose the kth user has L_k receive antennas and each user operates according to the spectral efficiency maximizing scheme introduced in Section 6.2.1 in order to achieve its maximum throughput. Then, the CDF and PDF of the output SNR for the kth user is given respectively by

$$F_k(x) = \begin{cases} 1 - \displaystyle\sum_{i=0}^{L_k-1} [F_{\gamma_k}(\gamma_T^N)]^i \{1 - F_{\gamma_k}(x)\}, & x \ge \gamma_T^N \\ [F_{\gamma_k}(x)]^{L_k}, & x < \gamma_T^N \end{cases} \tag{A.22}$$

and

$$f_k(x) = \begin{cases} \displaystyle\sum_{i=0}^{L_k-1} [F_{\gamma_k}(\gamma_T^N)]^i f_{\gamma_k}(x), & x \ge \gamma_T^N \\ L_k [F_{\gamma_k}(x)]^{L_k-1} f_{\gamma_k}(x), & x < \gamma_T^N, \end{cases} \tag{A.23}$$

where $F_{\gamma_k}(x)$ and $f_{\gamma_k}(x)$ are the CDF and PDF of a single channel of the kth user evaluated at x, respectively. Let γ_T^{ψ} denote the SNR threshold decided by the base station for user switching. Suppose that each user sends a full feedback, which contains the current channel state. Based on the mode of operation, the base station switches to another user when the current user has a lower receive SNR than γ_T^{ψ}. Therefore, its operation can be viewed as switched diversity with post examining selection (SECps) with γ_T^{ψ} as its switching threshold which is embedded with SECps with γ_T^{N} as its switching threshold. The PDF of output SNR for the base station is thus given by

$$f(x) = \begin{cases} \sum_{k=0}^{K-1} [F_k(\gamma_T^{\psi})]^k f_{k+1}(x), & x \geq \gamma_T^{\psi} \\ K \prod_{k=1}^{K-1} [F_k(x)] f_{k+1}(x), & x < \gamma_T^{\psi}. \end{cases} \tag{A.24}$$

where $F_k(x)$ and $f_k(x)$ are given in Eq. (A.22) and Eq. (A.23), respectively. After some manipulation, Eq. (A.24) can be rewritten as

$$f(x) = \begin{cases} \sum_{k=0}^{K-1} \mathcal{G}_k \sum_{j=0}^{L_{k+1}-1} [F_{\gamma_{k+1}}(\gamma_T^{N})]^j f_{\gamma_{k+1}}(x), & x \geq \gamma_T^{N} \\ \sum_{k=0}^{K-1} \mathcal{G}_k L_{k+1} [F_{\gamma_{k+1}}(x)]^{L_{k+1}-1} f_{\gamma_{k+1}}(x), & \gamma_T^{\psi} \leq x < \gamma_T^{N} \\ \sum_{k=1}^{K} \prod_{\substack{i=1 \\ i \neq k}}^{K} F_{\gamma_i}(x) f_{\gamma_k}(x), & x < \gamma_T^{\psi}, \end{cases} \tag{A.25}$$

where $\mathcal{G}_k = \prod_{i=1}^{k} [F_{\gamma_i}(\gamma_T^{\psi})]^{L_i}$.

If all the users have the same number of receive antennas, then Eq. (A.25)

simplifies to

$$f(x) = \begin{cases} \sum_{k=0}^{K-1} \sum_{i=0}^{L-1} [F_\gamma(\gamma_T^\psi)]^k [F_\gamma(\gamma_T^N)]^i f_\gamma(x), & x \geq \gamma_T^N \\ L \sum_{k=0}^{K-1} [F_\gamma(\gamma_T^\psi)]^k [F_\gamma(x)]^{L-1} f_\gamma(x), & \gamma_T^\psi \leq x < \gamma_T^N \\ KL[F_\gamma(x)]^{KL-1} f_\gamma(x), & x < \gamma_T^\psi. \end{cases} \tag{A.26}$$

Even though in the TOSch scheme each user send a reduced feedback indicating the highest modulation level that can be supported for transmission instead of the current channel state, the average system spectral efficiency for the TOSch scheme is the same for using a full feedback or a reduced feedback since the probability of a certain number of users belong to a modulation level is identical. Therefore, the average system spectral efficiency for the TOSch scheme can be calculated by

$$\text{ASE} = \sum_{n=1}^{N} SE_n \int_{\gamma_T^n}^{\gamma_T^{n+1}} f(x)dx. \tag{A.27}$$

Substituting Eq. (A.25) into Eq. (A.27) and after some manipulations, the average system spectral efficiency for the TOSch scheme is finally given in Eq. (6.25).

Appendix B

Some Integrals involving Average Error Rate Analysis

In this appendix, we derive closed-forms of some integral equations that need to be involved to analyze average error rate performance of diversity combining schemes with adaptive modulation shown previously.

B.1 Derivation of $\mathcal{I}[\alpha_n, \lambda, \delta]_{y_n}^{y_{n+1}}$

$$\mathcal{I}\Big[\alpha_n, \lambda, \delta\Big]_{y_n}^{y_{n+1}} = \int_{y_n}^{y_{n+1}} Q(\sqrt{\alpha_n y}) y^{\lambda} e^{-\delta y} dy \tag{B.1}$$

Using the alternative Q function in [65] and some mathematical manipulation, we can rewrite Eq. (B.1) as

$$\begin{aligned}\mathcal{I}\Big[\alpha_n, \lambda, \delta\Big]_{y_n}^{y_{n+1}} = \frac{\lambda!}{\delta^{\lambda+1}}\Bigg\{&\mathcal{J}_1\Big[\lambda+1, \frac{\alpha_n}{2\delta}, y_n\delta\Big] \\ &- \mathcal{J}_1\Big[\lambda+1, \frac{\alpha_n}{2\delta}, y_{n+1}\delta\Big]\Bigg\}\end{aligned} \tag{B.2}$$

where

$$\mathcal{J}_1\Big[k,a,b\Big] = \frac{1}{\Gamma(k)\pi}\int_0^{\frac{\pi}{2}}\left(\frac{\sin^2\theta}{\sin^2\theta+a}\right)^k \Gamma\Big[k, b\frac{\sin^2\theta+a}{\sin^2\theta}\Big]d\theta \tag{B.3}$$

Using the series representation of Gamma function, Eq. (B.3) is rewritten as

$$\mathcal{J}_1\Big[k,a,b\Big] = \sum_{n=0}^{k-1}\frac{b^n}{n!}\mathcal{I}_1\Big[k-n,a,b\Big] \tag{B.4}$$

where

$$\mathcal{I}_1\Big[k,a,b\Big] = \frac{1}{\pi}\int_0^{\frac{\pi}{2}}\left(\frac{\sin^2\theta}{\sin^2\theta+a}\right)^k e^{-b(\frac{\sin^2\theta+a}{\sin^2\theta})}d\theta. \tag{B.5}$$

The detailed derivation of Eq. (B.5) as a closed-form is given in Appendix B.2. Using the closed-form in Eq. (B.10) and an identity given by

$$e^{-b}\sum_{n=0}^{L-1}\frac{b^n}{n!}\frac{\Gamma[L-n,-b]}{\Gamma[L-n]} = 1, \tag{B.6}$$

Eq. (B.4) is derived with a simple closed form as

$$\begin{aligned}\mathcal{J}_1\Big[k,a,b\Big] &= \frac{\Gamma[k,b]}{2\Gamma[k]}\ \mathrm{erfc}[\sqrt{ab}] \\ &\quad - \frac{\sqrt{a}}{2\sqrt{\pi(a+1)}}\sum_{j=0}^{k-1}\frac{\Gamma[j+\frac{1}{2},(a+1)b]}{j!(a+1)^j}.\end{aligned} \tag{B.7}$$

Substituting Eq. (B.7) into Eq. (B.2) provides a closed form for $\mathcal{I}[\alpha_n,\lambda,\delta]_{y_n}^{y_{n+1}}$.

B.2 Derivation of $\mathcal{I}_1[k, a, b]$

$$\mathcal{I}_1\Big[k, a, b\Big] = \frac{1}{\pi}\int_0^{\frac{\pi}{2}} \left(\frac{\sin^2\theta}{a+\sin^2\theta}\right)^k e^{-b(\frac{a+\sin^2\theta}{\sin^2\theta})} d\theta \tag{B.8}$$

Using variable substitution of $t = b(\frac{a+\sin^2\theta}{\sin^2\theta})$ and partial fraction recursively, Eq. (B.8) is written as

$$\begin{aligned}\mathcal{I}_1\Big[k, a, b\Big] = \frac{\sqrt{ab}}{2\pi}\Bigg[&\int_{ab}^{\infty} \frac{1}{t}\sqrt{\frac{1}{t-ab}}\; e^{-t-b} dt \\ &- \sum_{i=1}^{k} \int_{(a+1)b}^{\infty} \frac{b^{i-1}}{t^i}\sqrt{\frac{1}{t-(a+1)b}}\; e^{-t} dt\Bigg]\end{aligned} \tag{B.9}$$

Using identities given as $\Gamma[\frac{1}{2}, x] = \sqrt{\pi}\ \mathrm{erfc}[\sqrt{x}]$ and $\Gamma[1+n, x] = n\Gamma[n, x] + e^{-x}x^n$, Eq. (B.9) can be represented as

$$\mathcal{I}_1\Big[k, a, b\Big] = \frac{1}{2}\Bigg\{e^{-b}\ \mathrm{erfc}[\sqrt{ab}] - \frac{\mu}{\sqrt{\pi}} e^{-b} \sum_{j=0}^{k-1} \frac{\Gamma[k-j, -b]\ \Gamma[j+\frac{1}{2}, (a+1)b]}{j!(1+a)^j\ \Gamma[k-j]}\Bigg\} \tag{B.10}$$

where $\mathrm{erfc}(\cdot)$ is the complementary error function defined by

$$\mathrm{erfc}(x) = \frac{2}{\sqrt{\pi}}\int_x^{\infty} e^{-t^2} dt. \tag{B.11}$$

and $\mu = \sqrt{\frac{a}{1+a}}$.

B.3 Derivation of $\mathcal{I}_2[k, a, b, c]$

$$\mathcal{I}_2\Big[k, a, b, c\Big] = \frac{1}{\pi}\int_0^{\frac{\pi}{2}} \left(\frac{\sin^2\theta}{c+\sin^2\theta}\right)^k e^{-b(\frac{a+\sin^2\theta}{\sin^2\theta})} d\theta \tag{B.12}$$

Similarly, using variable substitution of $t = b(\frac{a+\sin^2\theta}{\sin^2\theta})$ and recursive partial fraction shown above, Eq. (B.12) is written as

$$\mathcal{I}_2\Big[k,a,b,c\Big] = \frac{\sqrt{ab}}{2\pi}e^{-b(1-\frac{a}{c})}\Bigg[e^{-\frac{ab}{c}}\int_{ab}^{\infty}\frac{1}{t}\sqrt{\frac{1}{t-ab}}\;e^{-t-b}dt - \sum_{i=1}^{k}\int_{ab(1+\frac{1}{c})}^{\infty}\left(\frac{ab}{c}\right)^{i-1}\frac{1}{t^i}\sqrt{\frac{1}{t-ab(1+\frac{1}{c})}}\;e^{-t}dt\Bigg], \tag{B.13}$$

which can be expressed with a closed-form as

$$\mathcal{I}_2\Big[k,a,b,c\Big] = \frac{1}{2}\Bigg\{e^{-b}\;\mathrm{erfc}[\sqrt{ab}] - \frac{\eta}{\sqrt{\pi}}e^{-b}\sum_{j=0}^{k-1}\frac{\Gamma[k-j,-\frac{ab}{c}]\;\Gamma[j+\frac{1}{2},(a+\frac{a}{c})b]}{j!(1+c)^j\;\Gamma[k-j]}\Bigg\} \tag{B.14}$$

where $\eta = \sqrt{\frac{c}{1+c}}$.

Bibliography

[1] Tapan K. Sarkar, Robert Mailloux, Arthur A. Oliner, Magdalena Salazar-Palma, and Dipak L. Sengupta, *History of Wireless*, 2006, Wiley-IEEE Press.

[2] Marvin K. Simon and Mohamed-Slim Alouini, *Digital Communications over Fading Channels: A unified approach to performance analysis*, Wiley, New York, second edition, 2004.

[3] Bengt Holter and Geir Egil Øien, "On the amount of fading in MIMO diversity systems," *IEEE Transactions on Wireless Communications*, vol. 4, no. 5, pp. 2498–2507, Sept. 2005.

[4] Mohamed-Slim Alouini and Andrea J. Goldsmith, "Capacity of Rayleigh fading channels under different adaptive transmission and diversity-combining techniques," *IEEE Transactions on Vehicular Technology*, vol. 48, no. 4, pp. 1165–1181, July 1999.

[5] Ranjan K. Mallik, Moe Z. Win, Joshua W. Shao, Mohamed-Slim Alouini, and Andrea J. Goldsmith, "Channel capacity of adaptive transmission with maximal ratio combining in correlated Rayleigh fading," *IEEE Transactions on Wireless Communications*, vol. 3, no. 4, pp. 1124–1133, July 2004.

[6] Jooeung Kim, Inkyoung Kim, Sangmin Ro, Daesik Hong, and Changeon Kang, "Performance analysis of adaptive modulation system combined

with transmit/receive diversity," in *Proceedings of IEEE Vehicular Technology Conference (VTC'02)*, May 2002, vol. 2, pp. 837–841.

[7] Andrea J. Goldsmith and Soon-Ghee Chua, "Adaptive coded modulation for fading channels," *IEEE Trans. Commun.*, vol. 46, no. 5, pp. 595–602, May 1998.

[8] Andrea J. Goldsmith and Soon-Ghee Chua, "Variable-rate variable-power M-QAM for fading channels," *IEEE Trans. Commun.*, vol. 45, no. 10, pp. 1218–1230, October 1997.

[9] Kjell J. Hole, Henrik Holm, and Geir E. Øien, "Adaptive multidimensional coded modulation over flat fading channel," *IEEE Journal on Selected Areas in Communications*, vol. 18, no. 7, pp. 1153– 1158, July 2000.

[10] Xiaoxin Qiu and Kapil Chawla, "On the performance of adaptive modulation in cellular systems," *IEEE Transactions on Communications*, vol. 47, no. 6, pp. 884–895, June 1999.

[11] Seong Taek Chung and Andrea J. Goldsmith, "Degrees of freedom in adaptive modulation: A unified view," *IEEE Transactions on Communications*, vol. 49, no. 9, pp. 1561–1571, Sept. 2001.

[12] Gordon L. Stüber, *Principles of Mobile Communications*, Boston, MA: Kluwer Academic Publishers, 1996.

[13] W. C. Jakes, *Microwave Mobile Communications*, Piscataway, NJ: IEEE, second edition, 1994.

[14] Theodore S. Rappaport, *Wireless Communications*, Prentice-Hall, Upper Saddle River, NJ, 1996.

[15] Pramod Viswanath, David N. C. Tse, and Rajiv Laroia, "Opportunistic beamforming using dumb antennas," *IEEE Transactions on Information Theory*, vol. 48, no. 6, pp. 1277–1294, June 2002.

[16] S. O. Rice, "Statistical properties of a sine wave plus random noise," *Bell System Technical Journal*, vol. 27, pp. 109–157, Jan. 1948.

[17] Minobu Nakagami, "The m-distribution - a general formula of intensity distribution of rapid fading," in *Statistical Methods in Radio Wave Propagation*. 1960, pp. 3–36, Pergamon Press, Oxford, U. K.

[18] Hirofumi Suzuki, "A statistical model for urban multipath propagation," *IEEE Transactions on Communications*, vol. COM-25, no. 7, pp. 673–680, July 1977.

[19] Tor Aulin, "Characteristics of a digital mobile radio channel," *IEEE Transactions on Vehicular Technology*, vol. VT-30, pp. 45–53, May 1981.

[20] Homayoun Hashemi, "The indoor radio propagation channel," *Proceedings of IEEE*, vol. 81, no. 7, pp. 943–968, July 1993.

[21] Thomas Zwick, Troy Beukema, and Haewoon Nam, "Wideband channel sounder with measurements and model for the 60GHz indoor radio channel," *IEEE Transactions on Vehicular Technology*, vol. 54, no. 4, pp. 1266–1277, July 2005.

[22] Adel A. M. Saleh and Reinaldo A. Valenzuela, "A statistical model for indoor multipath propagation," *IEEE Journal on Selected Areas in Communications*, vol. SAC-5, no. 2, pp. 128–137, Feb. 1987.

[23] Jeffrey R. Foerster, Marcus Pendergrass, and Andreas F. Molisch, "A channel model for ultrawideband indoor communication," in *International Symposium on Wireless Personal Multimedia Communications*, Oct. 2003.

[24] Andrea J. Goldsmith, *Wireless Communications*, Cambridge University Press, 2005.

[25] Jack H. Winters, "On the capacity of radio communication systems with diversity in Rayleigh fading environment," *IEEE Journal on Selected Areas in Communications*, vol. 5, no. 5, pp. 871–878, June 1987.

[26] Q. T. Zhang, "Probability of error for equal-gain combiners over Rayleigh channels: Some closed-form solutions," *IEEE Transactions on Communications*, vol. COM-45, no. 3, pp. 270–273, Mar. 1997.

[27] George K. Karagiannidis, Dimitris A. Zogas, Nikos C. Sagias, Stavros A. Kotsopoulos, and George S. Tombras, "Equal gain and maximum ratio combining over weibull fading channels," *IEEE Transactions on Wireless Communications*, vol. 4, no. 3, pp. 841–846, May 2005.

[28] Adnan A. Abu-Dayya and Norman C. Beaulieu, "Analysis of switched diversity systems on generalized-fading channels," *IEEE Transactions on Communications*, vol. COM-42, no. 11, pp. 2959–2966, Nov. 1994.

[29] Adnan A. Abu-Dayya and Norman C. Beaulieu, "Switched diversity on Microcellular Ricean channels," *IEEE Transactions on Vehicular Technology*, vol. VT-43, no. 4, pp. 970–976, Nov. 1994.

[30] Young-Chai Ko, Mohamed-Slim Alouini, and Marvin K. Simon, "Analysis and optimization of switched diversity systems," *IEEE Transactions on Vehicular Technology*, vol. 49, no. 5, pp. 1813–1831, Sept. 2000.

[31] Yao Ma, Robert Schober, and Subbarayan Pasupathy, "Performance of M-PSK with GSC and EGC with Gaussian weighting errors," *IEEE Transactions on Vehicular Technology*, vol. 54, no. 1, pp. 149–162, Jan. 2005.

[32] Thomas Eng, Ning Kong, and Laurence B. Milstein, "Comparison of diversity combining techniques for Rayleigh-fading channels," *IEEE Transactions on Communications*, vol. 44, no. 9, pp. 1117–1129, Sept. 1996.

[33] J. N. Pierce and S. Stein, "Multiple diversity with nonindependent fading," *Proceedings of IRE*, vol. 48, pp. 89–104, Jan. 1960.

[34] K. S. Packard, "Effect of correlation on combiner diversity," *Proceedings of IRE*, vol. 46, pp. 362–363, Jan. 1958.

[35] Donald Brennan, "Linear diversity combining techniques," *Proceedings of IRE*, vol. 47, no. 6, pp. 1075–1102, June 1959.

[36] Bruce B. Barrow, "Diversity combining of fading signals with unequal mean strengths," *IEEE Transactions on Communications*, vol. CS-11, pp. 73–78, Mar. 1963.

[37] Emad K. Al-Hussaini and Abdel Aziz M. Al-Bassiouni, "Performance of MRC diversity systems for the detection of signals with Nakagami fading," *IEEE Transactions on Communications*, vol. COM-33, no. 12, pp. 1315–1319, Dec. 1985.

[38] Valentine A. Aalo, "Performance of maximal-ratio diversity systems in a correlated Nakagami-fading environment," *IEEE Transactions on Communications*, vol. COM-43, no. 8, pp. 2360–2369, Aug. 1995.

[39] H. A. David, *Order Statistics*, New York, NY :John Wiley & Sons, Inc., 1981.

[40] Ning Kong, Thomas Eng, and Laurence B. Milstein, "A selection combining scheme for RAKE receivers," *Proc. IEEE Int. Conf. Universal Personal Communications (ICUPC '95), Tokyo, Japan*, pp. 426–429, Nov. 1995.

[41] Mohamed-Slim Alouini and Marvin K. Simon, "An MGF-based performance analysis of generalized selection combining over Rayleigh fading channels," *IEEE Transactions on Communications*, vol. 48, no. 3, pp. 401–415, Mar. 2000.

[42] Moe Z. Win and Jack H. Winters, "Analysis of hybrid selection/maximal-ratio combining of diversity branches with unequal SNR in Rayleigh fading," in *Proc. IEEE Veh. Technol. Conf. VTC'99*, Houston, TX, May 1999, pp. 215–220.

[43] Ning Kong and Laurence B. Milstein, "SNR of generalized diversity selection combining with nonidentical Rayleigh fading statistics," *IEEE Transactions on Communications*, vol. 48, no. 8, pp. 1266–1271, Aug. 2000.

[44] Marvin K. Simon and Mohamed-Slim Alouini, "A compact performance analysis of generalized selection combining with independent but non-identically distributed Rayleigh fading paths," *IEEE Transactions on Communications*, vol. 50, no. 9, pp. 1409–1412, Sept. 2002.

[45] Mohamed-Slim Alouini and Marvin K. Simon, "Performance evaluation of generalized selection combining over Nakagami fading channels," in *Proceedings of IEEE Vehicular Technology Conference (VTC'99)*, Sept. 1999, vol. 2, pp. 953–957.

[46] Annamalai Annamalai and Chintha Tellambura, "Performance evaluation of generalized selection diversity systems over Nakagami-m fading channels," *Wireless Commununications and Mobile Computing*, pp. 99–116, 2003.

[47] Annamalai Annamalai and Chintha Tellambura, "Error rates for hybrid SC/MRC systems on Nakagami-m channels," in *Wireless Communications and Networking Conference, 2000. IEEE*, Sept. 2000, vol. 1, pp. 227 – 231.

[48] Yao Ma and Chin Choy Chai, "Unified error probability analysis for generalized selection combining in Nakagami fading channels," *IEEE Journal on Selected Areas in Communications*, vol. 18, no. 11, pp. 2198–2210, Nov. 2000.

[49] Ranjan K. Mallik and Moe Z. Win, "Analysis of hybrid selection/maximal-ratio combining in correlated Nakagami fading," *IEEE Transactions on Communications*, vol. 50, no. 8, pp. 1372–1383, Aug. 2002.

[50] Moe Z. Win and Jack H. Winters, "Virtual branch analysis of symbol error probability for hybrid selection/maximal-ratio combining in Rayleigh fading," *IEEE Transactions on Communications*, vol. 49, no. 11, pp. 1926–1934, Nov. 2001.

[51] Marvin K. Simon and Mohamed-Slim Alouini, "Performance analysis of generalized selection combining with threshold test per branch (T-GSC)," *IEEE Transactions on Vehicular Technology*, vol. 51, no. 5, pp. 1018–1029, Sept. 2002.

[52] Suk Won Kim, Dong S. Ha, and Jeffrey H. Reed, "Minimum selection GSC and adaptive low-power rake combining scheme," in *IEEE International Symposium on Circuits and Systems, 2003. (ISCAS '03)*, May 2003, vol. 4, pp. 25–28.

[53] Hong-Chuan Yang, "Exact performance analysis of minimum-selection generalized selection combining (GSC)," in *Proc. IEEE Int. Conf. on Commun. (ICC '2005)*, May 2005, pp. 3979–3983.

[54] Pranay Gupta, Nidhi Bansal, and Ranjan K. Mallik, "Analysis of minimim selection GSC in Rayleigh fading," in *2004 IEEE International Conference on Communications*, June 2004, vol. 6, pp. 3364–3368.

[55] Ranjan K. Mallik, Pranay Gupta, and Q. T. Zhang, "Minimum selection GSC in independent Rayleigh fading," *IEEE Transactions on Vehicular Technology*, vol. 54, no. 3, pp. 1013–1021, May 2005.

[56] Hong-Chuan Yang and Mohamed-Slim Alouini, "MRC diversity with an output threshold," in *Proceedings of IEEE International Conference on Communications (ICC '2004)*, June 2004, vol. 1, pp. 219–223.

[57] Haewoon Nam, Young-Chai Ko, and Baxter F. Womack, "Performance analysis of OT-MRC over i.i.d. Nakagami and non-i.i.d. Rayleigh fading channels," *IEEE Transactions on Vehicular Technology*, vol. 55, no. 6, pp. 1941–1946, Nov. 2006.

[58] Hong-Chuan Yang and Mohamed-Slim Alouini, "Improving the performance of switched diversity with post-examining selection," in *Proc. IEEE Global Telecommu. Conf. (Globecom '2004)*, Dec. 2004, pp. 479–483.

[59] Mohamed-Slim Alouini and Hong-Chuan Yang, "Minimum estimation and combining generalized selection combining (MEC-GSC)," in *Proc. International Symposium on Information Theory (ISIT '2005)*, Sept. 2005, pp. 578–582.

[60] Ahmed I. Sulyman and Maan Kousa, "Bit error rate performance of a generalized diversity selection combining scheme in Nakagami fading channels," in *Proc. IEEE Wireless Commununications Networking Conference*, Sept. 2000, pp. 1080–1085.

[61] Mohamed-Slim Alouini and Marvin K. Simon, "Application of the Dirichlet transformation to the performance evaluation of generalized selection combining over Nakagami-m fading channels," in *Proceedings of IEEE Vehicular Technology Conference (VTC'99)*, Sept. 1999, pp. 953–957.

[62] Marvin K. Simon and Mohamed-Slim Alouini, "A compact performance analysis of generalized selection combining with independent but non-identically distributed Rayleigh fading channels," *IEEE Transactions on Communications*, vol. 50, no. 9, pp. 1409–1412, Sept. 2002.

[63] I. S. Gradshteyn and I. M. Ryzhik, *Table of Integrals, Series, and Products*, Academic, San Diego, CA, fifth edition, 1994.

[64] Mohamed-Slim Alouini and Andrea J. Goldsmith, "A unified approach for calculating the error rates of linearly modulated signals over generalized fading channels," *IEEE Transactions on Communications*, vol. 47, pp. 1324–1334, Sept. 1999.

[65] John W. Craig, "A new, simple, and exact result for calculating the probability of error for two-dimensional signal constellations," in *Proceedings of IEEE Military Communications Conference (MILCOM'91)*, Oct. 1991, pp. 571–575.

[66] John G. Proakis, *Digital Communications*, McGraw-Hill, New York, 4th edition, 2001.

[67] Athanasios Papoulis, *Probability, Random Variables, and Stochastic Processes*, McGraw-Hill, New York, 4th edition, 2002.

[68] Hong-Chuan Yang and Mohamed-Slim Alouini, "Performance analysis of multibranch switched diversity systems," *IEEE Transactions on Communications*, vol. 51, no. 5, pp. 782–794, May 2003.

[69] Hong-Chuan Yang, "New results on ordered statistics and analysis of minimum-selection generalized selection combining (GSC)," *IEEE Transactions on Wireless Communications*, vol. 5, no. 7, pp. 1876–1885, July 2006.

[70] A. M. D. Turkmani, A. A. Arowojolu, P. A. Jefford, and C. J. Kellett, "Experimental evaluation of the performance of two-branch space and polarization diversity schemes at 1800 MHz," *IEEE Transactions on Vehicular Technology*, vol. 44, no. 2, pp. 318–326, May 1995.

[71] Paul Bender, Peter Black, Matthew Grob, Roberto Padovani, Nagabhushana Sindhushayana, and Andrew Viterbi, "CDMA/HDR: a bandwidth-efficient high-speed wireless data service for nomadic users," *IEEE Communications Magazine*, pp. 70–77, July 2000.

[72] Tina Quach, Fred Bonn, Jeff Ortiz, and Mike Thomas, "A highly integrated commerical gaas transceiver MMIC for 2.45 GHz ISM applications," in *Proceedings of Wireless Communications Conference*, Aug. 1997, pp. 141–146.

[73] *MAXIM 2.4 GHz SiGe linear power amplifier data sheet.*

[74] Wen-Shen Wuen, "2.4 GHz CMOS RF transmitter for IEEE 802.11b wireless LAN," Trans. wireless technology, National Technical University, Jan. 2002.

[75] Ericsson, Motorola, and Nokia, *Common HSDPA system simulation assumptions*, 2000, TSGR1 15(00)1094.

[76] Troels Emil Kolding, Klaus Ingemann Pedersen, Jeroen Wigard, Frank Frederiksen, and Preben Elgaard Mogensen, "High Speed Downlink Packet Access: WCDMA evolution," *IEEE Vehicular Technology Society News*, pp. 4–10, Feb. 2003.

[77] *MAXIM 2.4 GHz 802.11b Zero-IF transceiver.*

[78] Shinsuke Hara and Ramjee Prasad, "Overview of multicarrier CDMA," *IEEE Communications Magazine*, vol. 35, no. 12, pp. 126–133, Dec. 1997.

[79] "Wimax forum," http://www.wimaxforum.org.

[80] Erik Dahlman, "Long-term 3G evoluation and 4G research," in *2005 BEATS/CUBAN/WIP Third Workshop*, May 2005.

[81] Arunabha Ghosh, David R. Wolter, Jeffrey G. Andrews, and Runhua Chen, "Broadband wireless access with WiMAX/802.16: current performance benchmarks and future potential," *IEEE Communications Magazine*, vol. 43, no. 2, pp. 129–136, Feb. 2005.

[82] Jeffrey G. Andrews, "Interference cancellation for cellular systems: a contemporary overview," *IEEE Wireless Communications Magazine*, pp. 19–29, Apr. 2005.

[83] Lizhong Zheng and David N. C. Tse, "Diversity and multiplexing: a fundamental tradeoff in multiple antenna channels," *IEEE Transactions on Information Theory*, vol. 49, no. 5, pp. 1073–1096, May 2003.

[84] Robert W. Heath Jr. and Arogyaswami J. Paulraj, "Switching between diversity and multiplexing in MIMO systems," *IEEE Transactions on Communications*, vol. 53, no. 6, pp. 962–968, June 2005.

[85] Runhua Chen, Jeffrey G. Andrews, and Robert W. Heath Jr., "Transmit selection diversity for multiuser spatial multiplexing wireless systems," in *Proc. IEEE Globalcom Conf.*, Dec. 2004, vol. 4, pp. 2625–2629.

[86] Antonio Forenza, Ashishi Pandharipande, Hojin Kim, and Robert W. Heath Jr., "Adaptive MIMO transmission scheme: exploiting the spatial selectivity of wireless channels," in *Proceedings of IEEE Vehicular Technology Conference*, May 2005.

[87] Andrea J. Goldsmith and Pravin P. Varaiya, "Capacity of fading channels with channel side information," *IEEE Transactions on Information Theory*, vol. IT-43, no. 6, pp. 1896–1992, Nov. 1997.

[88] Andrea J. Goldsmith and Soon-Ghee Chua, "Adaptive coded modulation for fading channels," *IEEE Transactions on Communications*, vol. 46, no. 5, pp. 595–602, May 1998.

[89] Andrea J. Goldsmith and Soon-Ghee Chua, "Variable-rate variable-power M-QAM for fading channels," *IEEE Transactions on Communications*, vol. 45, no. 10, pp. 1218–1230, Oct. 1997.

[90] Viljo O. Hentinen, "Error performance for adaptive transmission on

fading channels," *IEEE Transactions on Communications*, vol. COM-22, no. 9, pp. 1331–1337, Sept. 1974.

[91] Chang Heon Lim and John M. Cioffi, "Performance of the adaptive rate MQAM with on/off power control," *IEEE Communications Letters*, vol. 5, no. 1, pp. 16–18, Jan. 2001.

[92] Mohamed-Slim Alouini and Andrea J. Goldsmith, "Adaptive modulation over Nakagami fading channels," *Wireless Personal Communications*, vol. 13, pp. 119–143, May 2000.

[93] Mohamed-Slim Alouini, X. Tang, and Andrea J. Goldsmith, "An adaptive modulation scheme for simultaneous voice and data transmission over fading channels," *IEEE Journal on Selected Areas in Communications*, vol. SAC-17, no. 5, pp. 837–850, May 1999.

[94] G. David Forney Jr., Robert G. Gallager, Gordon R. Lang, Fred M. Longstaff, and Shahid U. Qureshi, "Efficient modulation for band-limited channels," *IEEE Journal on Selected Areas in Communications*, vol. SAC-2, no. 5, pp. 632–646, September 1984.

[95] *IEEE Standard 802.16a-2003: Air Interface for Fixed Broadband Wireless Access Systems - Amendment 2: Medium Access Control Modifications and Additional Physical Layer Specifications for 2-11GHz*, 2003.

[96] Raymond Knopp and Pierre A. Humblet, "Information capacity and power control in single cell multiuser communications," in *Proceedings of IEEE International Conference on Communications*, June 1995, vol. 1, pp. 331–335.

[97] Bengt Holter, Mohamed-Slim Alouini, Geir Egil Øien, and Hong-Chuan Yang, "Multiuser switched diversity transmission," in *Proceedings of IEEE Vehicular Technology Conference*, Sept. 2004, vol. 3, pp. 2038–2043.

[98] Yahya Al-Harthi, Ahmed Twefik, and Mohamed-Slim Alouini, "Multiuser diversity with quantized feedback," in *Proceedings of IEEE Global Telecommunications Conference*, Nov. 2005, vol. 6, pp. 3728–3732.

[99] Vegard Hassel, Mohamed-Slim Alouini, David Gesbert, and Geir E. Øien, "Exploiting multiuser diversity using multiple feedback thresholds," in *Proceedings of IEEE Vehicular Technology Conference*, May 2005, vol. 2, pp. 1302– 1306.

[100] Vegard Hassel, Mohamed-Slim Alouini, Geir E. Øien, and David Gesbert, "Rate-optimal multiuser scheduling with reduced feedback load and analysis of delay effects," in *European Signal Processing Conference (EUSIPCO)*, Sept. 2005.

[101] Hend Koubaa, Vegard Hassel, and Geir E. Øien, "Multiuser diversity gain enhancement by guard time reduction," in *IEEE Workshop on Signal Processing Advance in Wireless Communications (SPAWC)*, June 2005.

[102] Hend Koubaa, Vegard Hassel, and Geir E. Øien, "Contention-less feedback for multiuser diversity scheduling," in *Proceedings of IEEE Vehicular Technology Conference*, Sept. 2005, vol. 3, pp. 1574–1578.

[103] Taiwen Tang and Robert W Heath Jr., "Opportunistic feedback for downlink multiuser diversity," *IEEE Communications Letters*, vol. 9, no. 10, pp. 948–950, Oct. 2005.

[104] Lin Yang and Mohamed-Slim Alouini, "Performance analysis of multiuser selection diversity," *IEEE Transactions on Vehicular Technology*, vol. 55, no. 3, pp. 1003–1018, May 2006.

[105] David Gesbert and Mohamed-Slim Alouini, "How much feedback is multi-user diversity really worth?," in *Proceedings of IEEE International Conference on Communications*, June 2004, pp. 234–238.

[106] Mathias Johansson, "Diversity-enhanced equal access-considerable throughput gains with 1-bit feedback," in *Signal Processing Advances in Wireless Communications, IEEE 5th workshop on*, July 2004, pp. 6–10.

[107] Arogyaswami Paulraj, Dhananjay Gore, and Rohit Nabar, *Introduction to Space-Time Wireless Communications*, Cambridge University Press, 2003.

[108] Siavash M. Alamouti, "A simple transmit diversity technique for wireless communications," *IEEE Journal on Selected Areas in Communications*, vol. 16, no. 8, pp. 1451–1458, Oct. 1998.

Vita

Haewoon Nam received the Master of Science in electrical engineering from Seoul National University in 1999 and Bachelor of Science in electrical communication engineering from Hanyang University in 1997.

From February 1999 to July 2002, he was a member of technical staff in the telecommunication research center, Samsung electronics, where he was engaged in the design and development of CDMA and GSM/GPRS baseband processors for mobile handsets. In the summer of 2003, he was affiliated with the IBM T.J. Watson research center, Yorktown Heights, NY, where he performed extensive radio channel measurements at 60GHz. In the fall of 2005, he was with the wireless mobile system group, Freescale semiconductor where he was engaged in the design and test of WiMAX MAC layer. His industry experience also includes work at Samsung Advanced Institute of Technology where he participated the simulation of MIMO systems for the LTE standard.

He is a recipient of the Korean government fellowship for his doctoral studies in the field of electrical engineering.

Permanent Address: 11215 Research Blvd. APT 2102, Austin, TX 78759

This dissertation was typeset with LaTeX 2$_\varepsilon$[1] by the author.

[1] LaTeX 2$_\varepsilon$ is an extension of LaTeX. LaTeX is a collection of macros for TeX. TeX is a trademark of the American Mathematical Society. The macros used in formatting this dissertation were written by Dinesh Das, Department of Computer Sciences, The University of Texas at Austin, and extended by Bert Kay, James A. Bednar, and Ayman El-Khashab.